ACCEPTED
FACULTY OF GRADUATE STUDIES

1991 01 23 DEAN

DATE

FUNCTIONAL MORPHOLOGY OF THE HEART/KIDNEY COMPLEX, DIGESTIVE SYSTEM AND MANTLE OF *DENTALIUM RECTIUS* (MOLLUSCA, SCAPHOPODA)

by

PATRICK DENNIS REYNOLDS
B.Sc., University College Galway, National University of Ireland, 1983

A Dissertation Submitted in Partial Fulfillment of the
Requirements for the Degree of

DOCTOR OF PHILOSOPHY

in the Department of Biology

We accept this thesis as conforming
to the required standard

Dr. A.R. Fontaine (Supervisor, Department of Biology)

Dr. R.G.B. Reid (Department of Biology)

Dr. D.V. Ellis (Department of Biology)

Dr. A. McAuley (Department of Chemistry)

Dr. E. van der Flier-Keller (Department of Geography)

Dr. M.P. Morse (Northeastern University) (External examiner)

Supervisor: Dr. Arthur R. Fontaine

ABSTRACT

The functional morphology of the heart/kidney complex, digestive system and mantle was investigated in *Dentalium rectius* (Mollusca, Scaphopoda). While encompassing in-depth examination of the diverse roles of each organ system, these studies also contribute towards an overview of metal processing by the organism.

The heart/kidney complex departs substantially from typical molluscan form; morphological features demonstrate that the heart is reduced to a perianal sinus adjacent to the pericardium. Excretory function appears to be maintained, however; pericardial podocytes and a right renopericardial connection indicate that a blood ultrafiltrate passes to the kidney. Urine is modified by two nephrocyte types. While one may effect reabsorption, both secrete calcium, zinc and phosphate-containing granules into the urine.

Intracellular granules of the digestive system also contain calcium phosphate; iron is the only other metal accumulated, principally by oesophageal and stomach epithelia. Iron uptake occurs via digestive cells and by both undifferentiated and specialized mantle epithelia. Iron-containing granules, released into the haemocoel by the mantle epithelium, are phagocytosed and transported by amoebocytes. Iron is not excreted by the kidney, but by oesophageal secretion into the gut lumen and by radular mineralization, differing significantly from iron processing reported in other molluscs.

In addition to iron uptake, mantle functions include the creation of respiratory currents, gas exchange and sensory reception; the respective epithelial specializations described here constitute functional equivalents to ctenidia and osphradia, organs which are absent in this molluscan class. The ciliated bands of the mid-mantle region include supporting cells which possess high-domed, microvillous apices that facilitate diffusion

between the mantle cavity and underlying haemocoel. The posterior region of the mantle is richly endowed with innervated cells, considered putative sensory receptors. Cilia number, length and ultrastructure define three receptor types. They are heterogeneously distributed among specific regions of the pavilion, and probably function in respiratory current testing.

The maintenance of respiratory current passage to the scaphopod mantle cavity requires a secondary increase in posterior aperture size, which is otherwise progressively diminished by normal shell growth. Such an increase occurs in *D. rectius*, and is effected by periodic shell decollation through dissolution by the posterior mantle.

Examiners:

Dr. A.R. Fontaine

Dr. R.G.B. Reid

Dr. D.V. Ellis

Dr. A. McAuley

Dr. E. van der Flier-Keller

Dr. M.P. Morse

CONTENTS

LIST OF TABLES

LIST OF FIGURES

ACKNOWLEDGEMENTS

Many people patiently shared their knowledge of the techniques employed in this study, for which I am very grateful. Jack Dietrich, C.L. Singla, Louise Page and Arthur R. Fontaine contributed significantly to my learning of electron microscopy. Tom Gore provided considerable photographic instruction and expertise. Robert Reid, Dawna Brand, Doug Bright, Ronald L. Shimek and particularly Don Horn have my gratitude for assistance with collection of specimens. Damhnait McHugh and Rossi Marx obligingly helped with the translation of German literature, and Chris Blanton did likewise with Latin. My thanks are also due to the departmental graduate advisor, Robert D. Burke and graduate secretary, Annette Barath.

An integral part of the progress of this research was the development of ideas, interpretation of data, and critical assessment of both, all of which has been fostered by discussions with many interested people, including Arthur R. Fontaine, Diarmaid ó Foighil, Damhnait McHugh, Robert Reid, M. Patricia Morse, Ronald L. Shimek, Doug Bright and Chris Rose.

A final but heartfelt thanks to my family for their continuous support, and to my wife, Damhnait McHugh, for everything.

This small eccentric class comprises the 'tooth shells,' so called from their resemblance to the tusks or canine teeth of some animals. Their nature in a zoological point of view was but little understood until of late years. Linné placed them in his 'Vermes. Testacea;' Lamarck and Cuvier considered them Annelids; De Blainville and Deshayes restored them to the rank of Mollusca. But the skilful and patient investigations of Lacaze-Duthiers have at last solved a problem the interest of which, in the estimation of a conchologist, surpasses that of the still sought-for discovery of the sources of the Nile.

J. G. Jeffreys 1865
British Conchology vol.3

CHAPTER 1

GENERAL INTRODUCTION

OVERVIEW

Introduction to the Scaphopoda

The Scaphopoda are one of the smallest of the seven molluscan classes (ca. 1000 fossil and extant species, Palmer, 1974). They are commonly known for the characteristic shape of their shell — a hollow, slightly curved, conical tube open at both ends. All members of the class are marine subtidal infauna, ranging in size from a few millimeters to several centimeters, that burrow into silt/sand sediments from 10 to over 1000 m depth using a muscular, conical or vermiform foot. Although relatively rare and often restricted to deeper water, they are particularly prevalent near the Vancouver Island coast, and were used as a form of currency among natives of the Northwest region up to the mid 1800's (Clark, 1963). The Scaphopoda are radulate molluscs, feeding on a variety of microorganisms which are selected from the sediment and manipulated by the feeding tentacles or captacula, a distinguishing feature of the class. The mantle cavity is narrow and runs the length of the animal; the typical molluscan sensory osphradia and ctenidia or gills are absent. Sexes are separate, and the gametes are shed to the exterior via the mantle cavity, through the right kidney and excretory pore. Development includes a free-swimming veliger-like larval stage. A diagram of the generalized scaphopod body plan is shown in Figure 1.

Figure 1. A diagramatic representation of the scaphopod body plan, shell removed. Anterior is to the left, dorsal to the top (*A*, opening of rectum; *C*, captacula; *CB*, ciliated ridges of the mantle cavity; *DD*, digestive diverticula; *F*, foot; *G*, gonad; *K*, kidneys; *MC*, mantle cavity; *O*, oesophagus; *P*, posterior mantle or pavilion; *R*, radula; *S*, stomach). Adapted from Pelseneer, 1889.

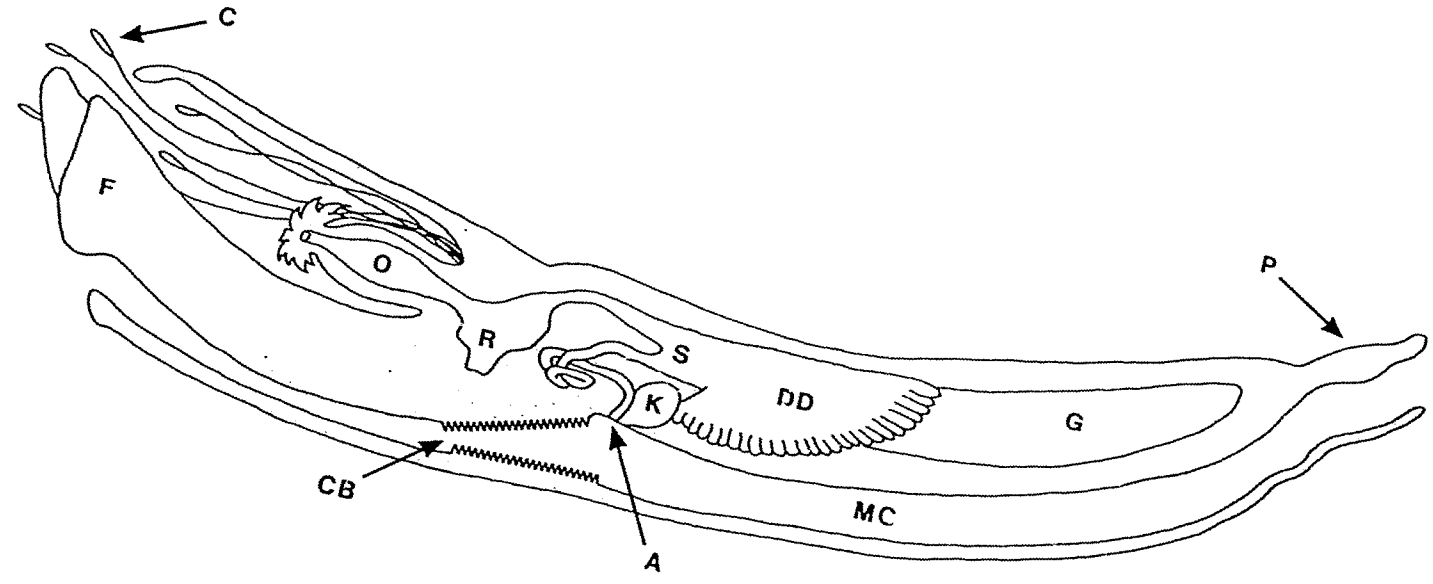

(1)

Evolution and phylogeny of the Class

The derivation of the unique morphological features of the Scaphopoda can be illuminated by consideration of the origins and evolution of the class. They are the last class of the Mollusca to have evolved (Runnegar & Pojeta, 1985); the oldest known scaphopod is represented by *Rhytiodentalium kentuckyensis* Pojeta and Runnegar 1979, dating from the late Middle Ordovician of Kentucky. The Scaphopoda probably descended from the extinct molluscan class Rostroconchia which had a bivalved shell. The rostrochonchs are also thought to have given rise to the bivalves, and are considered a subclass of the Bivalvia by Salvini-Plawen (1980). From the late Cambrian, two subtaxa of the rostroconchs, the Ribeiriida and Conocardida, showed a trend towards elongation of the anterior end (Pojeta & Runnegar, 1985); the genus *Pinnocaris* is a ribeirioid from the upper Cambrian to upper Ordovician that is often cited as a typical rostroconch which had developed the nasute shell that is likely of scaphopod ancestors. Subsequent fusion of the ventral mantle margins and predominantly anterior growth are necessary intermediate steps to the scaphopod body form (Pojeta and Runnegar, 1979). Anterior feeding tentacles or captacula are also thought to have been present in the Rostroconchia, the oldest form possessing them being the upper Cambrian *Pseudotechnophorus* (Pojeta & Runnegar, 1985).

An alternative interpretation of scaphopod origins was presented by Staurobogatov (1974). He suggested the Xenoconchia, a small group of fossils with a bullet-shaped shell, as common ancestors of the scaphopods and monoplacophores, and placed all of these groups as subclasses within the Class Solenoconchia. This was largely based on the common feature of a unspiralled, elongate shell, open at both ends or closed apically. Emerson (1978) considers the paleontological and neontological evidence of such

relationships to be insufficient; Pojeta & Runnegar (1979) believed the Class Solenoconchia to be an assemblage of not closely related taxa.

The modern Class Scaphopoda is divided into two subtaxa— the Dentaliida Gray, 1847, to which *Dentalium rectius* belongs, and the Gadilida Stoliczka, 1862 (≡ Siphonodentalioida Palmer, 1974). This division is based primarily on the shape of the central tooth of the radula and the constriction of the anterior aperture in the Gadilida (Emerson, 1962). The Dentaliida precede the Gadilida in the fossil record; the first gadilid fossils date from the Permian (Pojeta & Runnegar, 1985). *Entalina* is the first gadilid genus to appear, and is thought to have evolved with *Dentalium* from a common stock as it combines the foot of the Gadilida with the shell characteristics of the Dentaliida (Emerson, 1962). The evolution of the constricted anterior aperture typical of most gadilids is suggested by Shimek (1989) to permit greater burrowing efficiency, and is of use especially in predator avoidance. In the Dentaliida, evolution of shell sculpture suggests that the unornamented, smooth shell is the ancestral condition. This is retained in *Dentalium rectius*. The subgenus *Rhabdus*, which includes *D. rectius*, dates from the lower Miocene (Emerson, 1962).

Summary of literature on extant scaphopods

The common rostroconch ancestry and similarity in lifestyle of extant species of the Scaphopoda and Bivalvia suggests that the biology of these two classes could be closely correlated. However, this is difficult to adequately evaluate as recent research on the Scaphopoda is sparse and past work is almost exclusively based on Atlantic species of the genus *Dentalium*. Histological studies dating from the last century have described the general body form and the tissue morphology in most organs, some of which has been

confirmed by more recent investigations. While some early accounts such as those by Deshayes (1825) and Clark (1849) contained many inaccuracies, Lacaze-Duthier (1856, 1857) provided an extensive and accurate account of morphology, development and behaviour of *Dentalium*. Notable morphological contributions have been made by Fol (1885, 1889) and Plate (1888, 1890, 1892). Published ultrastructural research on scaphopoda is limited to transmission electron microscopic studies of *Dentalium* gametes (Gielenkirchen et al., 1971; Dufresne-Dube et al., 1983), scanning electron microscopy of the captacula (Shimek, 1988) and Chapter 2 of this dissertation (Reynolds, 1990).

Physiological investigations of small marine invertebrates are difficult, and in scaphopods are restricted to brief reports on excretory function (Kowalevsky, 1889) and digestion (Taib, 1981). Behavioural studies have examined the function of the mantle (Yonge, 1937) and of the foot in both burrowing (Dinamani, 1964; Trueman, 1968) and feeding (Morton, 1959; Gainey, 1972; Taib, 1980). The feeding biology of scaphopoda has generally received a good deal of attention, particularly in terms of habitat and prey selection (Bilyard, 1974; McFadien-Carter, 1973; Shimek, 1990), and captacular structure and function (Poon, 1987; Shimek, 1988).

Little is known of scaphopod reproduction. Although sexes are separate, D'Anna (1974) reported some hermaphroditic individuals in *Dentalium entalis*. Reproductive ecology has been examined only by Rokop (1974, 1977). *Dentalium* has, however, been used extensively in experimental embryology since the studies of Wilson (1904), and as a result a good deal is known of scaphopod early development. The embryological studies such as those by Verdonk et al. (1971) and Render & Guerrier (1984) focus on morphogenetic localization in the early embryos of *Dentalium*. Scaphopod reproduction and developmental studies on *Dentalium* are summarized in Reverberi (1971), McFadien-Carter (1979) and Moor (1983).

General reviews of scaphopod research are provided by Simroth (1894), Jutting (1926), Hoffman (1930) and Fischer-Piette & Franc (1969).

Research to date on Dentalium rectius

Despite several revisions of scaphopod classification, there is a lack of concensus regarding the nomenclature of *Dentalium rectius*. This species was originally described by Carpenter in 1864. It was subsequently placed in the newly created subgenus *Rhabdus* by Pilsbry & Sharp (1897). While included in the *Fustiaria* genus complex by Emerson (1962) in a revision of scaphopod classification, Palmer (1974) argued for the recognition of *Rhabdus* and other subgeneric groupings as full genera. As such, the species name *Rhabdus rectius* is in use among some malacologists (Emerson, 1962, 1978; Palmer, 1974; Boss 1982; Austin, 1985; Turgeon et al., 1988). However, use of the genus-taxon *Rhabdus* has not gained total acceptance, as this species is still often referred to the genus *Dentalium* (Bernard, 1970; Abbott, 1974; Kozloff, 1987; Shimek, 1988, 1989, 1990). A further source of confusion lies in the date of description; Carpenter named and summarily described the species in a 1864 publication (reproduced in Palmer, 1958), but an expanded description was published in 1865. Consequently, both "1864" (Bernard, 1970; Abbott, 1974; Ruhoff, 1980; Austin, 1985; Kozloff, 1987; Shimek, 1988, 1989, 1990) and "1865" (Emerson, 1962, 1978; Palmer, 1974; Boss 1982; Turgeon et al., 1988) have been cited. Other inconsistancies can be found in many areas of the taxonomy of the class. Unfortunately, many of the revisions to the classification of the scaphopods have lacked detailed information on soft part anatomy and radular characteristics (Emerson, 1978), and the over-reliance upon shell characters without sufficient knowledge of their relationship to the underlying soft tissues may have led to illegitimate systematic groupings in the

Scaphopoda (Shimek, 1989). The revisions of scaphopod classification by Starobogatov (1974), Palmer (1974), and Chistikov (1975, in Emerson, 1978), have been criticised for lack of sufficient detail in morphological criteria and, in the case of Chistikov, for nomenclatural identification of only one of the 24 species upon which he based his revisions (Emerson, 1978). It was in this study that Chistikov erected the superfamily Rhabdoidea and family Rhabdidae, containing *Rhabdus*. A further example of insufficient morphological detail in the taxonomic descriptions of this group is found in the taxon *Rhabdus* Pilsbry & Sharp, 1897 (type species, *Dentalium rectius* Carpenter 1864). In the original description, the absence of a slit or notch at the apical rim of the shell is cited as a distinguishing character, whereas my observations on apical shell morphology of *D. rectius* (Chapter 7) show that a shallow notch is usually present. While this shell character is not addressed in the original species descriptions (Carpenter, 1864 in Palmer, 1958; Carpenter, 1865), the description by Pilsbry & Sharp (1897) does appear in subsequent keys and summaries (Emerson, 1962; Abbott, 1974; Palmer, 1974). While recognising the apparent taxonomic validity of the genus name *Rhabdus*, it seems appropriate at this juncture to retain the generic name *Dentalium* while awaiting consensus and the application of more broadly based morphological criteria in the taxonomy of this group. This is supported by the reference to *Dentalium rectius* in the non-taxonomic literature dealing with this species (Shimek, 1988, 1990), and particularly by its use among systematists/taxonomists familiar with the local scaphopod fauna (Bernard, 1970; Kozloff, 1987; Shimek, 1989).

Apart from taxonomic descriptions and distributional checklists, only five published studies deal with this species. Reynolds (1990a) is reproduced here in Chapter 2; Reynolds (1990b) in Chapter 3. Shimek (1988) examined captacular morphology and function in several scaphopod species including *D. rectius*. Shell morphometric analysis of *D. rectius* was included in a taxonomic revision of Northeastern Pacific *Cadulus* species

(Shimek, 1989). The buccal contents and sediment characteristics of these scaphopod populations were investigated also by Shimek (1990) in a study of diet and habitat utilization.

OBJECTIVES AND RATIONALE

The Scaphopoda are one of the least studied classes of the Mollusca, despite substantial early morphological investigation dating from the mid 1800's. One possible explanation for this is the restriction of many species to deeper water and the consequent difficulty in obtaining specimens. This is not the case, however, in the near-shore waters of the Northeast Pacific where several species are found, some as shallow as 10 m at certain sites (Shimek, 1990; personal communication). The local availability of scaphopods presents an opportunity to address basic questions of structure and function in the class, which are prerequisite to significant cross-phylum comparisons encompassing the major molluscan classes. The importance of the Scaphopoda in this regard is emphasized by the fact that, on the basis of the small body of literature that exists, several organ systems of *Dentalium* species depart significantly from the molluscan ground plan as suggested by the available data on the major molluscan classes. Of these, the heart/kidney complex and mantle are are perhaps the most substantially modified from the general molluscan condition. The diverse roles performed by the coelom and the unique elaboration of the molluscan body wall signify the importance of these organ complexes to molluscan biology and the significance of an analysis of their functional morphology in the Scaphopoda. *Dentalium rectius* was chosen as the study organism for its accessibility and size, as it is an abundant and large scaphopod species that can be conveniently sampled.

The systems which are perhaps the most unclear in scaphopods are those of circulation and excretion. Recent reviews and current monographs are inconsistent on the nature of the scaphopod heart/kidney complex; some suggest that the Scaphopoda do not possess a heart, which would be a considerable departure from the circulatory and excretory systems in other molluscs. Chapters 2 and 3 address these areas of scaphopod biology in *Dentalium rectius*. Chapter 2 attempts to clarify the anatomy of the heart/kidney complex, which departs significantly from the typical molluscan plan. In addition, the ultrastructure of the heart/perianal sinus and pericardium is related to molluscan circulatory and excretory function. This is extended in Chapter 3, which examines the structure and function of the kidney.

Considerable attention has been given in recent years to heavy metal accumulation by marine invertebrates, particulary molluscs. In Chapter three, characterisation of nephrocyte secretory products in *D. rectius* is a contribution to the function of the kidney as a site of metal accumulation. Its metal processing role within the organism is pursued in Chapter 4, in which the digestive system, the other major site of metal uptake and storage in molluscs, is surveyed for intracellular metal accumulation. Based on these results, a model for iron processing in *D. rectius* is proposed.

Apart from the digestive system, the other general route for metal uptake in marine organisms is the external epithelia. In molluscs, the mantle provides an extensive surface exposed to the environment; the process of iron uptake across the mantle is reported in Chapter 5. The molluscan mantle is one of the distinguishing features of the class, but despite its extensive modifications compared to the typical molluscan condition, the scaphopod mantle has received little detailed study. In addition to its role in metal uptake, Chapter 5 examines the fine structure of a uniquely elaborated region of the mantle epithelium, the ciliated bands. This morphological feature has long been considered a

possible analogue to the molluscan ctenidia which have been lost in scaphopods. Chapter 5 addresses the possible role of the mantle ciliated bands in gas exchange.

Chapters 6 and 7 continue to examine the form and function of the mantle in *D. rectius*. Chapter 6 describes the ultrastrucure and distribution of sensory receptors in the uniquely modified posterior region of the scaphopod mantle, the pavilion. The function of this organ in the alteration of shell shape and its significance to growth of the organism is investigated in Chapter 7, in which a laboratory observation of shell decollation intiated an examination of the shell growth pattern and mechanism of apical shell loss.

The research presented in this dissertation provides the first detailed ultrastructural analysis of circulation, excretion, gas exchange and sensory reception in the Class Scaphopoda; additionally, more information has been added to our knowledge of the scaphopod digestive system and dynamics of shell growth. The results are presented as separate manuscripts in Chapters 2 through 7; Chapters 2 and 3 have been previously published (Reynolds, 1990a; 1990b). Although written independently, the results chapters appear in a sequence which leads the reader through a structural series linked by functional themes. In its entirety, this dissertation emphasizes the diverse roles performed by individual cell, tissue and organ components, and their integration within and between separate organ systems in *Dentalium rectius*.

LITERATURE CITED

Abbott, R. T. (1974). American Seashells (second ed.). Van Nostrand Reinhold, New York.

Austin, W. C. (1985). An annotated checklist of marine invertebrates in the cold temperate Northeast Pacific. Khoyatan Marine Laboratory, Cowichan Bay.

Bernard, F. R. (1970). A distributional checklist of the marine molluscs of British Columbia: based on faunistic surveys since 1950. Syesis, 3, 75-94.

Bilyard, G. R. (1974). The feedeing habits and ecology of *Dentalium entale stimpsoni* Henderson. The Veliger, 17(2), 126-138.

Boss, K. J. (1982). Phylum Mollusca. In Parker, S. P. (Ed.), Synopsis and Classification of Living Organisms (pp. 945-1166). McGraw-Hill.

Carpenter, P. P. (1865). Diagnoses Specierum et Varietum novarum Molluscorum, prope Sinum Pugetianum a Kennerlio Doctore, nuper decesso, collectorum. Proceedings of the Academy of Natural Sciences of Philadelphia, 1865, 54-64.

Clark, R. B. (1963). The economics of Dentalium. The Veliger, 6(1), 9-19.

Clark, W. (1849). On the animal of *Dentalium tarentinum*. The Annals and Magazine of Natural History. Series 2., 4, 321-378.

D'Anna, T. (1974). Ermafroditismo in *Dentalium entalis*. Academia Nazionale dei Lincei. Classe di Science Fisiche, Matematische e Naturali. Series 8., 57(6), 673-677.

Deshayes, M. (1825). Anatomie et monographie du genre Dentale. Memoires de la Société d'histoire naturelle de Paris, 2, 321-378, pls. 1-4.

Dinamani, P. (1964). Burrowing behavior of *Dentalium*. Biological Bulletin, 126, 28-32.

Dufresne-Dube, L., Picheral, B. & Guerrier, P. (1983). An ultrastructural analysis of *Dentalium vulgare* (Mollusca, Scaphopoda) gametes with special reference to early events at fertilization. Journal of Ultrastructure Research, 83(3), 242-257.

Emerson, W. K. (1962). A classification of the scaphopod mollusks. Journal of Paleontology, 36(3), 461-482.

Emerson, W. K. (1978). Two new eastern Pacific species of Cadulus, with remarks on the classification of the scaphopod mollusks. The Nautilus, 92(3), 117-123.

Fischer-Piette, E. & Franc, A. (1969). Classe des Scaphopodes. Mollusques, Gasteropodes et Scaphopodes (pp. 987-1017). Paris: Masson et Cie.

Fol, H. (1885). Sur l'anatomie microscopique du Dentale. Comptes rendu hebdomadaires des seances de l'academie des sciences. Serie D. Sciences naturelles., 1885, 1352-1355.

Fol, H. (1889). Sur l'anatomie microscopique du Dentale. Archives de Zoologie Experimentale et Génerale, Deuxième Série, 7, 91-148, pls. 5-8.

Gainey, L. F. Jr. (1972). The use of the foot and the captacula in the feeding of *Dentalium* (Mollusca: Scaphopoda). The Veliger, 15(1), 29-34.

Geilenkirchen, W. L. M., Timmermans, L. P. M., Van Dongen, C. A. M., Arnolds, W. J. R. (1971). Symbiosis of bacteria with eggs of Dentalium at the vegetal pole. Experimental Cell Research, 67, 477-478.

Hoffman, H. (1930). Polyplacophora (Schluss) Amphineura Allegmeines; Scaphopoda. Bronn's Klassen und Ordnungen des Tier-Reichs, Leipzig, Band 3, Nachträge zur Abteilung 1, Nachträge 3, 369-511.

Jutting, T. v. B. (1926). Scaphopoda. In G. Grimpe & E. Wagler (Ed.), Die Tierwelt der Nord- und Ostsee (pp. 67-80). Akad. Verlagsges., Leipzig.

Kowalevsky, A. (1889). Ein Beitrag zur Kenntnis der Exkretionsorgane. Biologisches Zentralblatt, 9(3), 65-76.

Kozloff, E. N. (1987). Marine Invertebrates of the Pacific Northwest. University of Washington Press, Seattle.

Lacaze-Duthiers, H. de (1856). Histoire de l'organisation et du développement du Dentale. Annales des Sciences Naturelles, Quatrième Séries, Paris, 6, 319-385, pls. 11-13.

Lacaze-Duthiers, H. de (1857). Histoire de l'organisation et du développement du Dentale. Annales des Sciences Naturelles, Quatrième Série, 7, 194-251, pls. 5-9.

McFadien-Carter, M. (1979). Scaphopoda. In A. C. Giese & J. S. Pearse (Ed.), Reproduction of Marine Invertebrates, Molluscs: Pelecypods and Lesser Classes (pp. 95-111). New York: Academic Press.

McFadien-Carter, M. S. (1973). Zoogeography and ecology of seven species of Panamic-Pacific Scaphopoda. The Veliger, 15(4), 340-347.

Moor, B. (1983). Organogenesis. In Verdonk, N. H., van den Biggelaar, J. A. M. & Tompa, A. S. (Eds.), The Mollusca, v. 3, Development (pp. 123-177). Academic Press, New York.

Morton, J. E. (1959). The habits and feeding organs of *Dentalium entalis*. Journal of the Marine Biological Association of the United Kingdom, 38, 225-238.

Palmer, C. P. (1974). A supraspecific classification of the scaphopod Mollusca. The Veliger, 17(2), 115-123.

Palmer, K. van W. (1958). Type specimens of marine mollusca described by P. P. Carpenter from the west coast (San Diego to British Columbia). Geological Society of America, Memoir 76, 376 pp.

Pelseneer, P. (1899). Reserches Morphologiques et Phylogenetiques sur les Mollusques Archaiques. Academie royale des sciences, des lettres et des beaux-arts de Belgique, Bruxelles, 113 pp.

Pilsbry, H. A. & Sharp, B. (1897). Class Scaphopoda. Manual of Conchology, Series 1, 17, i-xxxii, 1-144.

Pilsbry, H. A. & Sharp, B. (1898). Class Scaphopoda. Manual of Conchology, Series 1, 17, 145-280, pls. 1-39.

Plate, L. H. (1888). Bemerkungen zur Organisation der Dentalien. Zoologischer Anzeiger, 14, 78-80.

Plate, L. (1890). Ueber einige Organisationsverhältnisse der Dentalien. Sitzungsberichte der Gesellschaft zur Beförderung der gesammten Naturwissenschaften, 1890, 26-29.

Plate, L. H. (1892). Ueber den Bau und die Verwadtschaftsbeziehungen der Solenoconchen. Zoologische Jahrbucher Jena Abteilung für Anatomie, 5, 301-386, pls. 23-26.

Pojeta, J. Jr. & Runnegar, B. (1979). *Rhytiodentalium kentuckyensis*, a new genus and new species of ordovician scaphopod, and the early history of scaphopod mollusks. Journal of Paleontology, 53(3), 530-541.

Pojeta, J. Jr. & Runnegar, B. (1985). The early evolution of diasome molluscs. In Trueman, E. R. & Clark, M. R. (Eds.), Evolution. Academic Press, New York.

Poon, P. A. (1987). The diet and feeding behaviour of Cadulus tolmiei Dall, 1897 (Scaphopoda, Siphonodentalioida). The Nautilus, 101(2), 88-92.

Render, J. A. & Guerrier, P. (1984). Size regulation and morphogenetic localization in the *Dentalium* polar lobe. Journal of Experimental Zoology, 232, 79-86.

Reverberi, G. (1971). Dentalium. In Reverberi, G. (Ed.), Experimental Embryology of Marine and Freshwater Invertebrates (pp. 248-264). North-Holland.

Reynolds, P. D. (1990a). Functional morphology of the perianal sinus and pericardium of *Dentalium rectius* (Mollusca: Scaphopoda) with a reinterpretation of the scaphopod heart. American Malacological Bulletin, 7(2), 137-146.

Reynolds, P. D. (1990b). Fine structure of the kidney and characterization of secretory products in *Dentalium rectius* (Mollusca, Scaphopoda). Zoomorphology, 110(1), (in press).

Rokop, F. J. (1974). Reproductive patterns in the deep-sea benthos. Science, 186, 743-745.

Rokop, F. J. (1977). Seasonal reproduction of the brachiopod *Frieleia halli* and the scaphopod *Cadulus californicus* at bathyal depths in the deep sea. Marine Biology, 43, 237-246.

Ruhoff, F. A. (1980). Index to the species of Mollusca introduced from 1850 to 1870. Smithsonian Contributions to Zoology, number 294, 1-640.

Runnegar, B. & Pojeta, J. Jr. (1985). Origin and diversification of the Mollusca. In E.R. Trueman & M.R. Clarke (Eds.) The Mollusca, volume 10, Evolution (pp. 1-57).

Salvini-Plawen, L. v. (1980). A reconsideration of systematics in the Mollusca (phylogeny and higher classification). Malacologia, 19(2), 249-278.

Shimek, R. L. (1988). The functional morphology of scaphopod captacula. The Veliger, 30(3), 213-221.

Shimek, R. L. (1989). Shell morphometrics and systematics: a revision of the slender, shallow water *Cadulus* of the northeastern Pacific (Scaphopoda: Gadilida). The Veliger, 32(3), 233-246.

Shimek, R. L. (1990). Diet and habitat utilization in a Northeastern pacific ocean scaphopod assemblage. American Malacological Bulletin, 7(2), 147-169.

Simroth, H. (1894). I. Abteilung: Amphineura und Scaphopoda. Mollusca (pp. 356-467, tafel XV-XXII). Winter, Leipzig.

Starobogatov, Y. I. (1974). Xenoconchias and their bearing on the phylogeny and systematics of some molluscan classes. Paleontological Journal, 8(1), 1-13.

Taib, N. T. (1980). Some observations on the living animals of *Dentalium entalis* L. Journal of the College of Science, University of Riyadh, Saudi Arabia, 11, 129-144.

Taib, N. T. (1981). Sites of absorption and food storage in the gut of *Dentalium entalis* L.. Journal of the College of Science, University of Riyadh, Saudi Arabia, 12(1), 147-154.

Trueman, E. R. (1968). The burrowing process of *Dentalium* (Scaphopoda). Journal of Zoology, London, 154, 19-27.

Turgeon, D. D., Bogan, A. E., Coan, E. V., Emerson, W. K., Lyons, W. G., Pratt, W. L., Roper, C. F. E., Scheltema, A., Thompson, F. G. and Williams, J. D. (1988). Common and scientific names of aquatic invertebrates from the United States and Canada: mollusks. American Fisheries Society Special Publication 16.

Verdonk, N. H., Geilenkirchen, W. L. M. & Timmermans, L. P. M. (1971). The localization of morphogenetic factors in uncleaved eggs of *Dentalium*. Journal of Embryology and experimental Zoology, 25(1), 57-63.

Wilson, E. B. (1904). Experimental studies on germinal localization. Journal of Experimental Zoology, 1(1), 1-72.

Yonge, C. M. (1937). Circulation of water in the mantle cavity of *Dentalium entalis*. Proceedings of the Malacological Society of London, 22, 333-337.

CHAPTER 2

FUNCTIONAL MORPHOLOGY OF THE PERIANAL SINUS AND PERICARDIUM OF *DENTALIUM RECTIUS* (MOLLUSCA: SCAPHOPODA) WITH A REINTERPRETATION OF THE SCAPHOPOD HEART

ABSTRACT

The anatomy and ultrastructure of the perianal blood sinus and pericardium in the scaphopod *Dentalium rectius* Carpenter were investigated. The perianal blood sinus surrounds the rectum and lies adjacent to the anterior wall of the pericardial coelom; it is enclosed by smooth musculature with additional muscular trabeculae traversing the sinus. The pericardium is contractile, and consists of a simple, flat epithelium with interspersed muscle fibres; both are separated from the haemocoel by a basal lamina. The pericardial musculature is arranged as laterally oriented trabeculae which produce localised transverse constrictions of the dorsal pericardial wall. There is no evidence for a heart enclosed by the dorsal wall of the pericardial coelom in a position ventral to the stomach as interpreted by earlier workers, since both a myocardium and distinct epicardium are absent. A portion of the pericardial epithelium apposing the perianal sinus musculature is developed into podocytes and, based on functional analogy, may be the site of primary urine production. Although organogenetic information on scaphopod coelom formation is lacking, structural similarities of the perianal sinus and pericardium in *D. rectius* to the heart and pericardium in other molluscan classes support the homology of these organs.

INTRODUCTION

The morphology of scaphopod circulatory structures received a great deal of attention up to the early part of this century, producing several conflicting interpretations of structure and function. Deshayes' (1825) and Clark's (1849) descriptions of a heart in *Dentalium* spp. appear to be mistaken identifications of the oesophagus and stomach respectively. Lacaze-Duthiers (1857) found no structure analogous to a molluscan heart in *Dentalium* sp. i.e., a pulsatile vessel within a pericardium responsible for the movement of blood, and he considered the contractions of the pedal, perianal and abdominal blood sinuses to be sufficient for circulation. A small serous sac within the anterior abdominal sinus, lying between the stomach and ventral body wall, was suggested by Lacaze-Duthiers (1857) as the pericardial rudiment; he also noted the structural similarities of the perianal sinus to the bivalve ventricle. Fol (1889), studying *D. entalis*, concluded that the perianal sinus is homologous with the heart of other molluscs.

Plate (1891, 1892) described a completely different stucture as representing the scaphopod heart: an invagination of the dorsal pericardial wall, lying ventral to the stomach and within the pericardial coelom. Boissevain (1904) and Distaso (1905) confirmed these results and agreed with this interpretation. While Potts (1967) states that the pericardium is absent in scaphopods and the heart is represented by a contractile vessel, most recent reviews accept Plate's interpretation, at least tentatively (Fischer-Piette & Franc, 1968; Martin, 1983; Andrews, 1988).

Defining the structure of the scaphopod heart and pericardium accurately and conclusively is of importance not only in ascertaining the level of organization of the circulatory system, but also in determining the role of the heart in excretion or, alternatively, the structural modification of the excretory system in the absence of a

functional heart in this molluscan class. The general organization of the excretory system in the Mollusca is based on a haemocoel-pericardium-kidney complex. Physiological work on prosobranchs (Harrison, 1962; Little, 1965), coleoid cephalopods (Harrison & Martin, 1965; Martin & Aldrich, 1970) and bivalves (Jones & Peggs, 1983; Hevert, 1984) has established that primary urine is produced by ultrafiltration into the pericardial coelom. The site of ultrafiltration, as characterized ultrastructurally by the presence of podocytes, varies from the auricular or ventricular wall in prosobranch gastropods (Andrews, 1981), polyplacophorans (Økland, 1980), protobranch and pteriomorph bivalves (Pirie & George, 1979; Meyhöfer et al., 1985), to the branchial heart wall in cephalopods (Witmer & Martin, 1973; Schipp & Hevert, 1981) and the antero-dorsal wall of the pericardium in heterodont bivalves (Meyhöfer et al., 1985). In all cases, the ultrafiltrate enters the pericardial cavity from the haemocoel and passes through a renopericardial connection to the kidney lumen. Further modification of the primary urine by reabsoprtion and secretion takes place in the kidney before excretion to the external environment via the mantle cavity.

Localization of an ultrafiltration barrier by ammoniacal carmine injection, a technique used extensively in the study of circulation and excretion up to the early 1900's, has been attempted in most molluscan classes and has served as a useful basis for subsequent morphological and quantitative physiological investigation in many representative species (for review, see Martin, 1983). In scaphopods, however, it is the only physiological method applied to date, and possible sites of ultrafiltration have not been clearly indicated. Working with *Dentalium* sp., Kowalevsky (1889) noted the accumulation of ammoniacal carmine in unspecified blood spaces and connective tissue cells. Using the same method with *D. vulgare* Da Costa, Cuénot (1899) found that these cells contain yellowish, oily granules and described their distribution as broadly similar to that in amphineurans and gastropods, being found under the epithelium, between the

viscera and within the interstices of muscle fibres. On the basis of an uncertain but presumed common excretory function, Cuénot (1899) aligned these ammoniacal carmine accumulating cells and those of amphineurans and gastropods with the pericardial glands of bivalves and branchial hearts of cephalopods. Strohl (1924) agreed, labelling the cells collectively as carmine athrocytes.

An internal opening between the paired kidneys and another coelomic (pericardial) space is absent in *Dentalium* sp. according to Lacaze-Duthiers (1857), Fol (1885; 1889) and Plate (1888, 1892). Of those investigations which describe a pericardium, only Distaso (1905) noted a morphological connection represented by a pore leading to the left kidney.

This study of *Dentalium rectius* Carpenter (Order Dentaliida) aims to clarify the morphological relationship between the perianal and abdominal haemal sinuses, the pericardial coelom and the kidney using light and electron microscopy. The tissues of the pericardium and associated blood sinuses are described ultrastructurally with particular reference to contractile elements, and with a view to identifying possible sites for ultrafiltration of blood. The information contributes towards a better understanding of circulation and excretion in the Scaphopoda, and relationships of the class within the Mollusca.

MATERIALS AND METHODS

Specimens of *Dentalium rectius* were dredged from approximately 60 m at Satellite Channel, close to Victoria, British Columbia, Canada.

For anatomical examination at the light microscope level, tissues were fixed in 10% seawater-buffered formalin, dehydrated in a graded ethanol series and embedded in paraffin. Serial sections of 6-8 µm thickness were stained with eriochrome cyanin (Chapman, 1977). Additionally, serial 1 µm sections of resin embedded material, prepared as described below for transmission electron microscopy (TEM), were stained with methylene blue-azure II.

Tissues for electron microscopical examination were dissected from specimens and fixed in 2.5% glutaraldehyde in 0.2M phosphate buffer (pH 7.4) and 0.14M NaCl for 2 hours at room temperature. After rinsing in 0.2M phosphate buffer and 0.3M NaCl, they were post-fixed using 1% osmium tetroxide in 0.1M phosphate buffer and 0.375M NaCl for one hour at $4^{o}C$. Tissues were rinsed in distilled water and dehydrated in a graded series of ethanol. Specimens for scanning electron microscopy (SEM) were critical point dried from CO_2, sputter coated with gold and examined in a JEOL JSM-35. Specimens for TEM were transferred to propylene oxide before embedding in Epon resin. Ultrathin sections (grey-silver-pale gold interference colour) were obtained on a Reichert ultramicrotome and stained with uranyl acetate and lead citrate (Reynolds, 1963) prior to viewing in a Philips EM-300 transmission electron microscope.

Observations of live animals were made using a Wild M5A dissecting microscope. Removal of the shell and a ventral dissection of the mantle wall revealed the anus and transparent ventral body wall through which the pericardium could be easily seen.

RESULTS

Perianal sinus

The perianal sinus surrounds the rectum (Figure 1) as it passes between the kidneys to the mantle cavity. The sinus is positioned antero-ventrally to the kidneys and the pericardium, and no other coelomic space surrounds or apposes it (Figure 2). The sinus is surrounded by circular and longitudinal musculature, is traversed by an array of muscle fibres or trabeculae, and has additional longitudinal and circular fibres along the inner wall of the sinus enveloping the rectum (Figure 3).

The musculature of the perianal sinus is smooth. Neural processes occur adjacent to muscle cells, although no synapses have been observed (Figure 4). The muscle cells contain thick (29-58 nm diameter) and thin (5.8 nm diameter) myofilaments which are interspersed with α- glycogen granules (17.4 nm). Similar granules are also found concentrated at the periphery of the cell adjacent to the 6-11 nm wide sarcolemma (Figure 5). Thick myofilaments have an axial periodicity of 9-15 nm (Figure 6). Mitochondria are located in clusters within sarcoplasmic bulges adjacent to contractile elements (Figure 5).

Observations of live animals show that the muscular walls of the perianal sinus repeatedly contract, causing an extension of the rectum and closing of the anus, followed by relaxation of the rectum and dilation of the anus, occurring at a rate of approximately 40-60 contractions per minute. Occasional periods of relaxed dilation last from 10 to 30 seconds. These contractions, in addition to propelling blood through the sinus, appear to facilitate the voiding of strings of faecal material from the rectum.

Figure 2. Longitudinal section through the perianal sinus (*pa*), kidney (*n*), and anterior portion of stomach (*s*) and pericardium (*arrowheads*) (*ab*, abdominal sinus; *mc*, mantle cavity; *pc*, pericardial cavity; *r*, rectum). Scale bar = 0.1 mm.

Figure 3. Oblique cross section of the perianal sinus (*pa*), showing traversing muscular trabeculae (*arrowheads*) (*mc*, mantle cavity; *r*, rectum). Scale bar = 40 μm.

Figure 4. Muscle cells of the perianal sinus (*sm*) and the pericardium (*pm*). Note neural process adjacent to perianal sinus musculature (*arrowhead*) (*h*, haemocoel; *pc*, pericardial cavity; *pe*, pericardial epithelial cell). Scale bar = 1 μm.

Figure 5. Cytoplasmic extensions of a pericardial epithelial cell overlying a muscle cell of the perianal sinus (*arrowheads*, dense bodies; *arrow*, attachment plaque; *g*, glycogen granules; *h*, haemocoel; *jsr*, junctional sarcoplasmic reticulum; *m*, mitochondrion; *pc*, pericardial cavity; *sr*, sarcoplasmic reticulum; *th*, thick myofilaments). Scale bar = 0.5 μm.

Figure 6. Thick myofilaments of the smooth perianal sinus muscle cell. Note axial periodicity within the filaments. Scale bar = 0.2μm.

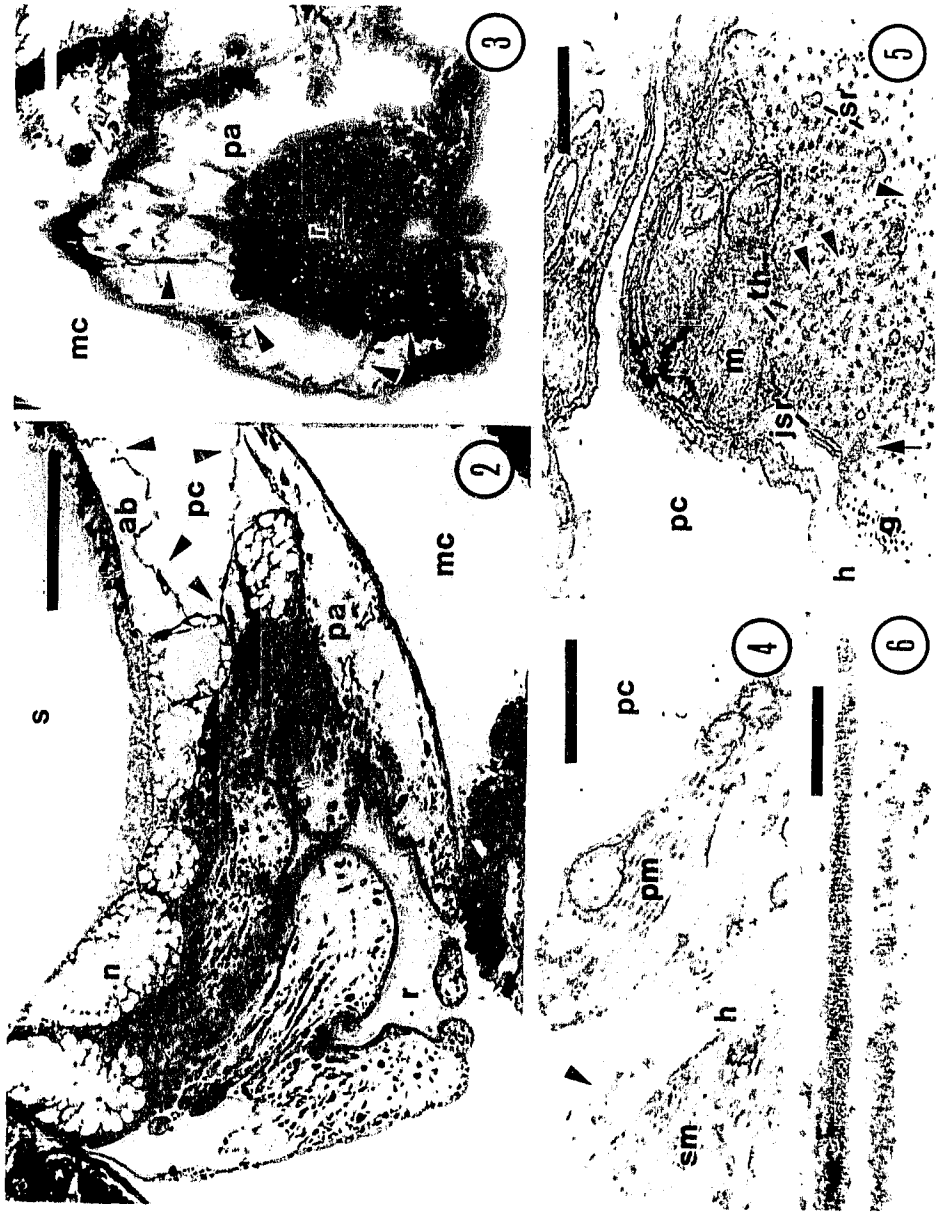
s
n
ab
pc
pa
r
mc
2
mc
pa
3
pc
m
jsr
sr
g
h
5
pc
pm
sm
h
4
6

Pericardium and Dorsal Pericardial Folds

The pericardial coelom lies within the abdominal blood sinus, ventral to the stomach, and extends from the posterior end of the stomach to the kidneys and perianal sinus, to which it adheres anteriorly (Figures 2, 7-9). The ventral pericardial epithelium is always in close contact with the body wall, while irregular infoldings of the dorsal pericardial wall project into the coelomic cavity. There is no myocardium or any type of endothelium within these infoldings (Figures 2, 8, 9); the only musculature adjacent to the pericardium is that of the body wall ventrally and perianal sinus anteriorly (Figure 7, 8). A connection exists between the pericardial coelom and the right kidney (Figure 10), although it was not found in all specimens.

The pericardial wall is composed of three cell types: simple flat epithelium, interspersed with muscle cells, and modified in the region adjacent to the perianal sinus to include podocytes. The arrangement and ultrastructure of epithelial and muscle cells is similar throughout the pericardium (Figure 7). The epithelial cells (Figure 11) typically possess a cell body with a small amount of cytoplasmic material surrounding the nucleus. The cell bodies extend into the pericardial cavity, with the continuous basal lamina lining the haemocoel. Thin cytoplasmic branches extend between cell bodies and contain one or a few isolated mitochondria (Figure 11), in addition to α- (15 nm) and β- (37 nm) glycogen granules (Figure 13). Desmosomes, with an intercellular distance of 9-15 nm, occur frequently where epithelial cell junctions appose the basal lamina (Figure 12) but were not observed in areas where cytoplasmic extensions overlap adjoining muscle cells (Figure 13). Adjoining plasmalemmae are not highly infolded and do not interdigitate (Figure 13).

The pericardial musculature is arranged as trabeculae which run in an entirely transverse direction, and are discontinuous in both anterior-posterior and lateral axes of the

Figure 7. Schematic diagram showing the relative positions of the perianal sinus (*pas*), pericardium (*pc*) and kidneys (*n*) (*ab*, abdominal sinus; *bw*, body wall; *dd*, digestive diverticulum; *ma*, mantle; *mc*, mantle cavity; *pd*, podocytes; *pe*, epithelial cell of the pericardium; *pm*, muscle cell of the pericardium; *r*, rectum; *A-B* indicates cross-sectional view represented in Figure 8).

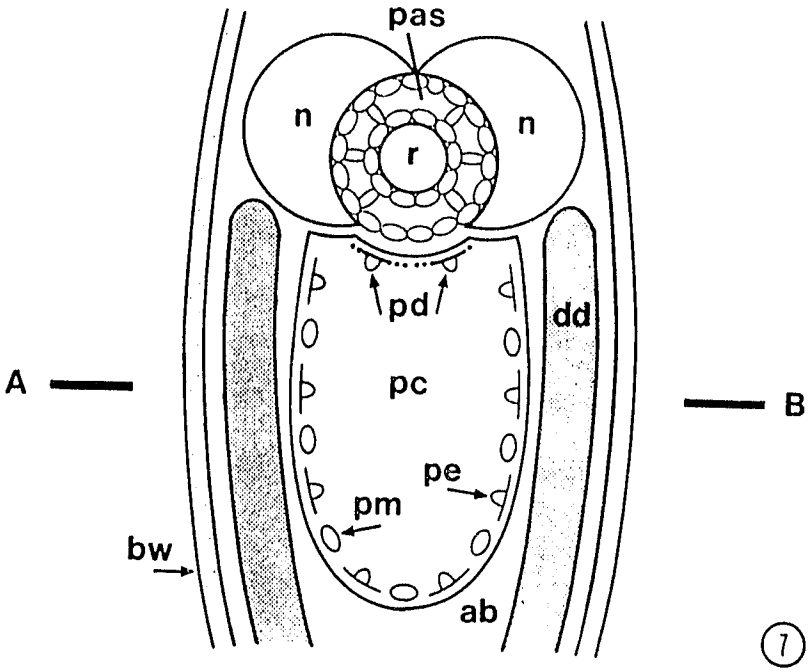

(7)

Figure 8. Schematic diagram showing the relative positions of the stomach (*s*), pericardium (*pc*) and mantle cavity (*mc*) (*ab*, abdominal sinus; *bw*, body wall; *dd*, digestive diverticulum; *ma*, mantle; *pe*, epithelial cell of the pericardium; *pm*, muscle cell of the pericardium; *rm*, retractor muscle; *C-D* indicates frontal section view represented in Figure 6) (see also Figure 18).

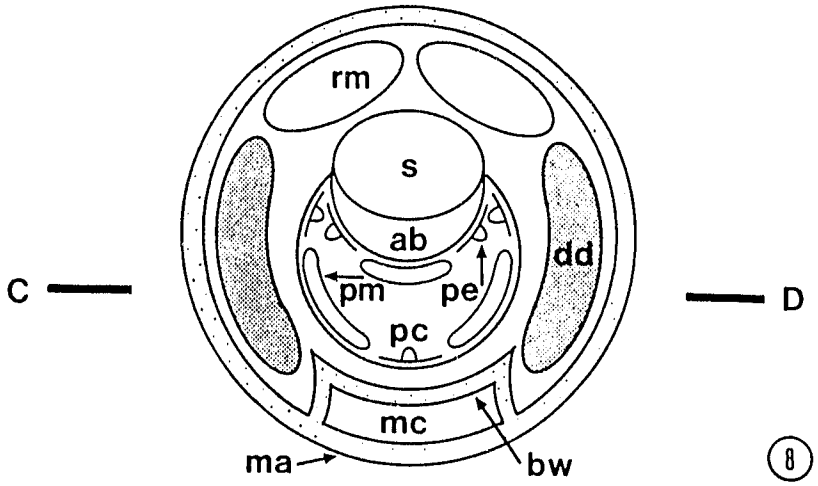

8

Figure 9. Longitudinal section through the pericardium (*pc*), stomach (*s*), perianal sinus (*pa*) and kidney (*n*) (*Arrowheads*, anterior and dorsal pericardial walls; *ab*, abdominal sinus; *dd*, digestive diverticulum; *i*, intestine; *mc*, mantle cavity). Scale bar = 0.15 mm.

Figure 10. Longitudinal section showing connection between the pericardial cavity (*pc*) and the right kidney (*n*) (*dd*, digestive diverticulum; *mc*, mantle cavity; *s*, stomach). Scale bar = 50 μm.

Figure 11. Pericardial epithelial cell (*arrow*, basal lamina; *h*, haemocoel; *m*, mitochondrion; *n*, kidney; *pc*, pericardial cavity). Scale bar = 2.5 μm.

Figure 12. Cytoplasmic extensions of the pericardial epithelium (*arrowhead*, desmosome; *h*, haemocoel; *pc*, pericardial cavity). Scale bar = 0.3 μm.

Figure 13. Epithelial (*pe*) and muscle cells (*pm*) of the pericardium. Note glycogen granules in region of epithelial cell cytoplasmic extension opposing basal lamina (*arrowhead*, basal lamina; *arrow*, myofilaments; *h*, haemocoel; *pc*, pericardial cavity; *sr*, sarcoplasmic reticulum). Scale bar = 0.6 μm.

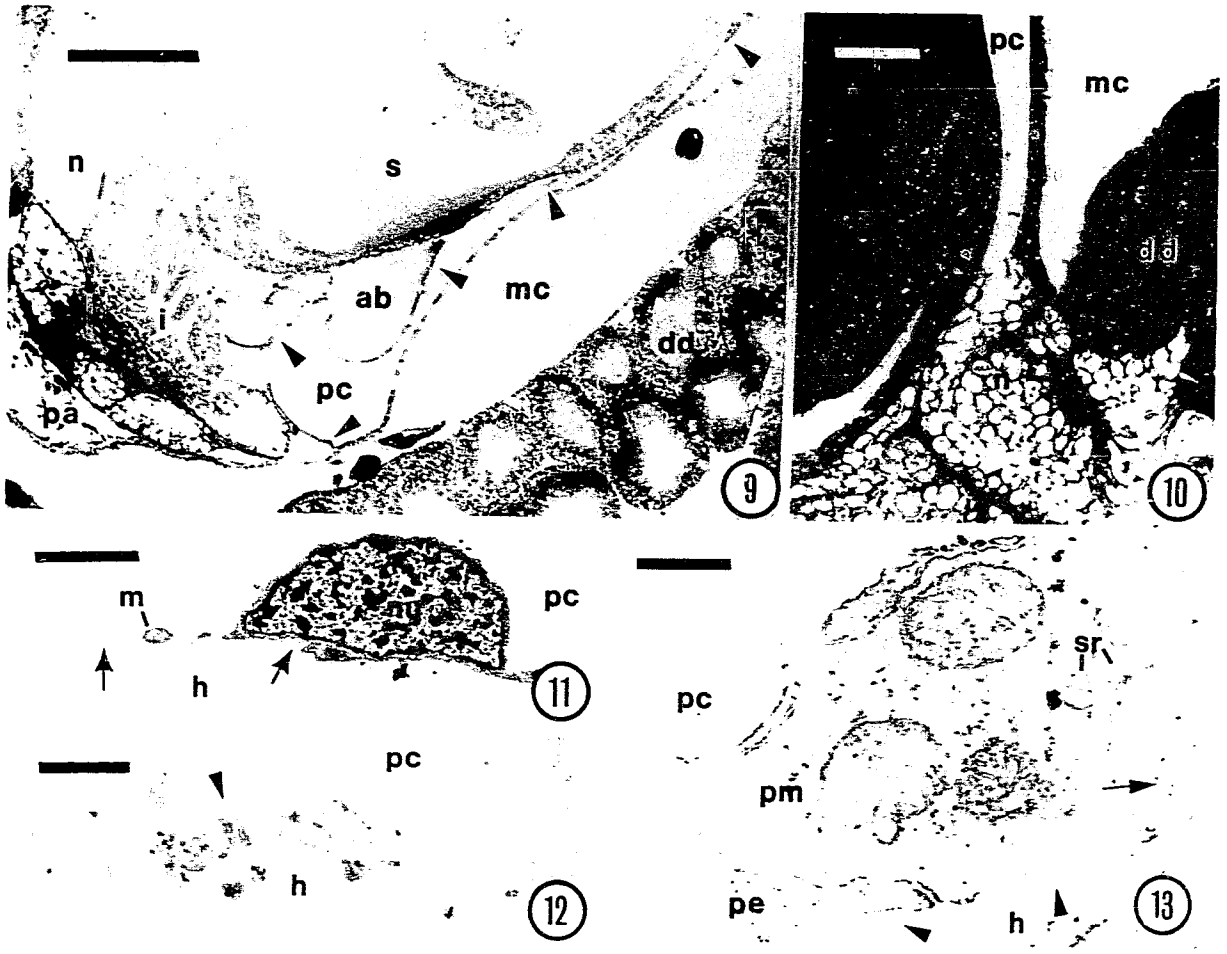
n
s
ab
mc
i
dd
pc
pa
9
pc
mc
dd
10
m
pc
h
11
pc
h
12
sr
pc
pm
pe
h
13

pericardium. The width of the trabeculae varies between 1 and 10 μm (Figures 14, 15). Muscle cells are interspersed between the epithelial cells and typically underlie extensions of the epithelial cytoplasm (Figures 13, 16-19). Adjoining plasmalemmae of the two cell types have an intercellular space of 7-15 nm within which no extracellular material has been observed (Figures 13, 16, 17, 19). Desmosomes occur at cell junctions apposing either the basal lamina or coelomic space, and have an intercellular width of 9-15 nm (Figure 17, 19). Both cell types are separated from the haemocoel by a continuous basal lamina, 18-40 nm thick (Figures 13, 16-19). A thin layer of collagen fibrils, varying in thickness from 0.11-0.53 μm, is often associated with the basal lamina (Figure 16). Neural elements are found adjacent to the muscle cells (Figure 18).

Muscle fibres of the pericardium fixed in a contracted state show near-alignment of dense bodies (0.12-0.14 μm length, 46-58 nm width) into Z-lines, with the intervening thick myofilaments creating A and I lines in a loose sarcomeral structure, approximately 1 μm in length (Figure 20). Occasional attachment plaques were observed anchoring the filaments to the sarcolemma (Figure 20). The muscle cells have a diameter at the nucleus of 3-3.5 μm (Figure 21). Thick and thin myofilaments do not appear to have a regular arrangement with respect to each other, and have diameters of 18-33 nm and 6-7.5 nm respectively (Figures 17, 19). Profiles of rough and smooth sarcoplasmic reticulum are present, as are those of junctional sarcoplasmic reticulum (Figures 17, 19, 20). A small quantity of α- and β-glycogen granules is present within the cytoplasm of the cell periphery (Figure 17). Clusters of mitochondria are positioned between the contractile elements and sarcolemma; sarcolemmal width is 7-15 nm (Figure 22).

The pericardium contracts independently of the perianal sinus in a regular though discontinuous manner; there is neither a gradual peristalsis of the pericardium nor a simultaneous uniform contraction of all muscle fibres. The contractions occur in an

Figure 14. Dorsal pericardial wall, viewed from the pericardial cavity. Anterior is to the top of the photomicrograph. Note lateral orientation of muscle fibres. Scale bar = 0.15 mm.

Figure 15. Dorsal pericardial wall, viewed from the pericardial cavity. Anterior is to the top of the photomicrograph. Note the discontinuity of the pericardial muscle cells (*pm*) along anterior-posterior and lateral axes. Scale bar = 40 μm.

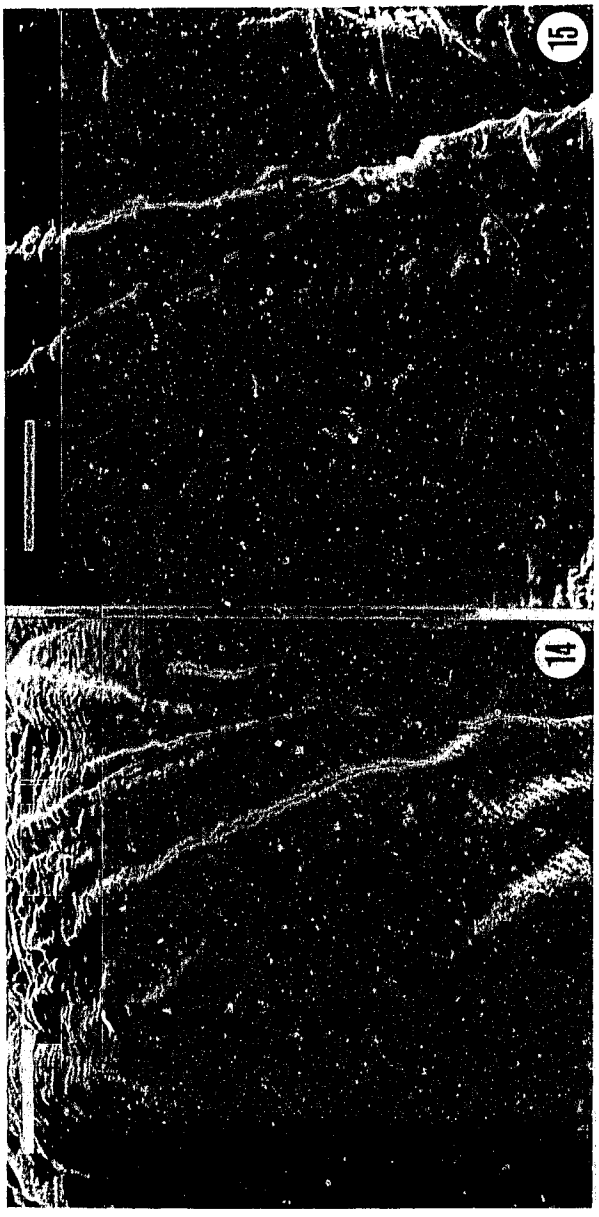
15
14

Figure 16. Epithelial (*pe*) and muscle cells (*pm*) of the pericardium (*arrowhead*, basal lamina; *arrow*, collagen fibres; *h*, haemocoel; *pc*, pericardial cavity; *sc*, subsarcolemmal cisternae). Scale bar = 2 μm.

Figure 17. Junction of epithelial (*pe*) and muscle cells (*pm*) of the pericardium (*arrowheads*, basal lamina; *arrow*, desmosome; *h*, haemocoel; *sr*, sarcoplasmic reticulum; *th*, thick myofilaments). Scale bar = 0.5 μm.

Figure 18. Longitudinal section of dorsal (top) and ventral (bottom) pericardial walls and body wall (*bw*) (*, muscle cells of the pericardium; *h*, haemocoel; *mc*, mantle cavity; *ne*, nerve process; *pc*, pericardial cavity; *sc*, subsarcolemmal cisternae). Scale bar = 10 μm.

Figure 19. Junction of epithelial and muscle cells of the pericardium (*arrowheads*, basal lamina; *arrow* desmosome; *h*, haemocoel; *jsr*, junctional sarcoplasmic reticulum; *ne*, nerve process; *pc*, pericardial cavity; *sr*, sarcoplasmic reticulum; *th*, thick myofilaments). Scale bar = 0.7 μm.

Figure 20. Longitudinal section through pericardial muscle cell. Note loose sarcomeral structure formed by alignment of dense bodies. Scale bar = 0.15 μm.

Figure 21. Oblique cross section through pericardial muscle cell (*arrowhead*, basal lamina; *h*, haemocoel; *nu*, nucleus; *pc*, pericardial cavity). Scale bar = 3μm.

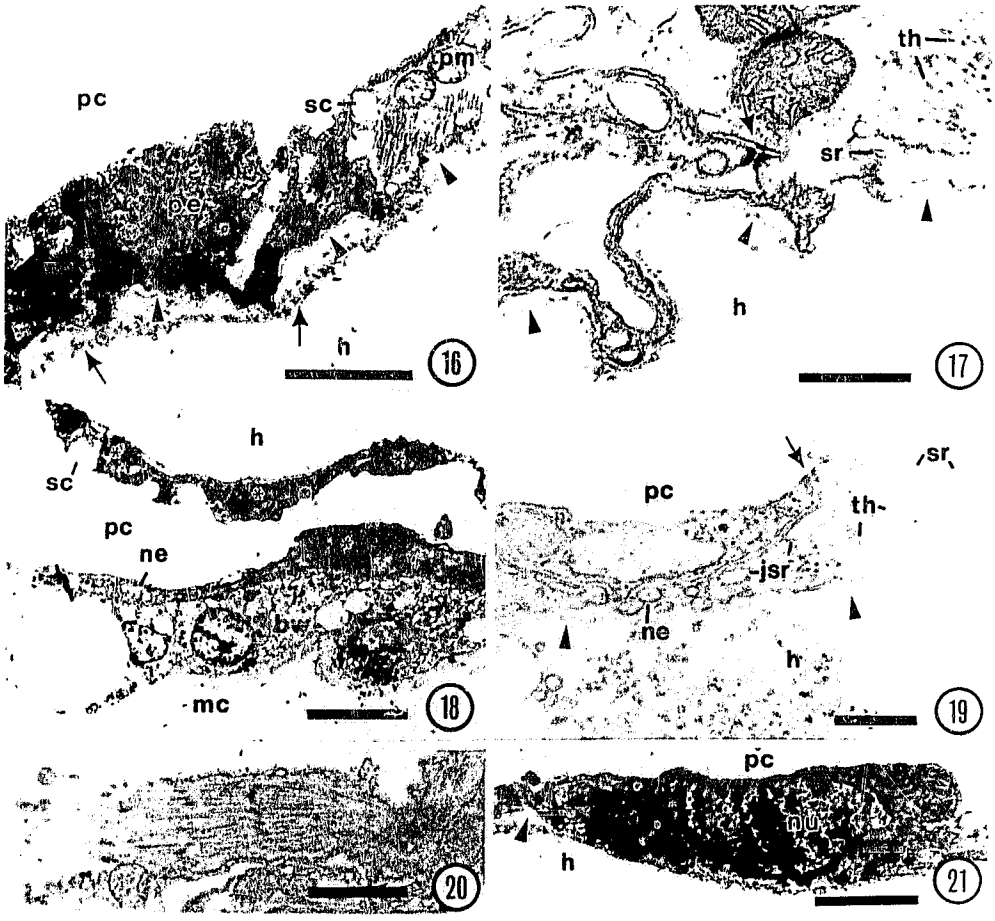
pc
sc
pm
pex
h
16
th
sr
h
17
h
sc
pc
ne
bw
mc
18
sr
pc
th
jsr
ne
h
19
pc
nu
h
21
20

anterior to posterior progression of 2-3 discrete constrictions of the dorsal pericardial wall, the wholly transverse orientation of the muscle fibres producing a single localized transverse constriction which is released as another, posterior to this, is produced. The posterior end of the pericardium appears to lie free within the abdominal sinus and moves in an anterior-posterior direction due to contraction of the muscle fibres. The anterior wall remains in close contact with the kidneys and perianal sinus, as the ventral pericardial wall does with the body wall. Very infrequently a slight contraction of the stomach was observed.

The third cell type of the pericardium is the podocyte, which is characterized by the presence of pedicels and fenestrations in the cytoplasmic branches of the pericardial epithelium (Figures 23-27). The cell type is not widespread and has only been observed in areas apposed by smooth musculature in the region of the perianal sinus i.e., the antero-ventral portion of the pericardium (Figures 7, 24, 25). Fenestrations, 13-32 nm in width, are distributed along cytoplasmic extensions (Figures 23-27), and raised pedicels have also been observed (Figure 26). In some sections, diaphragms in the form of electron opaque strands bridge the fenestrations (Figure 27). In all cases, the fenestrations overlie the basal lamina; there is no evidence of an apposing collagen layer. No microvilli line the luminal surface of these or any cells of the pericardium.

DISCUSSION

Structure of the molluscan heart

The anatomy of the molluscan heart generally consists of a single ventricle and one or two auricles which usually correspond to the number of ctenidia. The whole is enclosed

Figure 22. Junction of pericardial muscle cells (*m*, mitochondrion; *pc*, pericardial cavity; *th*, thick myofilaments). Scale bar = 1 μm.

Figure 23. Podocytes of the pericardium. Note fenestrations in the pericardial epithelium apposed by basal lamina (*arrowheads*) (*nu*, nucleus; *pc*, pericardial cavity). Scale bar = 1 μm.

Figure 24. View of perianal sinus muscle cells (*sm*) and pericardium. Note the highly infolded cytoplasmic extensions of the pericardium overlying the perianal sinus musculature, and the fenestrations apposed by basal lamina (*arrowheads*) (*h*, haemocoel; *pc*, pericardial cavity). Scale bar = 1 μm.

Figure 25. Muscle cell of perianal sinus (*sm*) and fenestrations (*arrowheads*) in the overlying pericardium (*g*, glycogen granules; *th*, thick myofilaments). Scale bar = 0.7 μm.

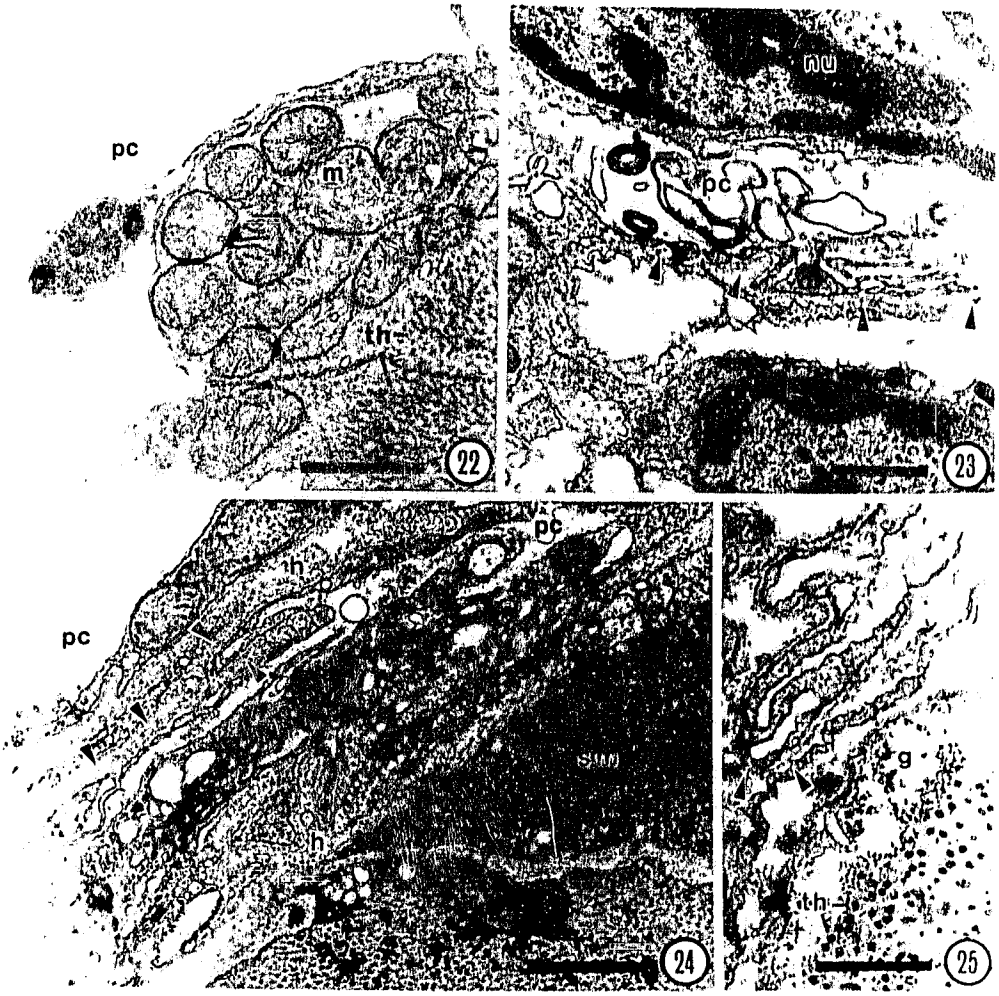
pc
m
th
22
nu
pc
23
pc
h
pc
h
SMM
24
g
th
25

Figure 26. Raised pedicels (*arrows*) of podocytes of the pericardium (*h*, haemocoel; *pc*, pericardial cavity). Scale bar = 0.3 μm.

Figure 27. Slit diaphragms of podocytes of the pericardium. Note fenestrations in epithelium apposed by basal lamina (*arrowheads*) and bridged by diaphragms (*arrows*) (*h*, haemocoel; *pc*, pericardial cavity). Scale bar = 0.3 μm.

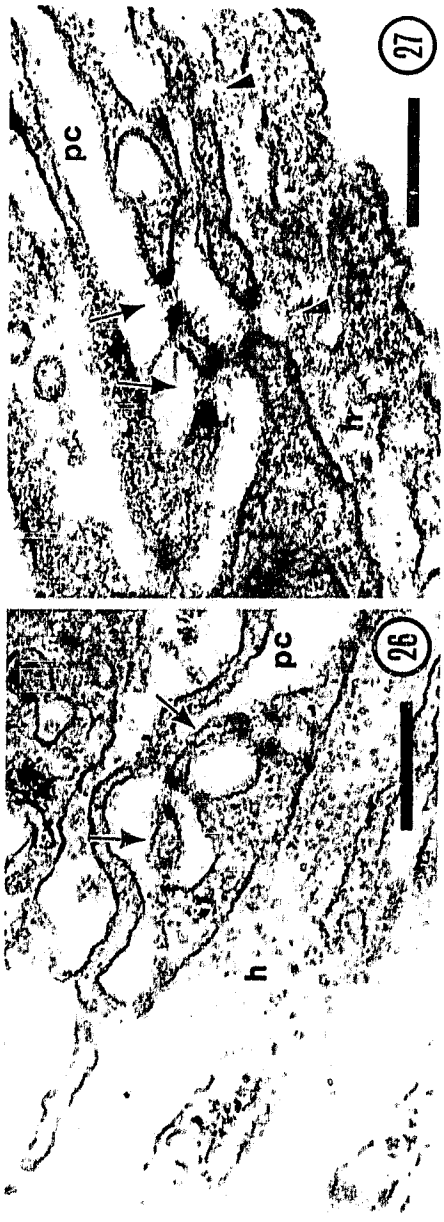
pc
h
27
pc
h
26

within a pericardium, and the ventricle in the Bivalvia and some Gastropoda is traversed by the rectum (Jones, 1983). At the height of molluscan heart organization, the Cephalopoda possess a complex systemic heart associated with a closed circulatory system (Wells, 1983); at the other extreme, the Scaphopoda have been described as having a rudimentary heart, relying on body musculature for circulation through a series of sinuses (Hill & Welsh, 1966). The molluscan heart lies freely within the pericardium, although the pericardial cavity does not extend dorsally over the ventricle in the Neomeniomorpha (Salvini-Plawen, 1985) and the bivalve *Pteria* (White, 1942). In some bivalve species the dorsal wall of the ventricle remains attached to the pericardium by connective tissue (Narain, 1976). The presence of the pericardium is critical to circulatory function; the pressure of the pericardial fluid is normally less than that of the blood in the heart, and cardiac refilling is maintained by a volume-compensating mechanism as originally proposed by Ramsay (1952) and Krijgsman & Divaris (1955), and reviewed by Jones (1983). The pericardium is drained by one or two renopericardial canals, which connect the lumina of the pericardium with those of the kidneys (Martin, 1983).

At the cellular level, the molluscan heart consists of an epicardium, which rests on a basal lamina, and an inner loose myocardium; an endothelium is lacking (Narain, 1976; Økland, 1980; Jones, 1983) except in cephalopods, where it is incomplete (Jensen & Tjønneland, 1977). While in some cases the epicardial cells possess microvilli and may also have a secretory role (Kling & Schipp, 1987), the ventricular epicardium generally consists of a continuous, simple epithelium. Podocytes are usually concentrated within the auricular epicardium, and are characterized by the presence of numerous thin cytoplasmic extensions, termed pedicels, which are aligned in a parallel array over the continuous basal lamina between the haemocoel and coelomic spaces (Andrews, 1976; Pirie & George, 1979; Økland, 1980). The gaps between the pedicels create fenestrations in the epithelium

or ultrafiltration slits; the basal lamina separates the haemocoel from the pericardial coelom and acts as the functional filter (Andrews, 1981; Morse, 1987). In many bivalves, gastropods and cephalopods, the ultrafiltration slits are bridged by slit diaphragms (Boer & Sminia, 1976; Andrews, 1979; Schipp & Hevert, 1981; Meyhöfer et al., 1985), although these have not been found in the podocytes of chitons (Økland, 1980). Portions of the auricular epicardium or pericardial epithelium are elaborated in many species, particularly in bivalves, to form pericardial glands (White, 1942), within which extensive areas of podocytes have been found (Meyhöfer et al., 1985). A similiar development of the haemocoel-pericardial interface is seen in the branchial heart appendages of coleoids and the pericardial appendages of nautiloid cephalopods (Fiedler & Schipp, 1987). The molluscan pericardium consists primarily of simple epithelial cells, although there have been few detailed ultrastructural studies. The polyplacophoran pericardial epithelium is continuous with, while differing from, the ventricular and auricular epicardium (Økland, 1980); it also possesses muscle cells and is pulsatile (Greenberg, 1962; Økland, 1981).

Interpretations of scaphopod circulatory structures to date

Two structures have been proposed as representing the scaphopod heart: (i) the perianal sinus, which has been described as having morphological similarities to (Lacaze-Duthiers, 1857) and homology with (Fol, 1889) the bivalve ventricle; and (ii) the dorsal infoldings of the pericardium ventral to the stomach, described by Plate (1891, 1892), Boissevain (1904), and Distaso (1905). Lacaze-Duthiers (1857) did not discuss the relationship between the perianal sinus and molluscan heart in any detail. Fol (1889), however, based their homology on structural similarities, and described the position of the sinus in relation to the rectum, the musculature and rhythmic contractions of the sinus, and

an endothelium, views which Plate (1892) and Boissevain (1904) later refuted. Lacaze-Duthiers (1857) placed the major responsibility for movement of the blood with the large pedal sinus, while Fol (1889) agreed that the perianal sinus makes little contribution to circulation.

The studies by Plate (1891, 1892), confirmed by Boissevain (1904) and Distaso (1905), described a contractile vessel ventral to the stomach surrounded by the pericardial coelom. Plate (1892) stated that the heart is extraordinarily simple, with no chambers or vessels, and lacks a strong development of musculature. He found that the pericardial and heart walls did not differ histologically, and were composed of epithelial cells with very thin, parallel and regularly arranged fibres. While Plate (1892) suggested that these may be muscle fibres, he concluded that this structure could not act as a centre of propulsion for the circulatory system.

Circulatory structures in Dentalium rectius

In *Dentalium rectius*, there is no evidence of the ultrastructural features associated with the typical molluscan heart (i.e., a myocardium with an associated epicardium) in a position ventral to the stomach and enclosed by the pericardium as described by Plate (1891, 1892), Boissevain (1904) and Distaso (1905) for other species of *Dentalium*. Without the benefit of ultrastructural study, it is likely that these early investigators considered the contractile dorsal pericardial wall as a ventricular epicardium. The lack of a myocardium or any ultrastructural differentiation of this portion of the pericardial epithelium discounts this interpretation, and no evidence supporting homology with the molluscan ventricle exists. While the scaphopod stomach is described as possessing a muscular tunic (Salvini-Plawen, 1988), the musculature in *D. rectius* is discontinuous and

closely applied to the stomach wall and as such is not associated with the pericardium and does not enclose a portion of the haemocoel.

The homology of the pericardial coelom described by Lacaze-Duthiers (1857), Plate (1891, 1892), Boissevain (1904) and Distaso (1905) with that of other molluscs is based solely on its general anatomy; i.e., a closed sac composed of squamous epithelium within the haemocoel. Ultrastructural features of the pericardial epithelium in *D. rectius* support this homology; the presence of long cytoplasmic branches, desmosomes and few other organelles suggest a simple delimiting epithelium, similar to that found in other molluscan peri- and epicardia. Furthermore, an excretory role inferred from the presence of podocytes and a renopericardial connection also supports this homology. On this basis, the term *pericardium* should be retained in describing this structure in scaphopods.

The arrangement of musculature in the *D. rectius* pericardium suggests transverse contractions of the dorsal pericardial wall, which are supported by the observations of live animals. The contractile pericardia in the Polyplacophora have been suggested by Økland (1981) to function in the circulation of pericardial fluid as part of the excretory system, with little effect on the contraction mechanisms of the heart. In *Tonicella*, the epithelial and muscle cells are separated by collagen and basal lamina, which is, however, continuous with the basal lamina lining the epithelial cells (Økland, 1981). In comparison, no extracellular material exists between cell types in the pericardium of *D. rectius*, and the basal lamina is limited to an unbranching layer between the pericardial elements and haemocoel. Contractions of the dorsal pericardial wall in *D. rectius* undoubtedly contribute to the circulation of blood through the relatively large abdominal sinus. These contractions do not lead directly to ultrafiltration of blood through the dorsal pericardial wall due to the absence of podocytes in this area of the pericardium. However, it is possible that local increases in blood pressure may be transferred anteriorly to the perianal sinus and may

ultimately facilitate ultrafiltration via the podocytes lining the perianal sinus. The irregular invaginations of the dorsal pericardial wall of *D. rectius* seen in section, and considered by Plate (1891, 1892), Boissevain (1904) and Distaso (1905) in other *Dentalium* species to be the heart, are due to the state of contraction of the dorsal pericardial wall at fixation and do not represent a permanently enclosed contractile vessel. The ventral pericardial wall was always observed in close adherence to the body wall in both fixed and live material.

The presence of podocytes is a development of the pericardial epithelium that is commonly observed and interpreted in other molluscan classes as the site of ultrafiltration of blood and production of primary urine. While ultrastructural features such as apposition of basal lamina, fenestration width and the presence of slit diaphragms in the podocytes of *D. rectius* are consistent with such a function, there is no evidence of an extensive array of pedicels and ultrafiltration slits as seen in representatives of some other molluscan classes (Andrews, 1979; Meyhöfer et al., 1985). Thus, the area available for ultrafiltration appears to be quite limited in *D. rectius*.

The renopericardial connection with the right kidney is small (20 μm in diameter), and was only noted in incidental thin (1 μm) sections. A left renopericardial canal in *Dentalium* was described by Distaso (1905), although his interpretation of the dorso-ventral orientation of the animal is opposite to that generally accepted by other investigators of the Scaphopoda. Therefore, considering the mantle cavity as ventral and the larger aperture as anterior, Distaso (1905) had, in fact, also described a connection between the pericardium and right kidney.

The ultrastructure of the perianal sinus in *D. rectius* does not differ significantly from that of smooth molluscan cardiac muscle. Thick myofilaments have an axial periodicity resembling paramyosin, while myofibre size, the arrangement of glycogen and

mitochondria, and the development of the sarcoplasmic reticulum is similar to that found in the cardiac musculature of the bivalves *Venus* (Kelly & Hayes, 1969), *Elliptio* (Rutherford, 1972) and *Geukensia* (Watts et al., 1981), and of the polyplacophorans *Lepidopleurus* and *Tonicella* (Økland, 1980). This is in contrast with the obliquely striated heart musculature of gastropods and cephalopods, as reviewed by Kling & Schipp (1987). The position of the sinus in *D. rectius* in relation to the rectum parallels that found in the bivalve ventricle. Also, the presence of traversing muscular trabeculae, which produce the regular contractions of the sinus (this study; Fol, 1889; Plate, 1892; Fischer-Piette & Franc, 1968) is also found in the ventricles of many bivalves and gastropods (Narain, 1976; Økland, 1982; Jones, 1983).

Whether the perianal sinus, pericardium and kidneys in *D. rectius* have an associated ontogenesis reflecting the developmental pattern of the heart, pericardium and kidneys from a common anlagen as seen in other classes of molluscs (Raven, 1966; Moor, 1983), with a subsequent movement of the pericardium from a position surrounding the ventricle to one more posterior to it, awaits further information on scaphopod organogenesis. If an homology between these organs exists, the lack of aortae, auricles or valves of any description, and the limited apposition of the pericardium, indicate a much reduced heart compared to that found in other molluscan classes. This reduction could have developed as a consequence of altered circulatory requirements, due in large part to the loss of ctenidia from the uniquely modified scaphopod mantle cavity.

Unidirectional flow of blood through the perianal sinus is not maintained (personal observations). While contractions may produce local pressures capable of driving limited ultrafiltration, it is unlikely to be capable of overcoming peripheral resistance of the circulatory system, or of even contributing significantly to circulation of the blood. As a consequence of the contractions of the foot and body musculature, however, the perianal

sinus may serve a role in facilitating equilibration of pressure gradients between the pedal and abdominal blood sinuses.

In conclusion, there is no evidence for a heart within the pericardium of *Dentalium* as interpreted by Plate (1891, 1892), Boissevain (1904), and Distaso (1905). Ultrastructural features in *Dentalium rectius* suggest that there may be an homology of the perianal sinus and pericardium with the heart and pericardium of other molluscs. Studies of scaphopod organogenesis are necessary to confirm this. The contractility of the dorsal pericardial wall and the perianal sinus may facilitate ultrafiltration of the blood via podocytes, which are limited to the anterior portion of the pericardium and overlie the perianal sinus. Further study into the blood pressures created by these and other contractile structures of the *Dentalium* haemocoel is necessary to further delineate their respective contributions to circulation.

LITERATURE CITED

Andrews, E. B. (1976). The fine structure of the heart of some prosobranch and pulmonate gastropods in relation to filtration. Journal of Molluscan Studies, 42, 199-216.

Andrews, E. B. (1979). Fine structure in relation to function in the excretory system of two species of *Viviparus*. Journal of Molluscan Studies, 45, 186-206.

Andrews, E. B. (1981). Osmoregulation and excretion in prosobranch gastropods, part 2: structure in relation to function. Journal of Molluscan Studies, 47, 248-289.

Andrews, E. B. (1988). Excretory systems of Molluscs. In Trueman, E. R. & Clarke, M. R. (Eds.), The Mollusca, v. 11, Form and Function (pp. 381-448). Academic Press, New York.

Boer, H. H. & Sminia, T. (1976). Sieve structure of slit diaphragms of podocytes and pore cells of gastropod molluscs. Cell and Tissue Research, 170, 221-229.

Boissevain, M. (1904). Beiträge zur Anatomie und Histologie von Dentalium. Jenaische Zeitschrift fur Naturwissenschaft, 38, 553-572, pls. 17-19.

Chapman, D. M. (1977). Eriochrome cyanin as a substitute for haematoxylin and eosin. Canadian Journal of Medical Technology, 39, 65-66.

Clark, W. (1849). On the animal of *Dentalium Tarentinum*. The Annals and Magazine of Natural History (Series 2), 4, 321-378.

Cuénot, L. (1899). L'excrétion chez les Mollusques. Archives de Biologie, 16, 49-96.

Deshayes, M. (1825). Anatomie et monographie du genre Dentale. Memoires de la Société d'histoire naturelle de Paris, 2, 321-378, pls. 1-4.

Distaso, A. (1905). Sull' Anatomia degli scafopodi. Zoologischer Anzeiger, 29, 271-278.

Fiedler, A. & Schipp, R. (1987). The role of the branchial heart complex in circulation of coleoid cephalopods. Experientia, 43, 544-553.

Fischer-Piette, E. & Franc, A. (1968). Classe des scaphopodes, Scaphopoda (Bronn 1862). In Grassé, P.-P. (Ed.) Traité de zoologie, anatomie, systematique, biologie, 5(3), Mollusques, Gasteropodes et Scaphopodes (pp. 987-1017). Masson et Cie, Paris.

Fol, H. (1885). Sur l'anatomie microscopique du Dentale. Comptes Rendu Hebdomadaires des Seances de l'Academie des Sciences, Série D, Sciences naturelles, 1885, 1352-1355.

Fol, H. (1889). Sur l'anatomie microscopique du Dentale. Archives de Zoologie Experimentale et Génerale, Deuxième Série, 7, 91-148, pls. 5-8.

Greenberg, M. J. (1962). Physiology of the heart of *Cryptochiton stelleri* Middendorff, 1847. American Zoologist, 2, 526.

Harrison, F. M. (1962). Some excretory processes in the abalone, *Haliotis rufescens*. Journal of Experimental Biology, 39, 179-192.

Harrison, F. M. & Martin, A. W. (1965). Excretion in the cephalopod *Octopus dofleini.* Journal of Experimental Biology, 42, 71-98.

Hevert, F. (1984). Urine formation in the Lamellibranchs: evidence for ultrafiltration and quantitative description. Journal of Experimental Biology, 111, 1-12.

Hill, R. B. & Welsh, J. H. (1966). Heart, circulation and blood cells. In Wilbur K. M. & Yonge C. M. (Eds.) Physiology of Mollusca, 2 (pp. 126-174). Academic Press, New York.

Jensen, H. & Tjønneland, A. (1977). Ultrastructure of the heart muscle cells of the cuttlefish *Rossia macrosoma.* Cell and Tissue Research, 185, 147-158.

Jones, H. D. (1983). The circulatory system of gastropods and bivalves. In Salueddin, A. S. M. & Wilbur, K. M. (Eds.) The Mollusca, v. 5, Physiology, Part 2 (pp. 189-238). Academic Press, New York.

Jones, H. D. & Peggs, D. (1983). Hydrostatic and osmotic pressures in the heart and pericardium of *Mya arenaria* and *Anodonta cygnea.* Comparative Biochemistry and Physiology, 76A(2), 381-385.

Kelly, R. E. & Hayes, R. L. (1969). The ultrastructure of smooth cardiac muscle in the clam, *Venus mercenaria.* Journal of Morphology, 127, 163-176.

Kling, G. & Schipp, R. (1987). Comparative ultrastructural and cytochemical analysis of the cephalopod systemic heart and its innervation. Experientia, 43, 502-511.

Kowalevsky, A. (1889). Ein Beitrag zur Kenntnis der Exkretionsorgane. Biologisches Zentralblatt, 9(3), 65-76.

Krijgsman, B. J. & Divaris, G. A. (1955). Contractile and pacemaker mechanism of the heart of molluscs. Biological Reviews, 30, 1-39.

Lacaze-Duthiers, H. de (1857). Histoire de l'organisation et du développement du Dentale. Annales des Sciences Naturelles, Quatrième Série, 7, 5-51, 171-255, pls. 2-9.

Little, C. (1965). The formation of urine by the prosobranch gastropod mollusc *Viviparus viviparus* Linn. Journal of Experimental Biology, 43, 39-54.

Martin, A. W. (1983). Excretion. In Saleuddin, A. S. M. & Wilbur, K. M. (Eds.) The Mollusca, 5, Physiology, Part 2 (pp. 353-405). Academic Press, New York.

Martin, A. W. & Aldrich, F. A. (1970). Comparison of hearts and branchial heart appendages in some cephalopods. Canadian Journal of Zoology, 48, 751-756.

Meyhöfer, E., Morse, M. P. & Robinson,W. E. (1985). Podocytes in bivalve molluscs: morphological evidence for ultrafiltration. Journal of Comparative Physiology B, 156, 151-161.

Moor, B. (1983). Organogenesis. In Verdonk, N. H., van den Biggelaar, J. A. M. & Tompa, A. S. (Eds.) The Mollusca, v. 3, Development (pp.123-177). Academic Press, New York.

Morse, M. P. (1987). Comparative functional morphology of the bivalve excretory system. American Zoologist, 27(3), 737-746.

Narain, A. S. (1976). A review of the structrue of the heart of molluscs, particularly bivalves, in relation to cardiac function. Journal of Molluscan Studies, 42, 46-62.

Økland, S. (1980). The heart ultrastructure of *Lepidopleurus asellus* (Spengler) and *Tonicella marmorea* (Fabricus) (Mollusca: Polyplacophora). Zoomorphology, 96, 1-19.

Økland, S. (1981). Ultrastructure of the pericardium in chitons (Mollusca: Polyplacophora), in relation to filtration and contraction mechanisms. Zoomorphology, 97, 193-203.

Økland, S. (1982). The ultrastructure of the heart complex in *Patella vulgata* L. (Archaeogastropoda, Prosobranchia). Journal of Molluscan Studies, 48, 331-341.

Pirie, B. J. S. & George, S. G. (1979). Ultrastructure of the heart and excretory system of *Mytilus edulis* (L.). Journal of the Marine Biological Association of the United Kingdom, 59, 819-829.

Plate, L. (1888). Bemerkungen zur Organisation der Dentalien. Zoologischer Anzeiger, 11, 509-515.

Plate, L. H. (1891). Über das Herz der Dentalien. Zoologischer Anzeiger, 14, 78-80.

Plate, L. H. (1892). Ueber den Bau und die Verwandtschaftsbeziehungen der Solenoconchen. Zoologische Jahrbucher Jena Abteilung für Anatomie, 5, 301-386, pls. 23-26.

Potts, W. T. W. (1967). Excretion in the Molluscs. Biological Reviews, 42, 1-41.

Ramsay, J. A. (1952). A physiological approach to the lower animals. Cambridge University Press, London. 148pp.

Raven, C. P. (1966). Morphogenesis: the analysis of molluscan development. Pergamon Press, Oxford. 365 pp.

Reynolds, E. S. (1963). The use of lead citrate at high pH as an electron opaque stain in electron microscopy. Journal of Cell Biology, 17, 208-212.

Rutherford, J. G. (1972). The structure of the ventricle of *Elliptio complanatus*, a freshwater lamellibranch. Journal of Morphology, 136, 421-432.

Salvini-Plawen, L. v. (1985). Early evolution and the primitive groups. In Trueman, E. R. & Clarke, M. R. (Eds.) The Mollusca, v. 10, Evolution (pp. 59-150). Academic Press, New York.

Salvini-Plawen, L. v. (1988). The structure and function of molluscan digestive systems. In Trueman, E. R. & Clarke, M. R. (Eds.) The Mollusca, v. 11, Form and Function (pp. 301-379). Academic Press, New York.

Schipp, R. & Hevert, F. (1981). Ultrafiltration in the branchial heart appendage of dibranchiate cephalopods: a comparative ultrastuctural and physiological study. Journal of Experimental Biology, 92, 23-35.

Strohl, J. (1924). Die Exkretion (Mollusken). In Winterstein, H. (Ed.) Handbuch der vergleichenden Physiologie, 2(2) (pp. 443-607). Fischer, Jena.

Watts, J. A., Koch, R. A., Greenberg, M. J. & Pierce, S. K. (1981). Ultrastructure of the heart of the marine mussel, *Geukensia demissa*. Journal of Morphology, 170, 301-319.

Wells, M. J. (1983). Circulation in cephalopods. In Saleuddin, A. S. M. & Wilbur, K. M. (Eds.) The Mollusca, v. 5, Physiology, part 2 (pp. 239-290). Academic Press, New York.

White, K. M. (1942). The pericardial cavity and the pericardial gland of the Lamellibranchia. Proceedings of the Malacological Society of London, 25, 37-88.

Witmer, A. and Martin, A. W. (1973). The fine structure of the branchial heart appendage of the cephalopod *Octopus dofleini martini*. Zeitschrift für Zellforschung und Mikroskopische Anatomie, 136, 545-568.

CHAPTER 3

FINE STRUCTURE OF THE KIDNEY AND CHARACTERIZATION OF SECRETORY PRODUCTS IN *DENTALIUM RECTIUS* (MOLLUSCA: SCAPHOPODA)

ABSTRACT

The ultrastructure of the scaphopod kidney and secretory product composition is described for the first time, in *Dentalium rectius*. The kidney epithelium consists of two primarily secretory cell types. The first exhibits extensive vacuolation, and scattered granules are formed within the vacuolar space by a process of surface accretion; the incorporation of glycogen particles in this process is associated with very fine, electron opaque threads which radiate from the granules. The second cell type possesses granules enclosed individually within secretory vesicles; intermediate stages in their growth are characterized by needle-like crystals on the granule surface. The secretory vesicles in some cases coalesce to form a large central vacuole filled with granules. This cell type possesses an apical membrane with sparse microvilli, which may indicate a secondary reabsorptive capacity. Granules in both cell types show a concentric ring ultrastructure, and are composed primarily of calcium phosphate with a small amount of zinc; there is also an organic component of protein, mucopolysaccharide and a large amount of glycogen. Ultrastructural and histochemical observations indicate a lysosomal origin for the granules, although granules of the second cell type develop intracellularly to a greater extent than those of the first. All granules are extruded into the kidney lumen by a process of merocrine secretion prior to release into the mantle cavity via an externally ciliated, muscular excretory pore.

INTRODUCTION

The molluscan excretory system functions by an interaction of the haemocoel, pericardium and coelomoduct kidneys, with our present understanding based to a great extent on the larger classes. Ultrafiltration of the blood, via podocytes in the epicardial or pericardial epithelium, produces primary urine which is received by the pericardial cavity (Andrews, 1988) and passes to the lumen of one or both kidneys by a renopericardial canal (for review, see Martin, 1983). Modification of the urine can take place by selective reabsorption of water, glucose and ions by various regions of the pericardial-kidney complex (Little, 1965, 1979), and by secretion of nitrogenous or other wastes by the kidney epithelial cells or nephrocytes (Potts, 1967; Andrews, 1981). Metal-containing granules or concretions, produced by lysosomal maturation and calcium phosphate biomineralisation (George et al., 1980; George et al., 1982; Sullivan et al., 1988), have been noted in the kidneys of many molluscan species (for review, see George, 1983). Such granules form part of a detoxification mechanism (Simkiss and Mason, 1983; Mason et al., 1984), and they are secreted into the kidney lumen to form a partially particulate urine (Pirie & George, 1979; George and Pirie, 1980) or are accumulated until cell death (Andrews, 1981).

The excretory system of the Scaphopoda is poorly known. Of the two subtaxa of scaphopods, the Dentaliida and Gadilida, most studies to date deal with the dentaliid *Dentalium*, whereas present knowledge of the gadilid kidney is limited to Odhner's (1931) description of *Cadulus dalli* var. *antarcticus* Odhner, 1931. The scaphopod heart is reduced, although podocytes are found within the pericardial epithelium overlying the perianal sinus musculature of *D. rectius* Carpenter, 1864 (Chapter 1; Reynolds, 1990). A

right renopericardial connection was described in *Dentalium* spp. by Distaso (1905) and is also present in *D. rectius* (see Reynolds, 1990). The paired kidneys lie in the mid ventrolateral region of the scaphopod body, one on either side of the rectum; in *Dentalium*, each kidney consists of a sac with pleated walls of a simple glandular epithelium (Fol, 1885). No confluence between the kidneys was found by Lacaze-Duthiers (1857), Plate (1892) and Boissevain (1904), although such a feature was described in *Dentalium* by Fol (1885, 1889). Odhner (1931) also reported no connection between the kidneys in *Cadulus*. The secretory function of the kidneys in *Dentalium* was demonstrated by Kowalevsky (1889) using indigo carmine injected into the pedal sinus. An excretory pore, rather than a canal, connects the kidney lumen with the mantle cavity. It is surrounded by strong musculature in *Cadulus* (see Odhner, 1931), and Lacaze-Duthiers (1857) describes a distinct sphincter in *Dentalium*. The right kidney serves as a conduit for the gametes in both *Cadulus* (see Odhner, 1931) and *Dentalium* (see Lacaze-Duthiers, 1857; Pelseneer, 1899; Boissevain, 1904).

The present study of the excretory system in *Dentalium rectius* describes the fine structure of the scaphopod kidney epithelium, with particular reference to the processes of reabsorption and secretion. Histochemical and elemental analyses were performed to characterize the secretory products, and to determine the extent of metal accumulation in the kidney. This account presents the first ultrastructural data on the *Dentalium* kidney, providing a broader morphological basis for consideration of the Scaphopoda in comparative studies of molluscan excretion.

MATERIALS AND METHODS

Specimens of *Dentalium rectius* were dredged from mud sediments approximately 60 m deep in Satellite Channel, near Victoria, British Columbia, Canada. For light microscopy, tissues were fixed in 10% seawater-buffered formalin, dehydrated in a graded series of ethanol and embedded in paraffin; serial 6 µm sections were stained with eriochrome cyanin (Chapman, 1977). Additionally, serial 1 µm sections of resin embedded material, prepared as described in Chapter 2 for transmission electron microscopy (TEM), were stained with methylene blue-azure II. Histochemical analysis of kidney tissue consisted of the tests listed in Table 1.

Tissues for electron microscopy were fixed for 2 hours at room temperature in 2.5% glutaraldehyde, buffered by 0.2M phosphate (pH 7.4) and 0.14M NaCl. After rinsing in 0.2M phosphate buffer and 0.3M NaCl, post-fixation using 1% osmium tetroxide in 0.1M phosphate buffer and 0.375M NaCl was carried out for one hour at $4^{o}C$. Tissues were rinsed in distilled water and dehydrated in a graded ethanol series. Specimens for scanning electron microscopy (SEM) were critical point dried in CO_2, sputter coated with gold and examined in a JEOL JSM-35. Specimens for TEM were transferred to propylene oxide prior to embedding in epon resin. Ultrathin sections (grey-silver-pale gold interference colour) were obtained on a Reichert ultramicrotome, stained with aqueous uranyl acetate and lead citrate and viewed in a Philips EM-300 transmission electron microscope.

For elemental analysis, tissues were fixed in 2.5% phosphate-buffered glutaraldehyde saturated with ammonium sulphide, dehydrated and embedded in resin as described above. Sulphide-saturated fixative reduces redistribution of metals such as copper and zinc from tissues during processing by precipitating them as sulphides, thus

preserving them for subsequent elemental analysis (George et al., 1978; Thomson et al., 1985). Thin sections (blue interference colour) were mounted on copper, nickel, or aluminium grids and examined unstained in a JEOL JEM-1200 EX scanning transmission electron microscope (STEM) in the TEM mode. Energy dispersive X-ray (EDX) microanalysis was carried out using a Tracor X-ray spectrometer with a Tracor Northern 5500 multichannel analyzer and display system. Analyses were performed at 80 kV accelerating voltage, 2 μm beam diameter, 10 μA beam current, 27.5^{o} tilt, and x4000 magnification for a 30 second acquisition period.

RESULTS

General morphology

The kidneys in *Dentalium rectius* consist of two separate sacs, situated ventrolaterally in the mid region of the animal. They are bounded dorsally by the intestine and anteriorly by the oesophagus; the distal part of the rectum passes between them (Figure 28), opening ventrally to the mantle cavity. The pericardium closely apposes the posterior ventral portion of both kidneys. The walls of the kidneys are infolded or pleated, giving the appearance, in section, of many convoluted tubules. They are composed of a single layer of glandular epithelium, the majority of which is highly vacuolated (Figure 28). The kidneys open to the mantle cavity via simple pores on either side of the anus. The pores are reflections of the glandular epithelium and, although the musculature of the body wall is well developed and extends to the opening, there does not appear to be a specialized sphincter muscle (Figure 29). The excretory pore (70 μm in diameter) is surrounded by tufts of cilia distinct from those otherwise lining the mantle cavity (Figure 30). The gametes are shed into the mantle cavity via the right kidney.

Figure 28. Section through the kidney showing tubules formed by kidney epithelium (*l*, kidney lumen; *mc*, mantle cavity; *r*, rectum). Light micrograph; glutaraldehyde/osmium fixation; resin embedded. Scale bar = 50 μm

Figure 29. Section through the excretory pore (*l*, kidney lumen; *m*, body wall muscle; *mc*, mantle cavity). Light micrograph; glutaraldehyde/osmium fixation; resin embedded. Scale bar = 20 μm.

Figure 30. Excretory pore viewed from the mantle cavity. Note emerging secretory granules, and ciliary tufts (*arrowheads*) which surround the pore. Scale bar = 25 μm.

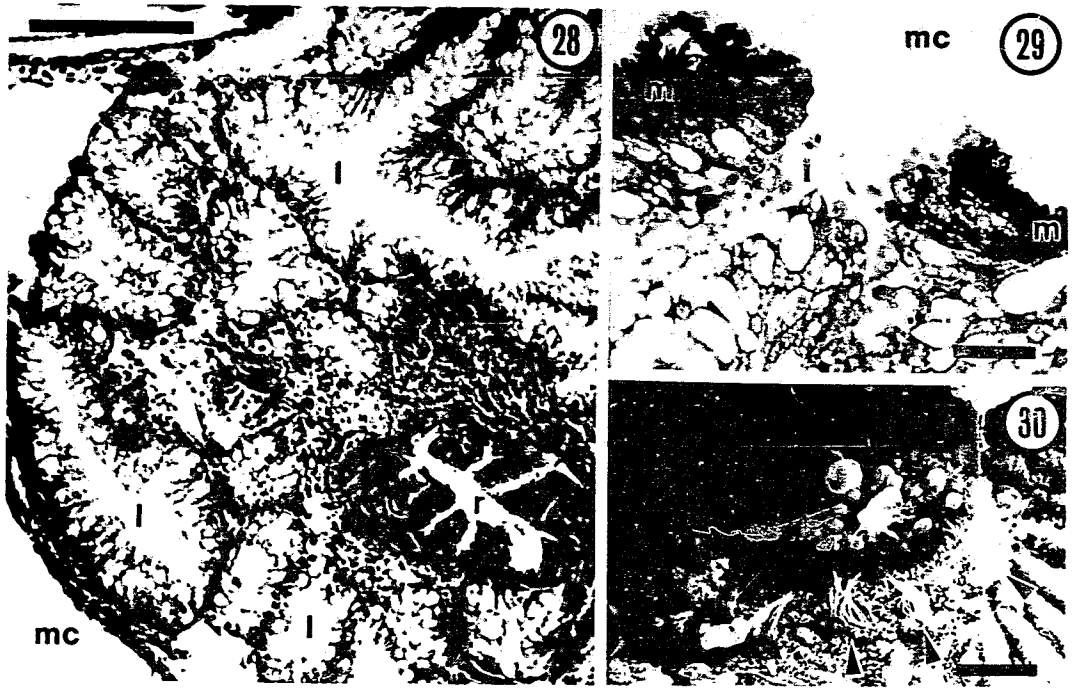
28
l
l
l
mc
mc
29
m
l
m
30

Nephrocyte type 1

There are no differentiated regions of the kidney epithelium, but two types of nephrocytes are distinguished on the basis of ultrastructural features (Figures 31, 32). Nephrocyte type 1 (Nc1) is the more common of the two types. It has a highly vacuolated cytoplasm and its secretory products appear in both light and electron micrographs to be granular material (*g*) within otherwise transparent vacuoles (*v*) (Figures 33-42). There is a highly infolded basal, and often lateral, cell membrane (*bm*) (Figures 35, 37) and a septate junction (Figure 34) between adjacent nephrocytes near the apices of the cells. The cells have a basally located nucleus (*nu*) surrounded by many mitochondria (*mi*) (Figure 35), in addition to Golgi bodies and smooth endoplasmic reticulum (Figure 34); residual bodies or lipofuscin granules are rare. The one to several vacuoles found in the cell originate in the basal cytoplasm. They coalesce to form the largest vacuole apically (Figures 35, 38) prior to fusion with the apical membrane and release of their contents (Figure 33). Secretory material devoid of cytoplasm is seen within the lumen of the kidney (Figures 41, 42), and many of the smooth apices of Nc1 appear indented or collapsed (Figure 43).

The granular material consists of clusters, 0.1-0.4 μm in diameter, of electron-opaque particles which resemble α- and β-glycogen (Figure 36). These glycogen particles, 50-90 nm in diameter, are also found within the cytoplasm and are released into basal vacuoles (Figures 34-37). In addition, membranous whorls are commonly found within the vacuoles (Figure 35). Larger granules (1-3 μm) are found scattered throughout the glycogen, usually within the apical vacuole (Figure 35); they have a mineralized appearance and a very distinctive concentric ring microstructure (Figures 39-42). Growth of these granules appears to be mediated by electron opaque strands which extend from the developing granule, and with which the β-glycogen granules or their α-subunits become associated, presumably prior to incorporation (Figures 39-41). Once released into the

Figure 31. Schematic drawing of nephrocyte type 1 (*bl*, basal lamina; *d*, desmosome; *h*, haemocoel; *mi*, mitochondria; *nu*, nucleus; *sj*, septate junction; *v*, secretory vacuoles; *arrows*, granules; *arrowhead*, glycogen).

Figure 32. Schematic drawing of nephrocyte type 2 (*bl*, basal lamina; *d*, desmosome; *h*, haemocoel; *mi*, mitochondria; *mv*, microvilli; *nu*, nucleus; *sj*, septate junction; *v*, secretory vacuoles; *arrow*, granule).

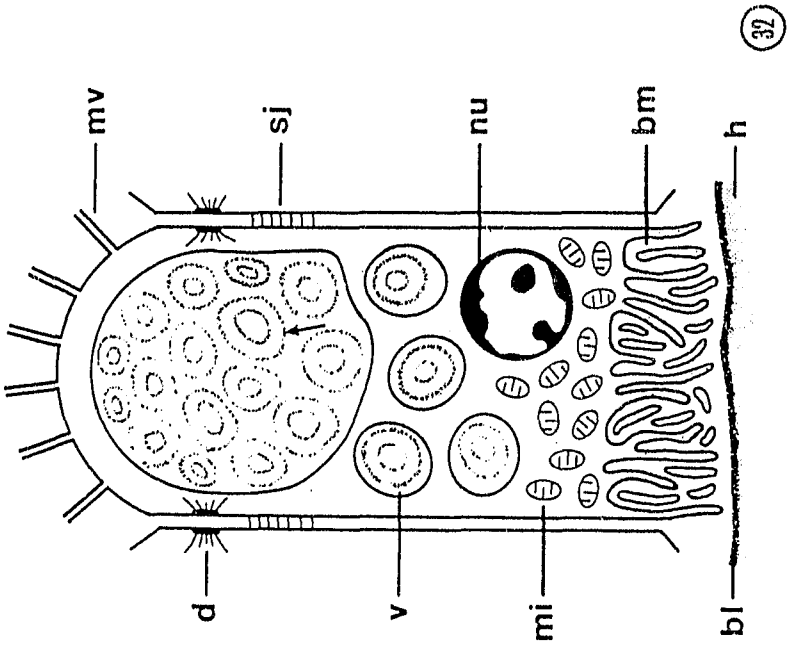

(32)

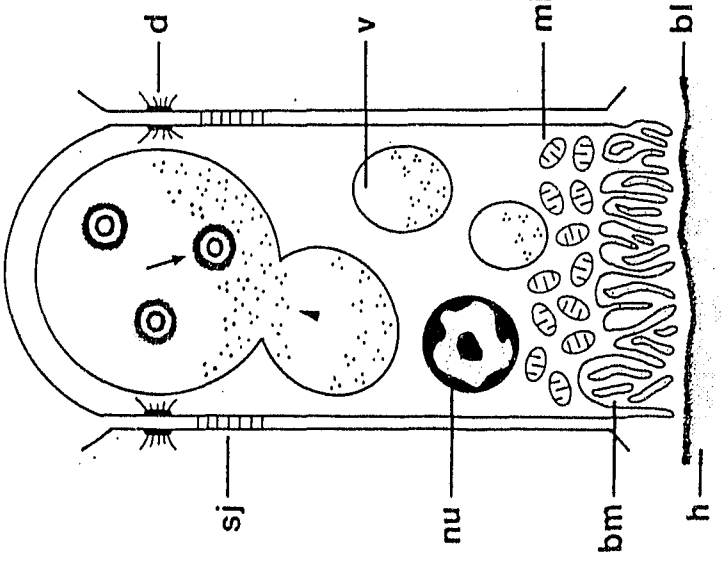

(31)

Figure 33. Cluster of type 1 nephrocytes in the kidney epithelium. Note collapsed apical membranes (*arrows*) and secretory material in kidney lumen (*arrowheads*) (*l*, kidney lumen). Light micrograph; glutaraldehyde/osmium fixation, resin embedded. Scale bar = 10 μm.

Figure 34. Septate junction between the lateral cell membranes near the apices (to the right) of adjacent nephrocyte type 1 cells (*v*, vacuole; *arrows*, endoplasmic reticulum; *arrowheads*, glycogen). Scale bar = 0.4 μm.

Figure 35. Nephrocyte type 1. Note infolding basal and lateral cell membranes (*arrowheads*) and larger mineralised granules (*arrows*); *g*, granules; *l*, kidney lumen; *mi*, mitochondria; *nu*, nucleus; *double arrowhead*, membranous whorl within vacuole. Scale bar = 10 μm.

Figure 36. Nephrocyte type 1 granules. The granules are composed of smaller granule subunits (*arrowheads*). Scale bar = 0.1 μm.

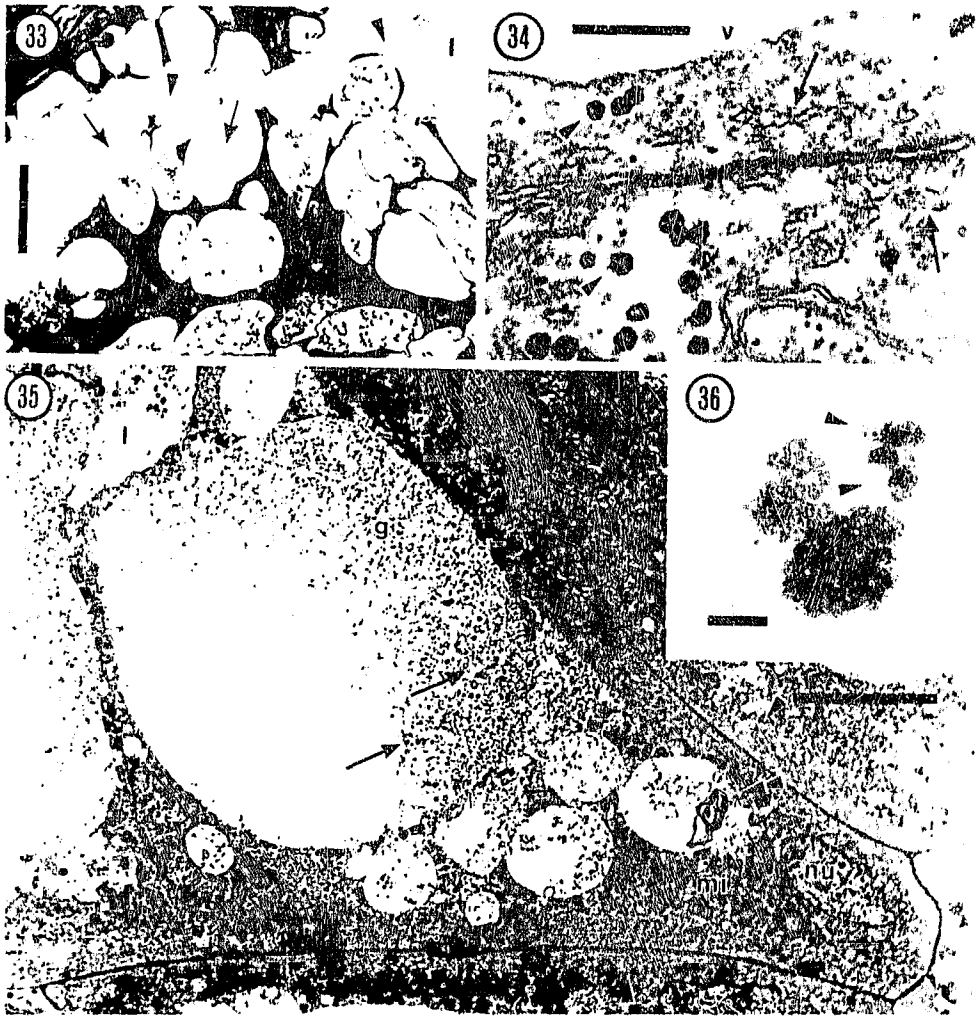
33
34
v
35
g
36
mi
nu

Figure 37. Basal area of nephrocyte type 1. Basal lamina (*arrowheads*) lines the haemocoel, and granules are secreted from the cytoplasm into vacuoles (*arrow*); *bm*, basal cell membrane; *g*, granules; *mi*, mitochondria. Scale bar = 0.5 μm.

Figure 38. Coalescence of vacuoles in nephrocyte type 1, showing point of vacuolar membrane separation (*arrowheads*) (*mi*, mitochondria; *v*, vacuole). Scale bar = 2 μm.

Figures 39-42. Development of granules in vacuoles of nephrocyte type 1 (Figures 39, 40; scale bars = 0.1 and 0.15 μm, respectively) and in the kidney lumen (Figures 41, 42; both scale bars = 0.5 μm).

Figure 43. View of the kidney lumen, showing cell apices of nephrocyte type 1 (*arrowheads*) and nephrocyte type 2 (*arrow*). Scale bar = 10 μm.

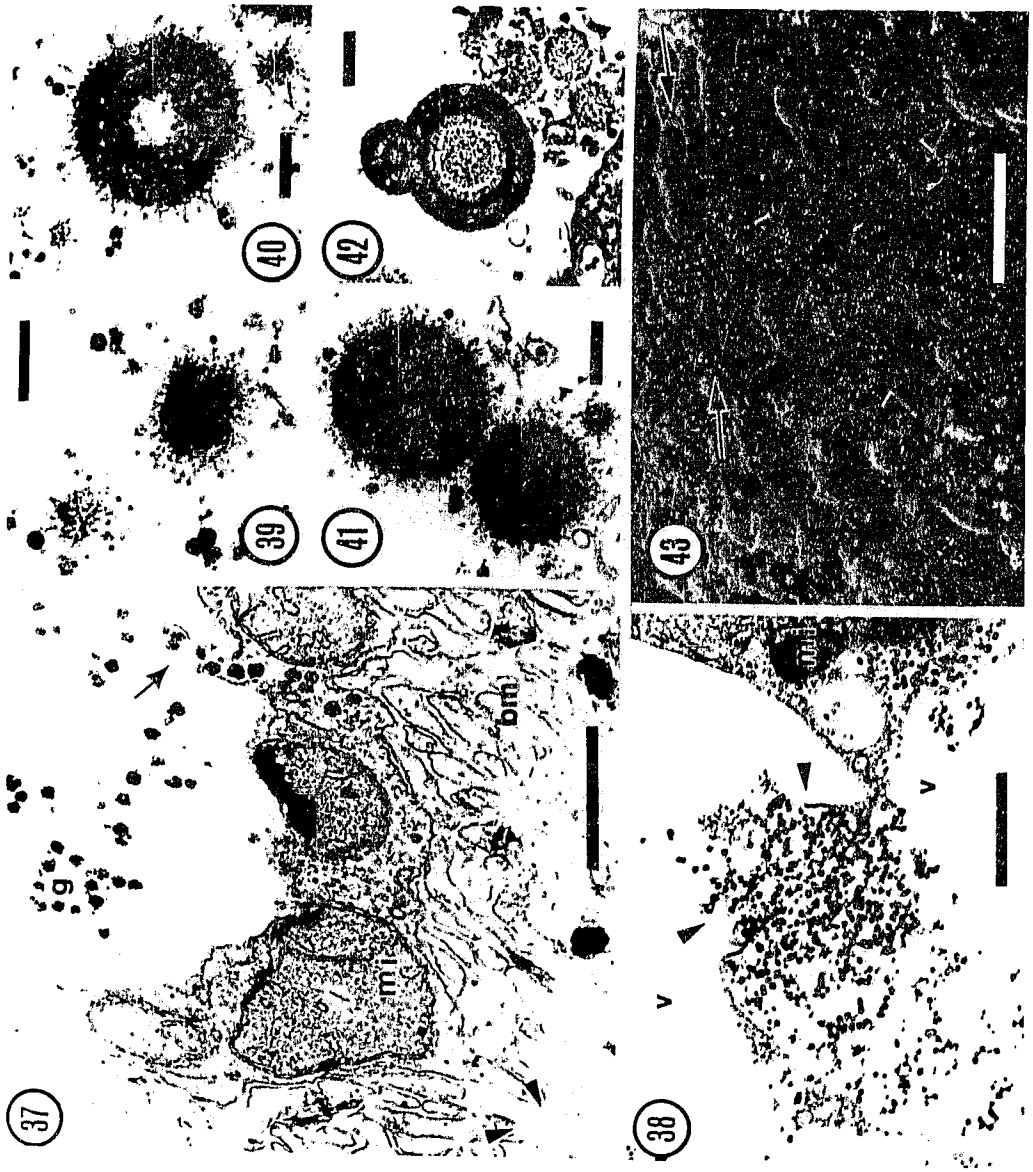
40
42
39
41
43
37
g
mi
bm
38
v
v

kidney lumen the radiating strands persist, and coalescence produces multilobed mineralized granules (Figure 41, 42).

Elemental analyses of the Nc1 intracellular granules and background vacuole contents indicate calcium and phosphorus, with a minor peak for zinc (Figures 44, 45).The granules react positively to histochemical stains for proteins, glycogen and polysaccharides, in addition to lipofuscin and phosphates (Table 1). The finely granular material within the secretory vacuoles is confirmed as glycogen (Table 1).

Nephrocyte type 2

In nephrocyte type 2 (Nc2) large transparent vacuoles filled with glycogen and scattered granules are absent, and instead, granules of 2-3 μm diameter fill the cell vacuoles (Figures 46, 47). These granules appear to form singly within membrane-limited vesicles, and some glycogen (*g*) is present within the limited space around the granule periphery (Figures 47, 48). The vesicles coalesce to form a large central vacuole within which the granules accumulate and may fuse (Figure 47). Other aspects of Nc2 ultrastructure are similar to those found in Nc1, in that a highly infolded basal membrane and basally located nucleus, mitochondria, Golgi bodies and smooth endoplasmic reticulum are present. The granule ultrastructure differs substantially from that of Nc1; the multilobed granules appear less densely mineralized, although the structure is also concentric (Figure 47, 48). The granules are released into the kidney lumen (*l*) either *en masse* from the apical vacuole (*v*) through the cell apex (Figure 49), or singly by exocytosis (Figure 50). The cells are also characterized by the presence of long, thin microvilli (*mv*) (Figures 46, 50) and small vesicles within the apical cytoplasm (Figure 50).

Figure 44. Elemental spectrum obtained from energy-dispersive X-ray microanalysis of a granule from nephrocyte type 1. Chlorine peak produced by embedding medium, nickel peak produced by specimen support grid.

Figure 45. Elemental spectrum obtained from energy-dispersive X-ray microanalysis of background vacuole contents of nephrocyte type 1. Chlorine peak produced by embedding medium, nickel peak produced by specimen support grid.

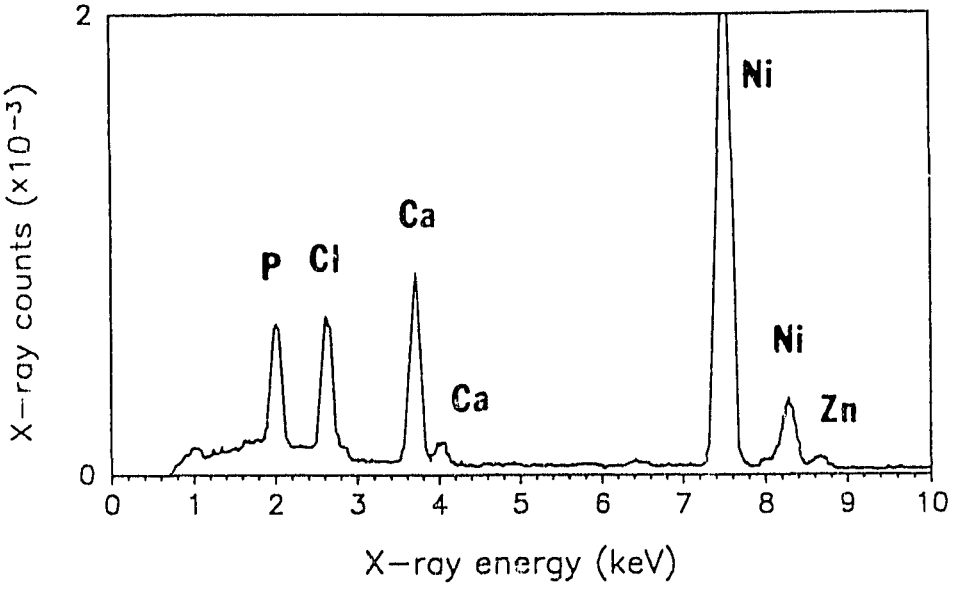
2
0
X-ray counts (x10⁻³)
P
Cl
Ca
Ca
Ni
Ni
Zn
0 1 2 3 4 5 6 7 8 9 10
X-ray energy (keV)

(44)

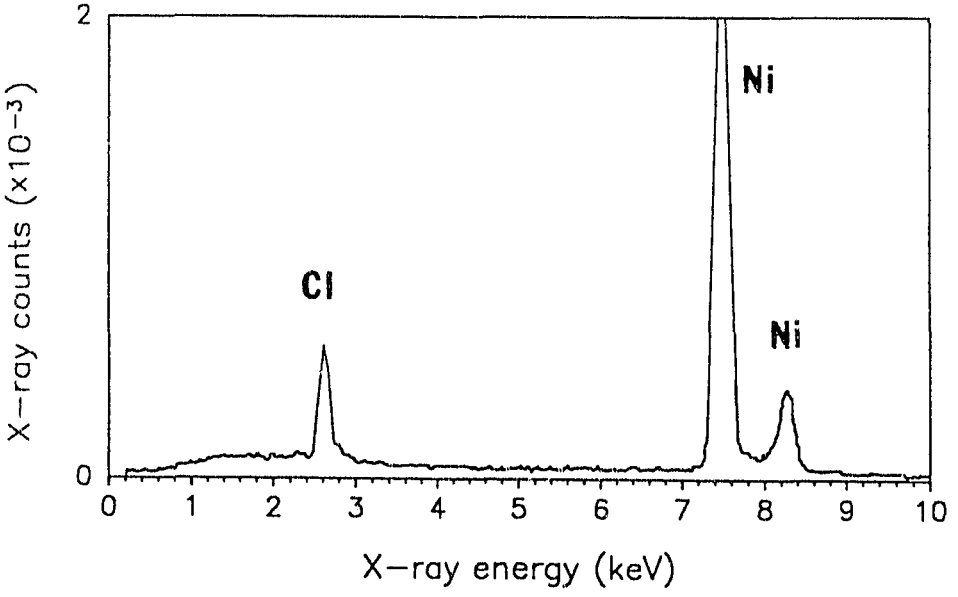
2
0
X-ray counts (x10⁻³)
Cl
Ni
Ni
0 1 2 3 4 5 6 7 8 9 10
X-ray energy (keV)

(45)

Table 1. Histochemical observations on nephrocyte secretory products.

Staining procedure	Reference	Constituent	Nephrocyte type 1	Nephrocyte type 2
Mercuric chloride-bromphenol blue	Pearse (1968)	proteins	++	++
Sudan black B	Humason (1979)	lipids	-	-
Hexamine silver	Pearse (1972)	uric acid, urates	-	-
Periodic acid-Schiff	Humason (1979)	carbohydrates	+++	++
PAS with diastase	Humason (1979)	carbohydrates, glycogen removed	-/+	-/+
Schiff reagent alone	Chayen et al. (1973)	pre-existing aldehydes	+	+
PAS for resin embedded tissue	Leeson and Leeson (1970)	carbohydrates	+++	++
PAS with diatase for resin embedded tissue	Leeson and Leeson (1970)	carbohydrates, glycogen removed	-/+	-/+
Schiff reagent alone, resin embedded tissue	Chayen et al.(1973) (mod.)	pre-existing aldehydes	+	+
Best's carmine	Pearse (1968)	glycogen	+++	+++
Toluidine blue	Pearse (1968)	mucins	-	-/+
Alcian blue pH 2.5	Pearse (1968)	polysaccharides	+	+
Alcian blue pH 1.0	Pearse (1968)	sulphated polysaccharides	-	-

Table 1. Histochemical observations on nephrocyte secretory products (cont'd).

Staining procedure	Reference	Constituent	Nephrocyte type 1	Nephrocyte type 2
Autofluorescence	Pearse (1972)	} melanins	-	-/+
Schmorl	Pearse (1972)	} &	++	+
Nile blue	Pearse (1972)	} lipofuscin	+	+
Sudan black B	Lillie (1965)	lipofuscin	+	+
Hueck	Pearse (1972)	lipofuscin	+	+
Perl's	Pearse (1972)	Fe^{+++}	-	-
Hutchinson's	Humason (1979)	Fe^{+++}	-	-
Hutchinson's with H_2O_2	Humason (1979)	masked Fe^{+++}	-	-
Hutchinson's with HNO_3	Humason (1979)	masked Fe^{+++}	-	-
Turnbull blue	Pearse (1972)	Fe^{++}	-	-
Dithiozone	Pearse (1972)	Zn^{++}	-	-
von Kossa	Pearse (1972)	phosphate	+	+
Ebel's	Chayen et al. (1973)	polyphosphate	+	+
Ammonium molybdate	Pearse (1972)	phosphate	+	+

- absent; + detectable reaction; ++ moderate reaction; +++ strong reaction.

Figure 46. Cluster of nephrocyte type 2 in the kidney epithelium (*g*, granules; *l*, kidney lumen; *arrows*, basal nuclei; *arrowheads*, microvilli). Light micrograph; glutaraldehyde/osmium fixation, resin embedded. Scale bar = 10 μm.

Figure 47. Apical region of nephrocyte type 2. Note granules enclosed in vacuoles individually (*arrowheads*) and grouped in a large central vacuole. Scale bar = 2 μm.

Figure 48. Nephrocyte type 2 granules. Note needle-like structures around the periphery of the granule (*g*, glycogen). Scale bar = 1 μm.

Figure 49. Merocrine secretion of nephrocyte type 2 granules (*g*) (*l*, kidney lumen; *v*, vacuole). Scale bar = 2 μm.

Figure 50. Exocytosis of nephrocyte type 2 granules (*mv*, microvilli; *arrow*, exocytosis of granule; *arrowheads*, membranes delimiting vacuoles). Scale bar = 2 μm.

Figure 51. Extracellular granule (*EG*) within the kidney lumen (*l*), surrounded by Nc1 and Nc2 cell apices. Light micrograph; glutaraldehyde/osmium fixation, resin embedded. Scale bar = 50 μm.

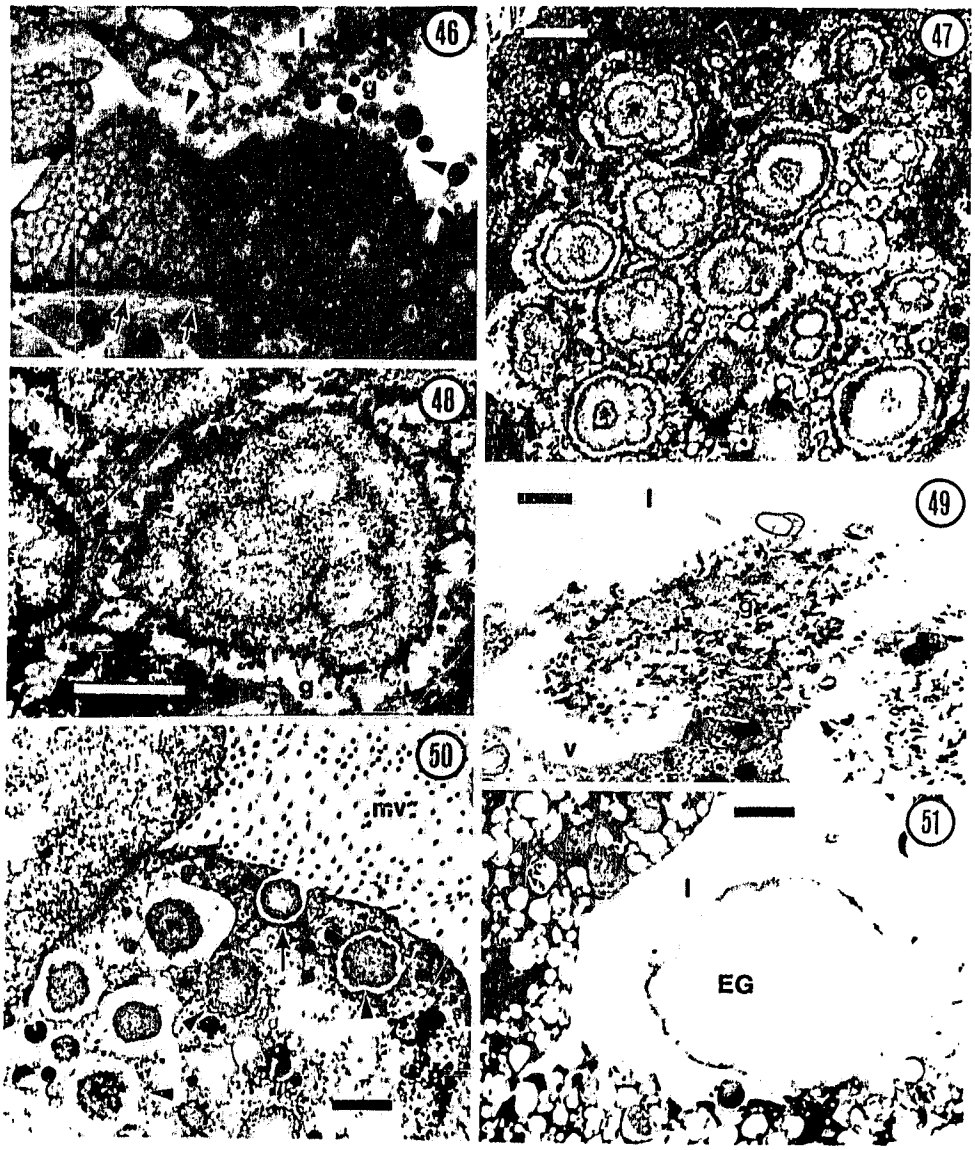
46
l
g
47
g
48
g
49
l
g
v
50
mv
51
l
EG

The elemental spectra produced by EDX microanalysis of Nc2 granules and background cytoplasm (Figures 52, 53) are similar to those obtained for the granules of Nc1, although X-ray counts were consistently higher (Figures 44, 52) because the smaller Nc1 granules provided less material for analysis. Calcium, phosphorus and a small amount of zinc are the major constituents. Likewise, the histochemical profile of the two cell types is very similar (Table 1). There is some metachromatic staining by toluidine blue of thesecretory products of Nc2.

Extracellular granules

Large (>20 μm) extracellular granules (*EG*) were occasionally encountered in the kidney lumen (*l*). They were present in several specimens prepared by both glutaraldehyde-osmium fixation/resin embedding and formalin fixation/paraffin embedding procedures, and only one or two were present per kidney. In some instances they were at the ends of tubules or sacs, surrounded by Nc1 epithelium with the cell apices close to the granule surface. The granules were usually shattered and largely lost by sectioning (Figure 51), and were generally not available for histochemical or EDX analysis, although incidental tests of single granules were positive for phosphate (von Kossa), zinc (dithizone) and glycogen (Best's), and negative for iron (Perl's). Fragments were entirely electron opaque when viewed by TEM. Their unstained appearance after formalin/paraffin preparation was as brittle concretions of yellow coloration, sometimes with a lamellar microstructure discernible.

Figure 52. Elemental spectrum obtained from energy-dispersive X-ray microanalysis of a granule from nephrocyte type 2. Chlorine peak produced by embedding medium; nickel peak produced by specimen support grid.

Figure 53. Elemental spectrum obtained from energy-dispersive X-ray microanalysis of background cytoplasm of nephrocyte type 2.

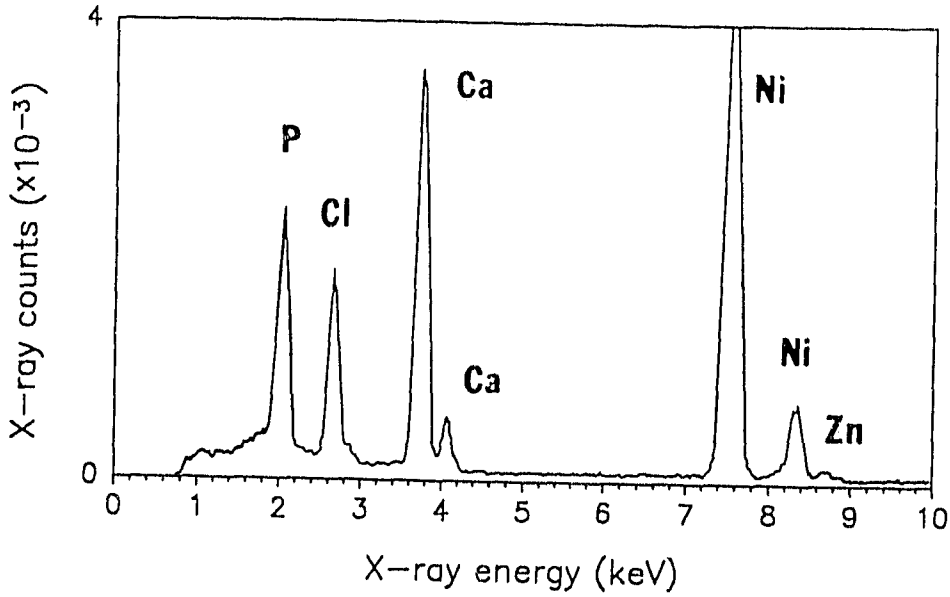
X-ray counts (x10⁻³)
4
0
P
Cl
Ca
Ca
Ni
Ni
Zn
0 1 2 3 4 5 6 7 8 9 10
X-ray energy (keV)

52

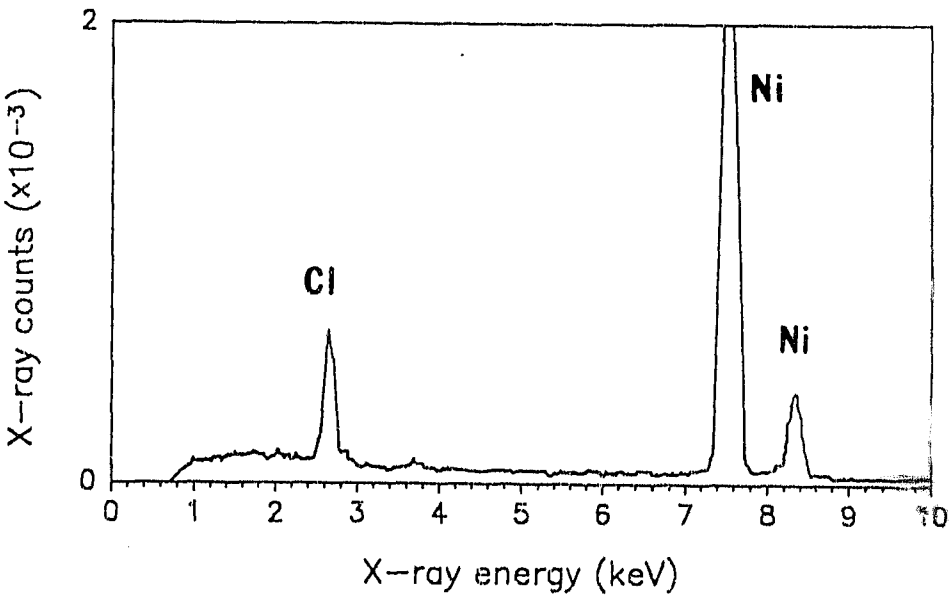
X-ray counts (x10⁻³)
2
0
Cl
Ni
Ni
0 1 2 3 4 5 6 7 8 9 10
X-ray energy (keV)

53

DISCUSSION

Kidney general morphology

The absence of a connection between the kidneys of *Dentalium rectius* concurs with studies of other scaphopods (Lacaze-Duthiers, 1857; Plate, 1892; Boissevain, 1904; Odhner, 1931); similiarly, the lack of ciliation within the kidneys has been reported in other species of *Dentalium* (see Lacaze-Duthiers, 1857; Plate, 1888, 1892; Fol 1889). A striated cuticle covering the nephrocytes, reported by Turchini (1923), was absent in *D. rectius*. The musculature around the excretory pore is not in the form of a concentric band of muscle as reported by Lacaze-Duthiers (1857) but may still effect closure, although this has not been observed directly. As such it may correspond to the muscular lips reported by Andrews (1988) to be typical of molluscan excretory pores.

Nephrocyte structure

The scaphopod kidney has been described as depuratory (Lacaze-Duthiers, 1857), and as functioning in continuous accumulation and elimination (Turchini, 1923). The nephrocytes of *D. rectius* exhibit ultrastructural features typical of secretory cells, such as an elaborately infolded cell membrane, basally located mitochondria, and an extensive vacuolation involved in the formation of secretory products which are released into the kidney lumen. The structure of Nc1 is consistent with light microscope descriptions of vacuolated kidney cells in other *Dentalium* species (Fol, 1889; Plate, 1892). Previous observations of non-vacuolated cells (Kowalevsky, 1889) and of the granule-filled nephrocytes (Plate, 1892) could correspond to Nc2 described in this study, in which the vacuoles are filled with granules. Although the considerable vacuolar spaces in the *D.*

rectius Nc1 did not react to the histochemical tests, they could represent a significant source of urine fluid as suggested for *Littorina littorea* nephrocytes (Mason and Nott, 1980). The merocrine secretion (exocytosis) of vacuole contents in *D. rectius* differs from the apocrine process found in most molluscs (Andrews, 1988), although the extrusion of granules by both apocrine and merocrine secretion has been observed in *Mytilus edulis* (Pirie and George, 1979; George and Pirie, 1980).

Little evidence of reabsorption was observed in the *D. rectius* kidney. The microvillous border found in Nc2 is the only observed ultrastructural feature that is characteristic of this process, although the small vesicles noted in the apical cytoplasm could result from pinocytotic activity. An extensive and well developed reabsorptive kidney epithelium, exhibiting a densly microvillous apical cell membrane with active pinocytosis, is more often observed in osmotically sensitive freshwater and terrestrial molluscs (Little, 1972; Andrews, 1976, 1988).

Granule composition

The elemental and histochemical tests suggest that both intracellular granule types are composed of calcium and zinc phosphates; the absence of a positive histochemical reaction for zinc, given the results of the EDX microanalysis, reflects the low concentration of the metal. The significance of zinc as a trace element in aquatic invertebrates has been outlined by George (1982). Sequestration of zinc in molluscan kidney granules could serve a detoxifying role (Moore, 1977; Lowe and Moore, 1979; Simkiss and Mason, 1983; Mason et al., 1984); high zinc levels have been found in similiarly structured calcium phosphate granules of bivalve kidneys from unpolluted environments (Doyle et al., 1978; George et al., 1980; Sullivan et al., 1988) and preferential accumulation by the kidney in

molluscs exposed to high zinc levels has been demonstrated (Bryan, 1973; Mason and Simkiss, 1983). The absence of iron in the *D. rectius* kidney contrasts with the high iron content of intracelluar granules in other tissues (Chapters 4, 5) and with many bivalve and gastropod species from unpolluted environments in which iron is a major inorganic component of the kidney granules, as indicated by histochemical or EDX techniques (Delhaye, 1976; Moore, 1977; George and Pirie, 1980; George et al., 1982; Mason et al., 1984; Thomson et al., 1985; Sullivan et al., 1988).

Strong protein staining is seen in both types of granules in *D. rectius*, and is a common constituent of molluscan kidney granules (Delhaye, 1976; Overnell, 1981; George et al., 1982; Reid et al., 1984). The fine granular material found in the basal cytoplasm and secretory vacuoles of Nc1 produces a strong histochemical reaction for glycogen which is consistent with its ultrastructural characteristics. A similar reaction is found for both Nc1 and Nc2 granules, and so it can be inferred that the glycogen which is peripherally associated with these granules is eventually incorporated and excreted. Glycogen has been found in the cytoplasm and vacuoles of secretory nephrocytes of several prosobranchs (Andrews, 1976, 1979), and the kidney granules of some bivalves (Reid et al., 1984; Sullivan et al., 1988) although not those of *Mytilus* (George et al., 1982). The glycogen and protein in the kidney granules of *D. rectius* could contribute to the initial organic matrix of the concentric layers prior to incorporation of inorganic calcium, as suggested for protein and mucopolysaccharides in bivalve kidney granules (Tiffany, 1982; Reid et al., 1984).

Urates were not detected in the kidneys of *D. rectius*, as is usual among other molluscs (Andrews, 1979; Reid et al., 1984), although uric acid and urates are present in the kidneys of the gastropod *Marisa cornuarietis* Linné, 1767 (Andrews, 1976), and a variety of "archaeogastropods" (Delhaye, 1976). The absence of significant amounts of

nitrogenous waste in the molluscan kidney has been related to the passive diffusion of ammonia across ctenidial and pallial epithelia (Potts, 1975) and the development of a larger role by the kidney in metal detoxification and reabsorption (Andrews, 1988).

Granule formation

Molluscan kidney granules have been identified as tertiary lysosomes and residual bodies by the presence of lipofuscin, lysosomal enzymes and ultrastructural characteristics such as dense electron opacity and the inclusion of membranous whorls (George et al., 1982; Andrews, 1985; Morse, 1987; Sullivan et al., 1988). While both intracellular granule types in *D. rectius* are produced within the lysosomal-vacuolar system of the nephrocytes, they do not resemble kidney granules identified by George et al. (1982) as residual bodies. The formation of granules in *D. rectius* appears to be initiated at an earlier stage in lysosomal maturation.

Fol (1889) described the colourless globules in the nephrocytes of *Dentalium entalis* as arising from a finely stippled mass, and this corresponds surprisingly well with the ultrastructural observations on Nc1 granule formation in *D. rectius*. The growth of the Nc1 granules and the formation of the concentric ring structure occur by a process of surface accretion, with glycogen incorporation and fusion with other granules being associated with thin electron opaque threads which radiate from the surface of the newly forming granule. A similiar process occurs in Nc2, although the periphery of the developing granules instead possesses many needle-like crystals, which have been previously described as an intermediary stage in intracellular calcium phosphate granule growth (Simkiss, 1976; Brown, 1982). Granule fusion has also been noted in other studies of molluscan excretory products (Reid et al., 1984; Sullivan et al., 1988). Formation of a

concentric banding pattern within metal-containing granules of invertebrates has been reviewed by Brown (1982). Carmichael et al. (1979) suggest the layering is produced by alternating accretion and resorption, while Hopkin & Nott (1979) demonstrated that layers of greater electron opacity contain higher metal levels. In the granules of both nephrocyte types in *D. rectius* the concentric banding probably reflects some periodicity in accretion or precipitation of the components involved, with the formation of electron opaque concentric rings related to the incorporation of calcium and zinc.

Nc2 secretory products appear to possess a significantly different origin and formation pathway than those of Nc1, as they arise individually in secretory vesicles and appear to be more developed before being released. Although they are not as highly mineralised (i.e., not as electron opaque), the granules are larger and often consist of two or more granules which have fused. The formation of extracellular granules is likely due to the fusion of Nc1 and Nc2 granules after they have been released. The histochemical indications of zinc phosphate and glycogen deposits within the extracellular granules support their origin from the two intracellular granule types.

The kidneys of *D. rectius* are similar in most aspects of their functional morphology to those generally found in marine molluscs from relatively unpolluted habitats, while exhibiting unique features in nephrocyte ultrastructure and granule development. While the kidney epithelium is simple, the process of merocrine secretion in *D. rectius* is uncommon among the Mollusca. The secretory materials possess those characteristics which form the basis for metal accumulation and excretion throughout the Mollusca, while some nephrocytes may provide a limited reabsorption capability.

LITERATURE CITED

Andrews, E. B. (1976). The ultrastructure of the heart and kidney of the pilid gastropod mollusc *Marisa cornuarietis*, with special reference to filtration throughout the Architaenioglossa. Journal of Zoology, 179, 85-106.

Andrews, E. B. (1979). Fine structure in relation to function in the excretory system of two species of *Viviparus*. Journal of Molluscan Studies, 45, 186-206.

Andrews, E. B. (1981). Osmoregulation and excretion in prosobranch gastropods. Part 2: structure in relation to function. Journal of Molluscan Studies, 47, 248-289.

Andrews, E. B. (1985). Structure and function in the excretory system of archaeogastropods and their significance in the evolution of gastropods. Philosophical Transactions of the Royal Society of London, Series B, 310, 383-406.

Andrews, E. B. (1988). Excretory systems of Molluscs. In Trueman, E. R. & Clarke, M. R. (Eds.), The Mollusca, v. 11, Form and Function (pp. 381-448). Academic Press, New York.

Boissevain, M. (1904). Beiträge zur Anatomie und histologie von *Dentalium*. Jenaische Zeitschrift für Naturwissenschaft, 38, 553-572, pls. 17-19.

Brown, B. E. (1982). The form and function of metal-containing "granules" in invertebrate tissues. Biological Reviews of the Philosophical Society of Cambridge, 57, 621-667.

Bryan, G. W. (1973). The occurrence and seasonal variation of trace metals in the scallops *Pecten maximus* (L.) and *Chlamys opercularis* (L.). Journal of the Marine Biological Association of the United Kingdom, 53, 145-166.

Carmichael, N. G., Squibb, K. S. & Fowler, B. A. (1979). Metals in the molluscan kidney: a comparison of two closely related bilvalve species (*Argopecten*), using X-ray microanalysis and atomic absorption spectroscopy. Journal of the Fisheries Research Board of Canada, 36, 1149-1155.

Chapman, D. M. (1977). Eriochrome cyanin as a substitute for haematoxylin and eosin. Canadian Journal of Medical Technology, 39, 65-66.

Chayen, J., Bitensky, L. & Butcher, R. G. (1973). Practical Histochemistry. John Wiley and Sons, Ltd., London.

Delhaye, W. (1976). Histophysiologie comparée des organes rénaux chez les archaeogastéropodes (Mollusca - Prosobranchia). Cahiers de Biologie Marine, 17, 305-322.

Distaso, A. (1905). Sull' Anatomia degli scafopodi. Zoologischer Anzeiger, 29, 271-278.

Doyle, L. J., Blake, N. J., Woo, C. C. & Yevich, P. (1978). Recent biogenic phosphorite: concretions in mollusk kidneys. Science, 199, 1431-1433.

Fol, H. (1885). Sur l'anatomie microscopique du Dentale. Comptes Rendu Hebdomadaires des Seances de l'Academie des Sciences, Série D, Sciences naturelles, 1885, 1352-1355.

Fol, H. (1889). Sur l'anatomie microscopique du Dentale. Archives de Zoologie Experimentale et Génerale, Duexième Série, 7, 91-148, pls. 5-8.

George, S. G. (1983). Subcellular accumulation and detoxication of metals in aquatic animals. In Vernderg, W. B., Calabrese, A., Thurberg, F. P. & Vernberg, E. J. (Eds.) Physiological mechanisms of marine pollutant toxicity (pp. 3-52). Academic Press, New York.

George, S. G. & Pirie, B. J. S. (1980). Metabolism of zinc in the mussel, *Mytilus edulis* (L.): a combined ultrastructural and biochemical study. Journal of the Marine Biological Association of the United Kingdom, 60, 575-590.

George, S. G., Pirie, B. J. S, Cheyne, A. R., Coombs, T. L. & Grant, P. T. (1978). Detoxification of metals by marine bivalves: an ultrastructural study of the compartmentation of copper and zinc in the oyster *Ostrea edulis*. Marine Biology, 45, 147-156.

George, S. G., Pirie, B. J. S. & Coombs, T. L. (1980). Isolation and elemental analysis of metal rich granules from the kidney of the scallop, *Pecten maximus* (L.). Journal of Experimental Marine Biology and Ecology, 42, 143-156.

George, S. G., Coombs, T. L. & Pirie, B. J. S. (1982). Characterization of metal-containing granules from the kidney of the common mussel, *Mytilus edulis*. Biochimica Biophysica Acta, 716, 61-71

Hopkin, S. P. & Nott, J. A. (1979). Some observations on concentrically structured, intracellular granules in the hepatopancreas of the shore crab *Carcinus maenas* (L.). Journal of the Marine Biological Association of the United Kingdom, 59, 867-877.

Humason, G. L. (1979). Animal Tissue Techniques (fourth ed). Freeman, San Francisco.

Kowalevsky, A. (1889). Ein Beitrag zur Kenntnis der Exkretionsorgane. Biologisches Zentralblatt, 9(3), 65-76.

Lacaze-Duthiers (de), H. (1857). Histoire de l'organisation et du développement du Dentale. Annales des Sciences Naturelles, Quatrième Série, 7, 5-51, pls. 2-4, 171-255, pls. 5-9.

Leeson, C. R. & Leeson, T. S. (1970). Staining methods for sections of epon-embedded tissues for light microscopy. Canadian Journal of Zoology, 48, 189-191.

Lillie, R. D. (1965). Histopathologic Technic and Practical Histochemistry (third ed). McGraw-Hill, New York.

Little, C. (1965). The formation of urine by the prosobranch gastropod mollusc *Viviparus viviparus* Linn. Journal of Experimantal Biology, 43, 39-54.

Little, C. (1972). The evolution of kidney function in the Neritacea (Gastropoda, Prosobranchia). Journal of Experimental Biology, 56, 249-261.

Little, C. (1979). Reabsorption of glucose in the renal system of *Viviparus*. Journal of Molluscan Studies, 45, 207-208.

Lowe, D. M. & Moore, M. N. (1979). The cytochemical distributions of zinc (Zn II) and iron (Fe III) in the common mussel, *Mytilus edulis*, and their relationship with lysosomes. Journal of the Marine Biological Association of the United Kingdom, 59, 851-858.

Martin, A. W. (1983). Excretion. In Saleuddin, A. S. M. & Wilbur, K. M. (Eds.) The Mollusca, v. 5, Physiology, part 2 (pp. 353-405). Academic Press, New York.

Mason, A. Z. & Nott, J. A. (1980). The association of the blood vessels and the excretory epithelium in the kidney of *Littorina littorea* (L.) (Mollusca, Gastropoda). Marine Biology Letters, 1, 355-365.

Mason, A. Z. & Simkiss, K. (1983). Interactions between metals and their distribution in tissues of *Littorina littorea* (L.) collected from clean and polluted sites. Journal of the Marine Biological Association of the United Kingdom, 63, 661-672.

Mason, A. Z., Simkiss, K. & Ryan, K. P. (1984). The ultrastructural localization of metals in specimens of *Littorina littorea* collected from clean and polluted sites. Journal of the Marine Biological Association of the United Kingdom, 64, 699-720.

Moore, M. N. (1977). Lysosomal responses to environmental chemicals in some maine (sic) invertebrates. In Giam, C. S. (Ed.) Pollutant effects on marine organisms (pp. 143-154). Lexington Books, Lexington.

Morse, M. P. (1987). Comparative functional morphology of the bivalve excretory system. American Zoologist, 27(3), 737-746.

Odhner, N. H. (1931). Die Scaphopoden. In Bock, S. (Ed.), Further Zoological Results of the Swedish Antarctic Expedition 1901-1903 (pp. 1-8, pls. 1, 2). Norsedt, Stockholm.

Overnell, J. (1981). Protein and oxalate in mineral granules from the kidney of *Pecten maximus* (L.). Journal of Experimental Marine Biology and Ecology, 52, 173-183.

Pearse, A. G. E. (1968). Histochemistry, Theoretical and Applied, 1 (third ed). Churchill, London.

Pearse, A. G. E. (1972). Histochemistry, Theoretical and Applied, 2, (third ed). Churchill Livingston, London.

Pelseneer, P. (1899). Reserches Morphologiques et Phylogenetiques sur les Mollusques Archaiques. Academie royale des sciences, des lettres et des beaux-arts de Belgique, Bruxelles, 113 pp.

Pirie, B. J. S. & George, S. G. (1979). Ultrastructure of the heart and excretory system of *Mytilus edulis* (L.). Journal of the Marine Biological Association of the United Kingdom, 59, 819-829.

Plate, L. (1888). Bemerkungen zur Organisation der Dentalien. Zoologischer Anzeiger, 11, 509-515.

Plate, L. (1892). Ueber den Bau und die Verwandtschaftsbeziehungen der Solenoconchen. Zoologische Jahrbucher Jena Abteilung für Anatomie, 5, 301-386, pls. 23-26.

Potts, W. T. W. (1967). Excretion in the Molluscs. Biological Reviews of the Philosophical Society, Cambridge, 42, 1-41.

Potts, W. T. W. (1975). Excretion in the Gastropods. Forschritte der Zoologie, 23(2/3), 76-88.

Reid, R. G. B., Fankboner, P. V. & Brand, D. G. (1984). Studies of the physiology of the giant clam *Tridacna gigas* Linné-II. Kidney function. Comparative Biochemistry and Physiology, 78A(1), 103-108.

Reynolds, P. D. (1990). Functional morphology of the perianal sinus and pericardium of *Dentalium rectius* (Mollusca: Scaphopoda) with a reinterpretation of the scaphopod heart. American Malacological Bulletin, 7(2), 137-146.

Simkiss, K. (1976). Intracellular and extracellular routes in biomineralization. In Duncan, C. J. (Ed.) Calcium in biological systems: Symposia of the Society for Experimental Biology # 30 (pp. 423-444). Cambridge University Press, London.

Simkiss, K. & Mason, A. Z. (1983). Metal ions: metabolic and toxic effects. In Hochachka, P. W. (Ed.) The Mollusca, v. 2, Environmental Biochemistry and Physiology (pp. 101-164). Academic Press, New York.

Sullivan, P. A., Robinson, W. E. & Morse, M. P. (1988). Isolation and characterization of granules from the kidney of the bivalve *Mercenaria mercenaria*. Marine Biology, 99, 359-368.

Thomson, J. D., Pirie, B. J. S. & George, S. G. (1985). Cellular metal distribution in the Pacific oyster, *Crassostrea gigas* (Thun.) determined by quantitative X-ray microprobe analysis. Journal of Experimental Marine Biology and Ecology, 85, 37-45.

Tiffany, W. J. (1982). Excretory concretions in the sunray venus clam, *Macrocallista nimbosa* (Bivalvia: Veneridae). The Veliger, 25(1), 77-79.

Turchini, J. (1923). L'excretion urinaire chez les Mollusques. Chap 5, Scaphopodes. In Dion, G. (Ed.) Contribution à l'étude de l'histologie comparée de la cellule rénale (pp114-115). Librairie Octave Dion, Paris.

CHAPTER 4

CYTOLOGY OF METAL STORAGE IN THE DIGESTIVE SYSTEM OF *DENTALIUM RECTIUS* (MOLLUSCA, SCAPHOPODA)

ABSTRACT

The ultrastructure, histochemistry and elemental analysis of intracellular metal accumulations in the digestive tract epithelia of the dentaliid scaphopod *Dentalium rectius* are described. Intracellular membrane-limited granules are found in all cell types investigated and contain varying levels of iron and calcium phosphate. No other accumulated metals were detected. Granules of the oesophageal and stomach epithelium have high iron content; in contrast, cells of the digestive and intestinal epithelia do not play an important role in iron storage. However, digestive cells may be a significant site of iron uptake from ingested materials, complementing uptake across the mantle from seawater. Iron excretion occurs solely through mineralisation of the radula and release of oesophageal granules into the gut; previous studies have shown that the kidney does not secrete iron. The pathway of iron processing in *D. rectius* differs substantially from that found in other molluscs from unpolluted habitats, and is likely dependant upon both the physiological requirements of radular mineralization and the temporal availability of iron in the environment.

INTRODUCTION

The morphology of the digestive system in Scaphopoda is well known in terms of anatomical relationships of the associated organs (Lacaze-Duthiers, 1856; Taib, 1981a).

While some attention has been given to description at the cellular level (Fol, 1885; 1889; Plate, 1888; 1892; Taib, 1981b), no ultrastructural data has yet been published. Similarly, little is known of intracellular metal storage in the scaphopod gut. The absence of metal accumulation in the calcium phosphate kidney granules of *Dentalium rectius* (Chapter 3; Reynolds, 1990) is unusual, as the kidney is a significant organ in the storage and excretion of metals in bivalves and gastropods from both unpolluted and polluted environments (Bryan, 1973; Delhaye, 1976; Moore, 1977; Doyle et al., 1978; George et al., 1980, 1982; George & Pirie, 1980; Mason & Simkiss, 1983; Mason et al., 1984; Thomson et al., 1985; Sullivan et al., 1988). This suggests that metabolic pathways of metal processing in scaphopods may differ significantly from other molluscs. A prerequisite to experimental study of the dynamics of metal uptake, accumulation and excretion is the identification of tissues involved in metal processing and the cellular sites of metal storage within the organism. Metal uptake normally occurs by two routes: across the gut epithelium from ingested material and via epithelia exposed to the external environment. In addition to the molluscan kidney, tissues of the digestive tract have also been found to be major sites of heavy metal accumulation in molluscs from polluted environments (Nott & Nicolaidou, 1989). Metal uptake by mantle tissues will be examined in Chapter 5. The purpose of this study is to describe the fine structure of selected epithelia in the scaphopod digestive system and to characterise intracellular sites of metal accumulation found in these tissues. These results will be compared to ultrastructural and compositional characteristics of metal processing by the gut in other molluscan classes, and applied towards a testable model of metal processing routes in the dentaliid scaphopod *Dentalium rectius* Carpenter 1864.

MATERIALS AND METHODS

Dentalium rectius was collected from mud dredged from 60 m depth in Satellite channel, off Vancouver Island, British Columbia. Specimens were kept in chilled seawater and returned to the laboratory, where they were shelled, quickly dissected, and fixed for light microscopy, histochemical analysis, scanning electron microscopy (SEM, transmission electron microscopy (TEM) or energy dispersive X-ray (EDX) microanalysis, as described in Chapter 3.

RESULTS

The digestive tract of *Dentalium rectius* (Figure 54) is similar to that described for other dentaliid scaphopods. The mouth leads to a buccal pouch; following the opening to the radular apparatus, the oesophagus gives off two lateral diverticula before opening to the posterior-dorsal portion of the stomach. Two lobes of digestive diverticulum arise posteriorly from the stomach. The intestine leaves the stomach anteriorly, ventral to the opening of the oesophagus, and undergoes several loops and turns before opening into the mantle cavity through the anus. The rectum, surrounded by the perianal sinus, projects ventrally into the mantle cavity, directed slightly towards the anterior (Chapter 2, Figure 54).

Radula

The radula has five teeth per row, consisting of paired marginals and laterals which overlay a central tooth (Figure 55) and is supported by a radular membrane. The

Figure 54. Longitudinal section through the mid-region of *Dentalium rectius*, showing the anatomical relationships of the digestive tract organs (*DD*, digestive diverticula; *I*, intestine; *O*, oesophagus; *S*, stomach). Scale bar = 0.25 mm.

Figure 55. The radula of *Dentalium rectius*. Note the paired marginal and lateral teeth, and the single central tooth. Scale bar = 0.3 mm.

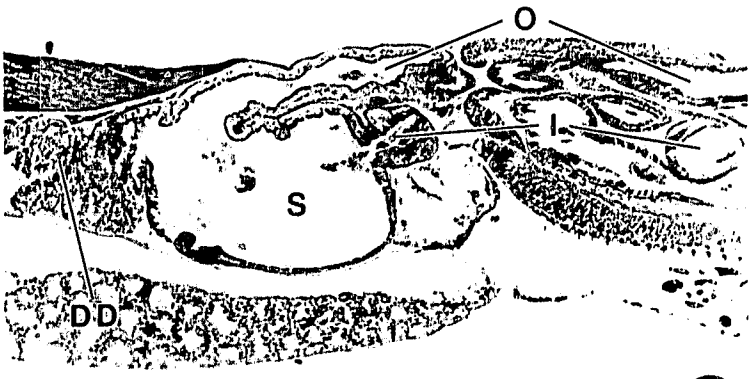

54

55

histochemical composition of the radular teeth and membrane is presented in Table 3. The teeth are highly mineralized, the organic matrix showing a strong reaction for protein, carbohydrates including polysaccharides but not substantial glycogen, and detectable levels of lipofuscin. Inorganic components include high quantities of both ferric and ferrous iron, with no detectable levels of zinc or copper. The positive reactions to the von Kossa, Ebel's and ammonium molybdate tests indicate that the two iron species are complexed with phosphate. The radular membrane, which secretes the teeth, differs significantly in both organic and inorganic constituents. While also testing strongly positive for proteins, the membrane has considerably less carbohydrate which, however, includes both glycogen and polysaccharide. There is a higher level of lipofuscin than is found in the radular teeth. Zinc and phosphate were the only inorganics detected; in sharp contrast to the teeth, there is no iron indicated by the several relevant histochemical tests employed.

Oesophageal epithelium

The oesophagus is lined with narrow columnar epithelium. The apical membrane is elaborated into a microvillous border, and in some instances bears cilia (Figure 56). Distributed throughout the cytoplasm are numerous membrane-delimited electron opaque granules (Figures 56-59), which are structurally differentiated into two granule types. One type has a 1 μm maximum diameter with a central, finely textured matrix surrounded by coarser material (Figures 57, 58). The core may have an angular outline and electron-opaque particles scattered within it. The second granule type is considerably larger (3.2 μm maximum diameter) and has a heterogeneous electron opacity (Figures 58, 59). Within these granules, membranous whorls with an irregular lamellate structure (11.4-22.9 nm thickness range) are evident. These granules appear to have incorporated smaller granules

Table 2. Histochemical observations on the radular apparatus.

Staining procedure	Reference	Constituent	Radula Teeth	Radula Membrane
Mercuric chloride-bromphenol blue	Pearse (1968)	proteins	+++	+++
Sudan black B	Humason (1979)	lipids	x	x
Hexamine silver	Pearse (1972)	uric acid, urates	-	-
Periodic acid-Schiff†	Humason (1979)	carbohydrates	+++	+
PAS with diastase†	Humason (1979)	carbohydrates, glycogen removed	x	x
Best's carmine	Pearse (1968)	glycogen	-	+
Toluidine blue	Pearse (1968)	mucins	-	-
Alcian blue pH 2.5	Pearse (1968)	polysaccharides	++	+
Alcian blue pH 1.0	Pearse (1968)	sulphated polysaccharides	-	-
Autofluorescence	Pearse (1972)	} melanins	+	+
Schmorl	Pearse (1972)	} &	+	+++
Nile blue	Pearse (1972)	} lipofuscin	+	+
Sudan black B	Lillie (1965)	lipofuscin	+	+
Hueck	Pearse (1972)	lipofuscin	+	++

Table 2. Histochemical observations on the radular apparatus (cont'd).

Staining procedure	Reference	Constituent	Radula Teeth	Radula Membrane
Perl's	Pearse (1972)	Fe^{+++}	+++	-
Hutchinson's	Humason (1979)	Fe^{+++}	+++	-
Hutchinson's with H_2O_2	Humason (1979)	masked Fe^{+++}	+++	-
Hutchinson's with HNO_3	Humason (1979)	masked Fe^{+++}	+++	-
Turnbull blue	Pearse (1972)	Fe^{++}	+++	-
Dithiozone	Pearse (1972)	Zn^{++}	-	+
Rubeanic Acid	Pearse (1972)	Cu^{++}	-	-
von Kossa	Pearse (1972)	phosphate	++	+
Ebel's	Chayen et al. (1969)	polyphosphate	+++	+
Ammonium molybdate	Pearse (1972)	phosphate	++	+

†control sections (Schiff reagent only) employed

-, no detectable reaction; +, detectably positive; ++, moderately positive; +++, strongly positive; x, not tested

Figure 56. Oesophageal epithelial cells. Note the microvilli and cilia extending into the oesophageal lumen (*O*), the electron-opaque intracellular granules, basally located nucleii and infolded basal cell membrane (*arrowheads*). Scale bar = 20 μm.

Figure 57. Small granules of oesophageal epithelial cells. Note angular outline of homogeneous electron-opaque core with scattered particles, and outer layer of course material. Scale bar = 0.6 μm.

Figure 58. Large granules of oesophageal epithelial cells. Note membranous whorls, spherical components, smaller granules (*arrowheads*), mitochondria (*M*). Scale bar = 5 μm.

Figure 59. Extra large granule found in oesophageal cell. Note similarity of structure to larger granules in Figure 58. Scale bar = 1 μm.


57
M
58
O
56
59

of similar material, and generally have the appearance of tertiary lysosomes or residual bodies (Figures 58, 59). Infrequently (< one per cell) these granules reach 6 μm maximum diameter (Figure 59), but maintain a similar ultrastructural appearance. The nucleus is located in the mid to lower region of the cell. Numerous mitochondria are found within the cytoplasm and the basal cell membrane is infolded, indicative of active transport between the cells and the haemocoel (Figure 56).

Typical spectra produced by EDX analysis of the larger oesophageal granules (>1 μm) and of the background cytoplasm are shown in Figures 60 and 61. The elemental composition of the granules includes significant portions of iron, calcium, sulphur and phosphorus, which are not indicated by analysis of the cytoplasm. Nickel, chlorine and silicon are attributable to contamination by specimen preparation and analysis techniques. The histochemical profile of these oesophageal granules is presented in Table 3. Their organic component consists of detectable levels of protein and complex carbohydrates. The granules test strongly positive for lipofuscin, supporting their identification as tertiary lysosomes. Intense reactions were also recorded for both ferric and ferrous iron and phosphate, which correlates with the EDX results. Additionally, positive reactions for lipid and glycogen were observed for other components of the cell cytoplasm (Table 3).

Stomach epithelium

The stomach epithelium is regionally differentiated into several cell types. Those with iron-containing granules are limited to the anterior portion of the ventral wall, adjacent to the opening of the intestine. They are columnar in shape and bear a densely microvillous apical membrane (Figure 62). Adjacent cells are joined by a zonula adherens near the apex, followed by a septate junction (Figure 63). The mid region of the cells are dominated by

Figure 60. Energy dispersive X-ray microanalysis spectrum of a large oesophageal granule. Note peaks for calcium, iron and phosphorous. Chlorine peak produced by embedding medium, nickel peak produced by specimen support grid, and silicon peak produced by analytical equipment.

Figure 61. Energy dispersive X-ray microanalysis spectrum of background oesophageal epithelium cytoplasm. Note the absence of peaks for calcium, iron and phosphorous. Chlorine peak produced by embedding medium, nickel peak produced by specimen support grid, and silicon peak produced by analytical equipment.

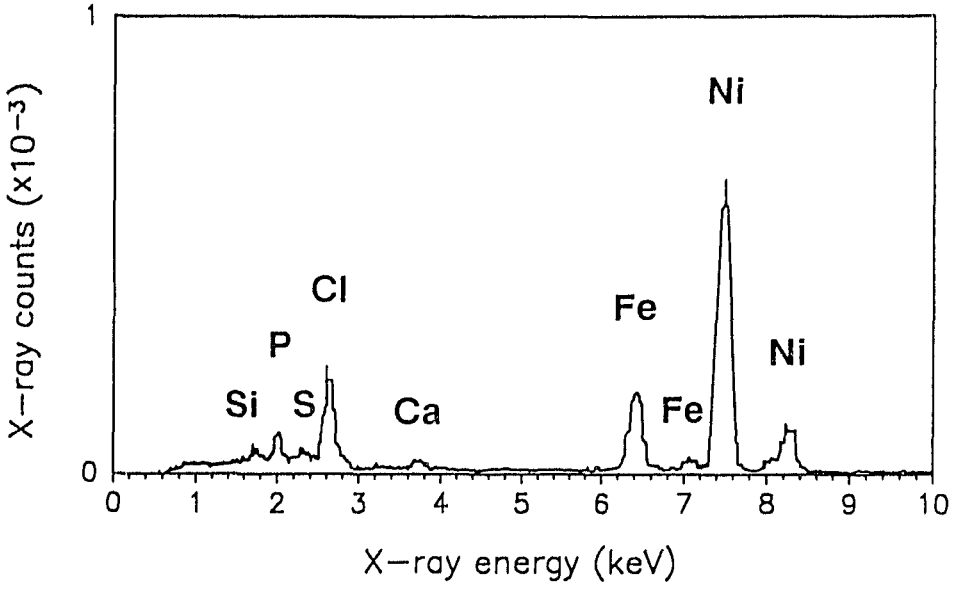
X-ray counts (x10⁻³)
1
0
0 1 2 3 4 5 6 7 8 9 10
X-ray energy (keV)
Si
P
S
Cl
Ca
Fe
Fe
Ni
Ni

60

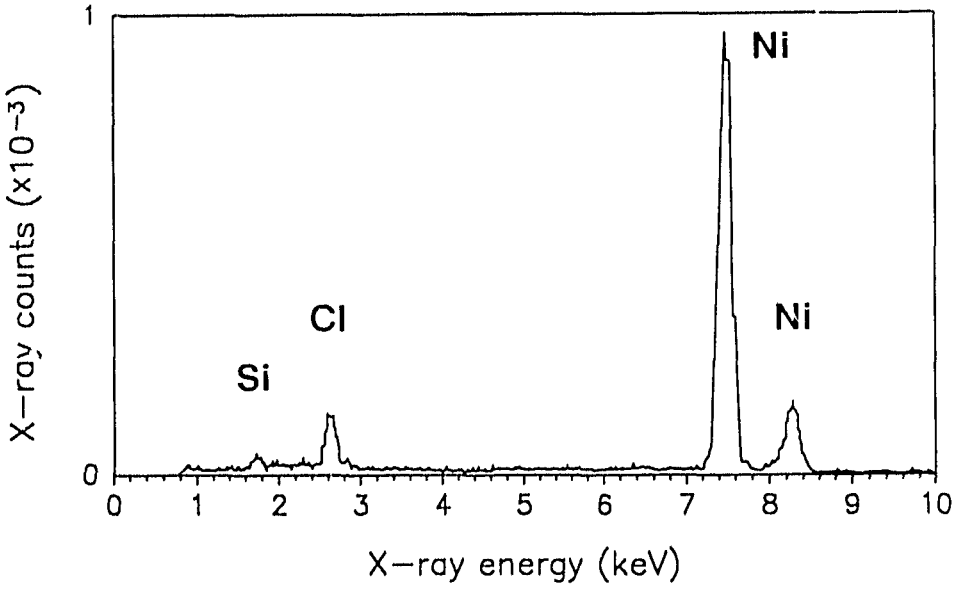
X-ray counts (x10⁻³)
1
0
0 1 2 3 4 5 6 7 8 9 10
X-ray energy (keV)
Si
Cl
Ni
Ni

61

Table 3. Histochemical observations on intracellular granules of digestive system tissues.

Staining procedure	Reference	Constituent	Cell Types						
			O	S	Da	Dm	Db	B	I
Mercuric chloride-									
bromphenol blue	Pearse (1968)	proteins	+	+	+++	++	+++	+	+
Sudan black B	Humason (1979)	lipids	++*	++	+	++	+++**	-	++
Hexamine silver	Pearse (1972)	uric acid, urates	-	-	-	-	-	-	-
Periodic acid-Schiff†	Humason (1979)	carbohydrates	+	++	++	+++	+++	++	+
PAS with diastase†	Humason (1979)	carbohydrates,							
		glycogen removed	+	++	++	+++	x	+***	+
Best's carmine	Pearse (1968)	glycogen	+****	+	+	+	+++	+**	+
Toluidine blue	Pearse (1968)	mucins	-	-	-	-	-	-	-
Alcian blue pH 2.5	Pearse (1968)	polysaccharides	+	+	++	+++	+	++**	++
Alcian blue pH 1.0	Pearse (1968)	sulphated							
		polysaccharides	-	-	++	+++	+	+**	x
Autofluorescence	Pearse (1972)	} melanins	++	x	-	+++	x	+++	x
Schmorl	Pearse (1972)	} &	++	+	++	+++	+	+++**	++
Nile blue	Pearse (1972)	} lipofuscin	+++	+++	+	++	+	+++	+++
Sudan black B	Lillie (1965)	lipofuscin	+++	+++	++	+++	++	+++	+++
Hueck	Pearse (1972)	lipofuscin	+++	+++	++	+++	++	+++	+++

Table 3. Histochemical observations on intracellular granules of digestive system tissues (cont'd).

Staining procedure	Reference	Constituent	Cell Types						
			O	S	Da	Dm	Db	B	I
Perl's	Pearse (1972)	Fe^{+++}	+++	+++	+	+	-	-	+
Hutchinson's	Humason (1979)	Fe^{+++}	+++	+++	+	+	-	-	+
Hutchinson's with H_2O_2	Humason (1979)	masked Fe^{+++}	+++	+++	+	+	-	-	+
Hutchinson's with HNO_3	Humason (1979)	masked Fe^{+++}	+++	+++	+	+	-	-	+
Turnbull blue	Pearse (1972)	Fe^{++}	+++	-	-	-	-	-	-
Dithiozone	Pearse (1972)	Zn^{++}	-	-	-	-	-	-	-
Rubeanic acid	Pearse (1972)	Cu^{++}	-	-	-	-	-	-	-
von Kossa	Pearse (1972)	phosphate	+++	++	+	++	-	+++	++
Ebel's	Chayen et al. (1969)	polyphosphate	+++	+++	+	++	+	++	++
Ammonium molybdate	Pearse (1972)	phosphate	+	+	+	++	-	+	+

†control sections (Schiff reagent only) employed

*large lipid droplet associated with cell, separate from granules

**reaction confined to perimeter of granule

***indicates glycogen is present

****cell cytoplasm strongly positive

-, no detectable reaction; +, detectably positive; ++, moderately positive; +++, strongly positive; x, not tested

Os, small granules of oesophogeal cells; *Ol*, large granules of oesophogeal cells; *S*, stomach ciliated cells; *Da*, microvilli of digestive cells; *Dm*, mid region granules of digestive cells; *Db*, basal granules of digestive cells; *B*, basophil cells of digestive diverticulum; *I*, intestinal cells.

granules, 2.0 μm maximum diameter, composed of material with mixed opacity and membranous whorls distinct from those found in the oesophageal cells (Figure 64). These whorls appear to be hollow, often collapsed, spheres of lamellate material (each lamella 4.5 nm thick), which form around and are embedded in flocculant material. Patterns resembling crystalline ferritin (Figure 64) are found within the granule matrix. The nucleii of the stomach epithelial cells are located in the basal cytoplasm, and the basal cell membrane is infolded (Figure 62).

The granules react positively for protein, lipid, complex carbohydrates with detectable levels of glycogen and polysaccharide, and lipofuscin; ferric iron and phosphate produce strong reactions to these tests in the granules, but unlike the oesophageal granules, no ferrous iron was detected (Table 3).

Digestive cells

The digestive diverticula of *D. rectius* are lined predominantly by digestive cells (Figures 65-70). These are characterized by a densely microvillous apical membrane, and many intracellular lysosomes in varying stages of maturation (Figures 66-68, 70). Secondary lysosomes, with an homogeneous electron-opaque appearance, have a wide variety of sizes with a 13.3 μm maximum diameter found usually at the base of the cell (Figures 66, 67, 70). Tertiary lysosomes, with a more heterogeneous appearance, reach a maximum diameter of 5.8 μm (Figures 66, 68, 70). Associated with the enzyme secreting role of these cells is the presence of Golgi and endoplasmic reticulum (Figures 67, 69). Nucleii are located basally (Figure 70).

Figure 62. Stomach epithelial cell. Note granules and basal nucleii. Scale bar = 5 μm.

Figure 63. Zonula adherens and septate junction between stomach epithelial cells (apex to the top). Scale bar = 0.5μm.

Figure 64. Intracellular granules of stomach epithelial cells. Note lamellar whorls, parallel line patterns (*arrowheads*) and dense granulation (*double arrowheads*) indicative of ferritin. Scale bar = 0.5 μm.


64
63
62

Figure 65. Sections through digestive diverticulum tubules. Note digestive cells and basophil cells (*arrowheads*). Scale bar = 50 μm.

Figure 66. Apex of digestive cells and basophil cell (*B*). Note microvilli, secondary (*S*) and tertiary (*T*) lysosomes. Scale bar = 10 μm.

Figure 67. Secondary lysosomes of digestive cell. Scale bar = 3 μm.

Figure 68. Tertiary lysosomes of digestive cell. Scale bar = 2 μm.

Figure 69. Golgi apparatus of digestive cell. Note secretory products with 29-44 nm lamellar substructure. Scale bar = 0.5 μm.

Figure 70. Basal region of digestive cells. Note large secondary and tertiary lysosomes in basal cytoplasm, and amoebocytes within haemocoel (H). Scale bar = 15 μm.

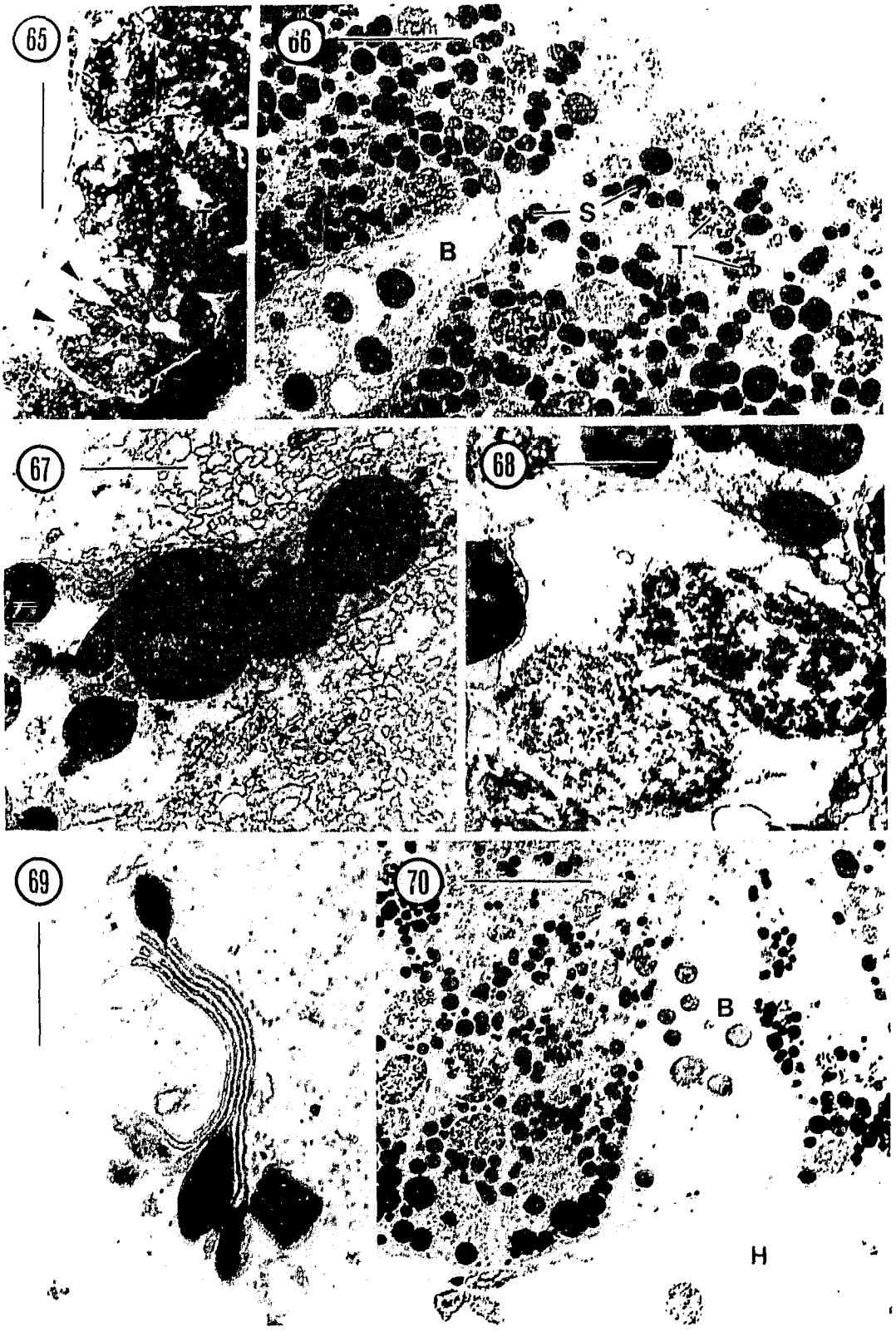
65
66
B
S
T
67
68
69
70
B
H

The histochemical characterization of the digestive cell granules differs according to intracellular region. Lipofuscin is found in granules throughout the cell, although those in the mid region react more strongly than those in the basal cytoplasm, consistent with their lysosomal origin and an increasing maturity from formation near the cell apex to digestion of contents in the mid-region lysosomes. Similarly, lipid content of the lysosomes increases with maturity, although these differences in staining densities may be a function of lysosome size (Figures 66-68, 70). Carbohydrates are found in all granules, with glycogen forming a major component of the carbohydrate store in the basal granules, and complex carbohydrates including polysaccharides found amongst the microvilli (probably mucus) and in the mid-region granules. The digestive cells are low in iron content compared to the oesophageal and stomach epithelium. Ferric iron was detected in the mucus surrounding the microvilli and in the mid-region granules, and absent in the basal granules; slightly higher phosphate levels are present in the mid-region granules (Table 3).

Basophil cells

The basophil cells of the digestive diverticulum are found between the digestive cells but are much less numerous (Figures 65, 66, 70). They are generally pyramidal in shape and smaller than the surrounding digestive cells. The luminal surface of the cells possesses microvilli (Figure 66), and septate junctions are found between the basophil and the digestive cells apically. The nucleus is located basally (Figure 70). The cytoplasm has an extensive rough endoplasmic reticulum and numerous vacuoles; granules within these vacuoles consist of alternately electron-opaque and transparent concentric bands (5.6 μm maximum diameter; Figures 66, 70-72). Flocculent material often appears to adhere to the granule periphery, suggesting formation by surface accretion (Figure 72). The granules

Figure 71. Cytoplasm and granules of basophil cells. Note rough endoplasmic reticulum and concentric substructure. Scale bar = 3 μm.

Figure 72. Granules of basophil cells. Note peripheral accretionary material (*H*, haemocoel). Scale bar = 2 μm.

Figure 73. Concentrically structured granule within amoebocyte. Scale bar = 4 μm.

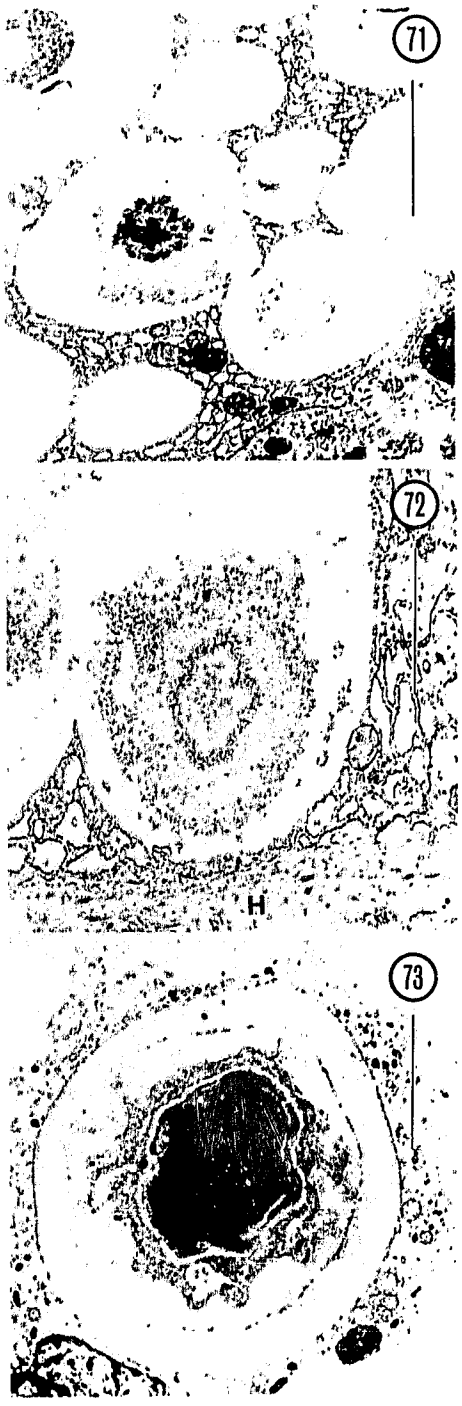
71
72
H
73

also incorporate a variety of larger materials, giving in some instances a heterogeneous appearance to the larger granules (Figure 71, 72). Similar granules are also found within amoebocytes circulating in the haemocoel of the digestive diverticulum (Figure 73).

Results of histochemical tests on the basophil granules show detectable levels of protein with a considerable quantity of carbohydrate present as both glycogen and polysaccharide. The prevalence of several reaction products in the periphery of the granule may be due to the highly mineralized nature of the deposits. Lipid is absent, but there is a strong positive reaction for lipofuscin (Table 3). There is no histochemical indication of iron, although a small peak appeared on EDX microanalytical spectra of basophil granules (Figures 74, 75). Peaks for calcium and phosphorus, probably present as phosphate (Table 4) were also obtained.

Intestinal epithelium

The intestinal epithelial cells (Figures 54, 76) have a microvillous apical membrane which also bears cilia; and nucleii are located basally. Considerable mucous secretion takes place (Figure 76). The cells often possess numerous intracellular granules which appear in light micrographs to have a mineralized appearance similar to the metal phosphate granules found in the oesophagus and stomach. Their histochemical properties shown in Table 3 indicate a very similar composition to those found within the stomach epithelium, with the exception that only very low levels of ferric iron are present.

Figure 74. Energy dispersive X-ray microanalysis spectrum of a basophil granule. Note peaks for calcium, iron and phosphorous. Chlorine peak produced by embedding medium, nickel peak produced by specimen support grid.

Figure 75. Energy dispersive X-ray microanalysis spectrum of background basophil cytoplasm. Note absence of peaks for calcium and iron. Chlorine peak produced by embedding medium, nickel peak produced by specimen support grid.

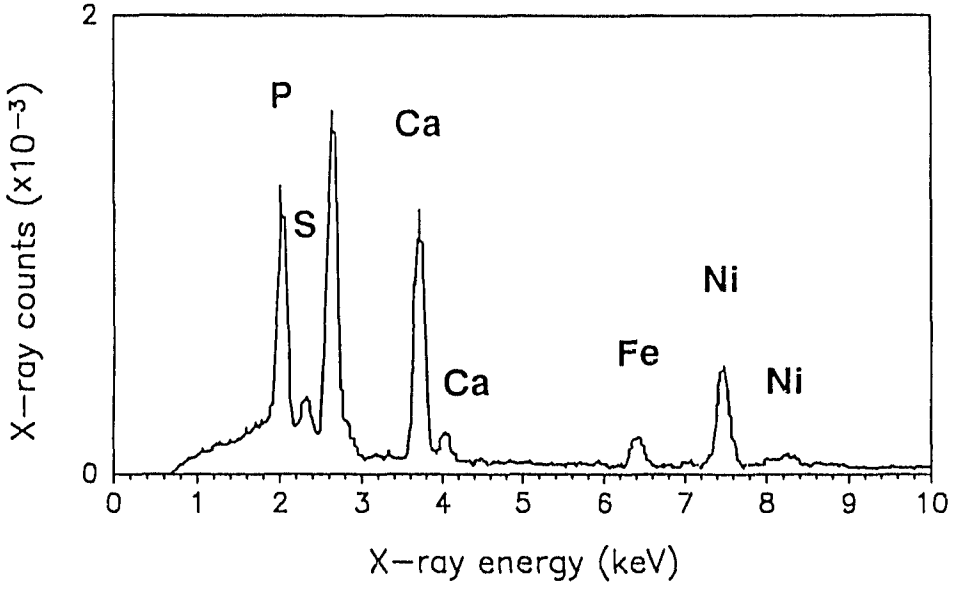
2
0
X-ray counts (x10⁻³)
P
S
Ca
Ca
Fe
Ni
Ni
0 1 2 3 4 5 6 7 8 9 10
X-ray energy (keV)

74

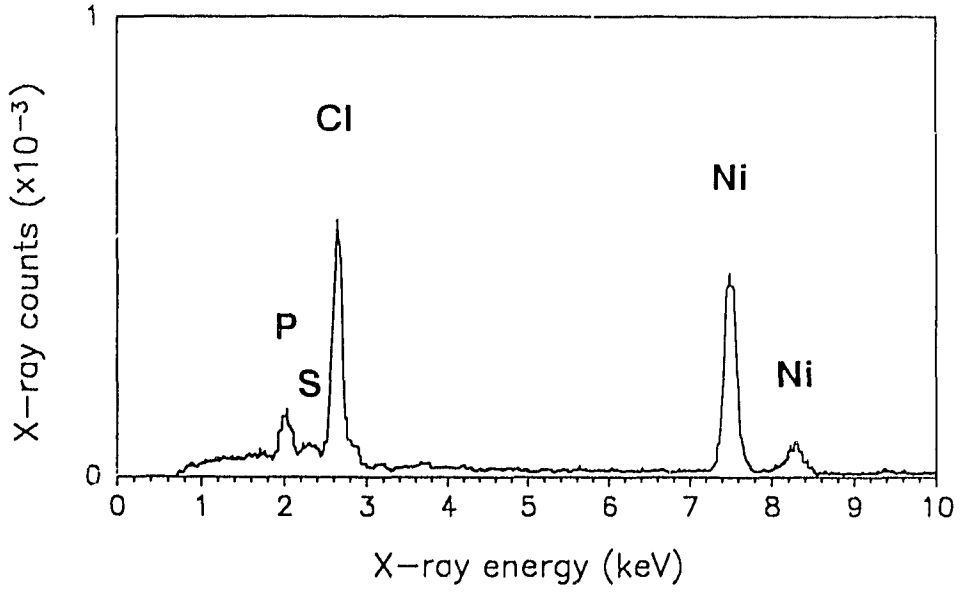
1
0
X-ray counts (x10⁻³)
Cl
P
S
Ni
Ni
0 1 2 3 4 5 6 7 8 9 10
X-ray energy (keV)

75

Figure 76. Intestinal epithelial cells. Note cilia (C) and microvilli (M) of apical membrane, mucous secretions (*arrowheads*), darkly staining intracellular granules and basal nucleii. Scale bar = 10 μm.

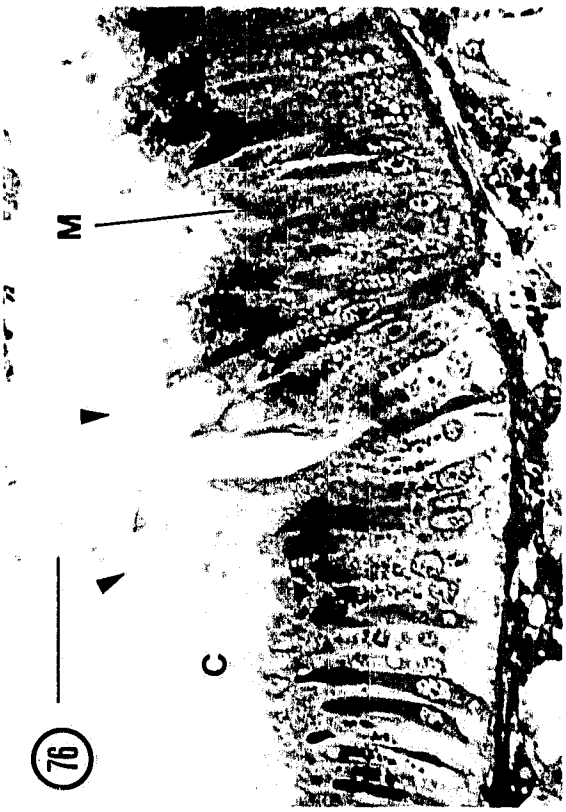
M
C
76

DISCUSSION

The anatomy of the scaphopod digestive system is summarized by Salvini-Plawen (1981), and the organisation of the gut in *Dentalium rectius* is similar to that of other dentaliid scaphopods. The radula has a simple arrangement common to all members of the class (Odhner, 1931; Morton, 1959; Taib, 1981a). The ultrastructure of the various cell types described is generally consistent with previous histological reports for *Dentalium* spp. (Lacaze-Duthiers, 1856; Fol, 1885, 1889; Plate, 1888; 1892; Morton, 1959; Taib, 1981a,b). The oesophageal cells in *D. rectius* release granules and secrete a mucus-like substance which reacts positively to histochemical tests for carbohydrates and polysaccharides (personal observations). This secretion likely functions in consolidating ingested material into a food bolus and initiating extracellular digestion. Mucus also coats the luminal surface microvilli of the digestive and intestinal cells. As in other molluscs, this probably facilitates adsorption of nutrients and is incorporated into lysosomes through pinocytotic uptake (Owen, 1972). While extracellular digestion occurs in the digestive diverticulum of scaphopods (Morton, 1959), there has been no characterisation of extracellular enzymes secreted by the digestive or basophil cells in *D. rectius* or other members of the class. Ciliated cells of the *Dentalium* stomach epithelium form several bands which serve as a sorting area and mix the ingested material (Morton, 1959; Salvini-Plawen, 1981). Oesophageal and stomach epithelia and digestive cells in *D. rectius* possess ultrastructural features indicative of transport across the basal cell membrane.

The only metals identified from the intracellular granules of the gut epithelia of *D. rectius* were calcium and iron. The ubiquitous presence of calcium phosphate granules is a common feature to many molluscan tissues involved in the elaboration of secretory materials, and they are generally considered to have a role in detoxification through the

incorporation of metal ions (Brown, 1982; Simkiss & Mason, 1983). They are also thought to be standby calcium resources for shell repair and for maintenance of blood calcium during periods of anoxia (Wilbur, 1985). Intracellular calcium phosphate granules, which contain zinc but no iron, have also been noted in the *D. rectius* kidney (Chapter 2; Reynolds, 1990).

The oesophageal and stomach epithelial cells of *D. rectius* are major sites of ferric iron accumulation in the gut. However, the low levels of iron in the granules of the basophil cells of the digestive gland and the intestinal epithelium suggest only a minor role in the iron metabolism of *D. rectius*. Ferric iron has been localised using histochemical or EDX methods in the digestive cells, labial palps, gut epithelium and gut contents of *Mytlilus edulis* (George et al., 1976; Lowe & Moore, 1979), and the iron content of intracellular granules in stomach (high), digestive (low) and basophil (absent) cells of *Littorina littorea* (Mason et al., 1984) parallels that found in *D. rectius*. Ferric iron is commonly a significant constituent of molluscan kidney granules (Delhaye 1976; Moore 1977; George and Pirie, 1980; George et al., 1982; Mason et al., 1984; Thomson et al., 1985; Sullivan et al., 1988), although it is absent from those of *D. rectius* (Chapter 2; Reynolds, 1990). Intracellular ferritin has been observed in studies of iron accumulation in molluscan tissues and is thought to maximize iron storage in intracellular granules (Simkiss et al., 1983). That ferritin may be involved in ferric iron storage in *D. rectius* is indicated by the parallel arrays noted within the iron-containing granules of the stomach epithelium. These are similar in appearance to intragranular ferritin identified from the gastropod *Biomphalaria* (Heneine et al. 1969) and the chiton *Acanthopleura* (Kim et al., 1989). Ferrous iron was found in the radular teeth and granules of the oesophageal cells. Ferrous iron is thought to be the ionic state of cytoplasmic iron attached to protein ligands, which is oxidised to ferric iron when stored attached to ferritin (Simkiss et al., 1983), and is also

thought to be actively transported from the surrounding epithelium to the tooth surface in radular mineralization (Kim et al., 1989).

Although scaphopods can generally be considered microcarnivores (Salvini-Plawen, 1981), the diet of *Dentalium rectius* is more diverse than other sympatrically occurring scaphopod species and has been described as omnivorous (Shimek, 1990). A considerable amount of ingested material is sediment, including mineral grains (Shimek, 1990). The sediment from which *D. rectius* was collected consists of very fine sand (48.7%) and medium-coarse silt (23.5%) with an organic content of 8.36% (±0.118 S.D.) (Reid & Brand, personal communication). The silty, high organic content of the sediments is comparable to other sites where *D. rectius* is found in abundance (Shimek, 1990). Iron is the most abundant metal present within the sediments ($38x10^3$ ppm), followed by aluminium ($35x10^3$ ppm) and calcium ($17x10^3$ ppm) (Reid & Brand, personal communication). Gut contents of *D. rectius* reacted positively to histochemical tests for both ferric and ferrous iron (personal observations). Iron found in oesophageal and stomach epithelia may be taken up directly from the contents of the gut lumen through the apical cell membrane, or transported to the oesophogeal and stomach cells from the digestive diverticulum and mantle epithelium, another site of significant iron uptake (Chapter 5), or a combination of all three. While studies of iron metabolism in *Mytilus* and *Nucella* indicate that uptake through ingested material is more significant than via external epithelium (Pentreath, 1973; George et al., 1975; Young, 1975; Young, 1977), experimental data are necessary to evaluate the respective contributions of iron uptake sites in *D. rectius*.

Iron transport occurs via amoebocytes, which phagocytose cytoplasmic packages of iron-containing granules released into the haemocoel from the mantle epithelium (Chapter 4). In *Mytilus edulis* and the limpets *Patella* and *Patelloida* haemolymph ferritin has been

identified as a high capacity iron binding protein capable of transporting iron and which may have a significant role in byssal formation and radular mineralization (George et al., 1975; Burford et al., 1986). Such proteins are likely present in *D. rectius*, although no studies have yet identified or examined the role of metalloproteins in Scaphopoda. Given the absence of iron excretion by the kidneys (Chapter 2; Reynolds, 1990), the ultimate fate of iron in *D. rectius* is either excretion with fecal material through release of oesophageal granules, or mineralization of the radula. The scaphopod radula is relatively large compared to that found in other molluscs (Morton, 1959) and has a high iron content some of which is in the form of magnetite (Shimek, personal communication). Shimek and Fontaine (personal communication) investigated the elemental composition of the radula in five species of scaphopods, including *D. rectius*, using EDX microanalysis. They found calcium, iron and zinc consistently, with zinc prevalent in the developing teeth; as in the chiton radula, iron probably replaces zinc as the teeth mature (Shimek & Fontaine, personal communication). Similar routes of iron excretion occur in all radulate molluscs, and accumulated iron is utilised in the byssus of the bivalve *Mytilus edulis*, where it plays a similar hardening role (George et al., 1976). Based on the present data, a summary of the iron pathway in *Dentalium rectius* is shown in Figure 77. Experimental studies are needed to further address the dynamics of this system, such as the extent of active and passive iron uptake across gut and mantle epithelia, the temporal nature and fate of oesophageal iron accumulation, and the role of the kidney in detoxification and excretion of excess or pollutant levels of iron and other metal ions.

Figure 77. Schematic diagram of iron pathway in *Dentalium rectius*. Note that no iron is excreted via the kidney. Ellipses represent relative proportions of sources and destinations based on qualitative comparisons of amount of iron present within tissues.

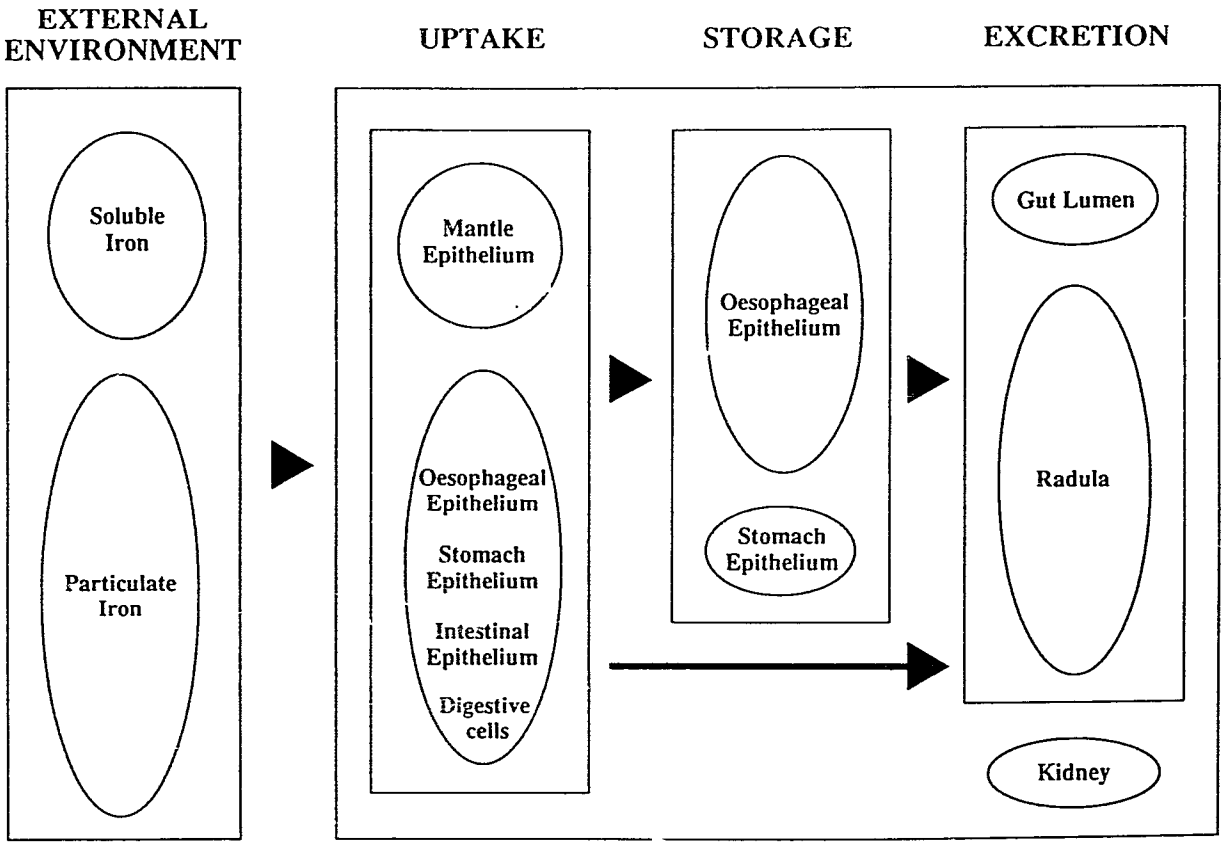
EXTERNAL ENVIRONMENT
UPTAKE
STORAGE
EXCRETION
Soluble Iron
Particulate Iron
Mantle Epithelium
Oesophageal Epithelium
Stomach Epithelium
Intestinal Epithelium
Digestive cells
Oesophageal Epithelium
Stomach Epithelium
Gut Lumen
Radula
Kidney

(77)

LITERATURE CITED

Brown, B. E. (1982). The form and function of metal-containing "granules" in invertebrate tissues. Biological Reviews of the Philosophical Society of Cambridge, 57, 621-667.

Bryan, G. W. (1973). The occurrence and seasonal variation of trace metals in the scallops *Pecten maximus* (L.) and *Chlamys opercularis* (L.). Journal of the Marine Biological Association of the United Kingdom, 53, 145-166.

Burford, M. A., Macey, D. J. & Webb, J. (1986). Hemolymph ferritin and radula structure in the limpets *Patelloida alticostata* and *Patella peronii* (Mollusca: Gastropoda). Comparative Biochemistry and Physiology, 83A(2), 353-358.

Chayen, J., Bitensky, L. & Butcher, R. G. (1973). Practical Histochemistry. John Wiley and Sons, Ltd., London.

Delhaye, W. (1976). Histophysiologie comparée des organes rénaux chez les archaeogastéropodes (Mollusca - Prosobranchia). Cahiers de Biologie Marine, 17, 305-322.

Doyle, L. J., Blake, N. J., Woo, C. C. & Yevich, P. (1978). Recent biogenic phosphorite: concretions in mollusk kidneys. Science, 199, 1431-1433.

Fol, H. (1889). Sur l'anatomie microscopique du Dentale. Archives de Zoologie Experimentale et Génerale, Deuxième Série, 7, 91-148, pls. 5-8.

Fol, M. H. (1885). Sur l'anatomie microscopique du Dentale,. Comptes rendu hebdomadaires des seances de l'academie des sciences. Serie D. Sciences naturelles., 1885, 1352-1355.

George, S. G., Coombs, T. L. & Pirie, B. J. S. (1982). Characterization of metal-containing granules from the kidney of the common mussel, *Mytilus edulis*. Biochimica Biophysica Acta, 716, 61-71.

George, S. G., Pirie, B. D. S. & Coombs, T. L. (1975). Transport of iron complexes in shellfish. In Hutchinson, T. C. (Ed.) International Conference on Heavy Metals in the Environment. Electrical Power Research Institute et al., Toronto.

George, S. G. & Pirie, B. J. S. (1980). Metabolism of zinc in the mussel, Mytilus edulis (L.): a combined ultrastructural and biochemical study. Journal of the Marine Biological Association of the United Kingdom, 60, 575-590.

George, S. G., Pirie, B. J. S. & Coombs, T. (1980). Isolation and elemental analysis of metal rich granules from the kidney of the scallop, Pecten maximus (L.). Journal of Experimental Marine Biology and Ecology, 42, 143-156.

George, S. G., Pirie, B. J. S. & Coombs, T. L. (1976). The kinetics of accumulation and excretion of ferric hydroxide in *Mytilus edulis* (L.) and its distribution in the tissues. Journal of Experimental Marine Biology and Ecology, 23, 71-84.

Heneine, F., Gazzinelli, G. & Tafuri, W. L. (1969). Iron metabolism in the snail *Biomphalaria glabrata*: uptake, storage and transfer. Comparative Biochemistry and Physiology, 28, 391-399.

Humason, G. L. (1979). Animal Tissue Techniques (fourth ed). Freeman, San Francisco.

Kim, K. -S., Macey, D. J., Webb, J. & Mann, S. (1989). Iron mineralization in the radula teeth of the chiton *Acanthopleura hirtosa*. Proceedings of the Royal Society of London, B 237, 335-346.

Lacaze-Duthiers, H. (1856). Histoire de l'organisation et du développement du Dentale. Annales des Sciences Naturelles, Quatrième Séries, Paris, 6, 319-385, pls. 11-13.

Leeson, C. R. & Leeson, T. S. (1970). Staining methods for sections of epon-embedded tissues for light microscopy. Canadian Journal of Zoology, 48, 189-191.

Lillie, R. D. (1965). Histopathologic Technic and Practical Histochemistry (third ed). McGraw-Hill, New York.

Lowe, D. M. & Moore, M. N. (1979). The cytochemical distributions of zinc (Zn II) and iron (Fe III) in the common mussel, *Mytilus edulis*, and their relationship with

lysosomes. Journal of the Marine Biological Association of the United Kingdom, 59, 851-858.

Mason, A. Z. & Simkiss, K. (1983). Interactions between metals and their distribution in tissues of *Littorina littorea* (L.) collected from clean and polluted sites. Journal of the Marine Biological Association of the United Kingdom, 63, 661-672.

Mason, A. Z., Simkiss, K. & Ryan, K. P. (1984). The ultrastructural localization of metals in specimens of *Littorina littorea* collected from clean and polluted sites. Journal of the Marine Biological Association of the United Kingdom, 64, 699-720.

Moore, M. N. (1977). Lysosomal responses to environmental chemicals in some maine (sic) invertebrates. In C. S. Giam (Ed.), Pollutant effects on marine organisms. (pp. 143-154). Lexington Books, Lexington.

Morton, J. E. (1959). The habits and feeding organs of *Dentalium entalis*. Journal of the Marine Biological Association of the United Kingdom, 38, 225-238.

Nott, J. A. & Nicolaidou, A. (1989). The cytology of heavy metal accumulations in the digestive glands of three marine gastropods. Proceedings of the Royal Society of London, B 237, 347-362.

Odhner, N. H. (1931). Die Scaphopoden. In Bock, S. (Ed.), Further Zoological Results of the Swedish Antarctic Expedition 1901-1903 (pp. 1-8, pls. 1, 2). Norsedt, Stockholm.

Owen, G. (1972). Lysosomes, peroxisomes and bivalves. Science Progress Series, Oxford, 60, 299-318.

Pearse, A. G. E. (1968). Histochemistry, Theoretical and Applied, 1 (third ed). Churchill, London.

Pearse, A. G. E. (1972). Histochemistry, Theoretical and Applied, 2, (third ed). Churchill Livingston, London.

Pentreath, R. J. (1973). The accumulation from water of ^{65}Zn, ^{54}Mn, ^{58}Co and ^{59}Fe by the mussel, Mytilus edulis. Journal of the Marine Biological Association of the United Kingdom, 53, 127-143.

Plate, L. (1890). Ueber einige Organisationsverhältnisse der Dentalien. Sitzungsberichte der Gesellschaft zur Beförderung der gesammten Naturwissenschaften, 1890, 26-29.

Plate, L. H. (1888). Bemerkungen zur Organisation der Dentalien. Zoologis her Anzeiger, 14, 78-80.

Plate, L. H. (1892). Ueber den Bau und die Verwadtschaftsbeziehungen der Solenoconchen. Zoologische Jahrbucher Jena Abteilung für Anatomie, 5, 301-386, pls. 23-26.

Reynolds, P. D. (1990). Fine structure of the kidney and characterization of secretory products in *Dentalium rectius* (Mollusca, Scaphopoda) Zoomorphology, 110(1), (in press).

Salvini-Plawen, L. v. (1981). The molluscan digestive system in evolution. Malacologia, 21(1-2), 371-401.

Shimek, R. L. (1990). Diet and habitat utilization in a Northeastern pacific ocean scaphopod assemblage. American Malacological Bulletin, 7(2), 147-169.

Simkiss, K. & Mason, A. Z. (1983). Metal ions: metabolic and toxic effects. In P. W. Hochachka (Ed.) The Mollusca, v. 2, Environmental Biochemistry and Physiology (pp. 101-164). Academic Press, New York.

Sullivan, P. A., Robinson, W. E. & Morse, M. P. (1988). Isolation and characterization of granules from the kidney of the bivalve Mercenaria mercenaria. Marine Biology, 99, 359-368.

Taib, N. T. (1981a). Gross anatomy of the alimentary canal of *Dentalium entalis* L. (Scaphopoda). Journal of the College of Science, University of Riyadh, Saudi Arabia, 12(1), 139-145.

Taib, N. T. (1981b). Sites of absorption and food storage in the gut of *Dentalium entalis* L. Journal of the College of Science, University of Riyadh, Saudi Arabia, 12(1), 147-154.

Thomson, J. D., Pirie, B. J. S. & George, S. G. (1985). Cellular metal distribution in the Pacific oyster, *Crassostrea gigas* (Thun.) determined by quantitative X-ray microprobe analysis. Journal of Experimental Marine Biology and Ecology, 85, 37-45.

Wilbur, K. M. (1985). Topics in molluscan mineralization: present status, future directions. American Malacological Bulletin, Special Edition(1), 51-58.

Young, M. L. (1975). The transfer of ^{65}Zn and ^{59}Fe along a *Fucus serratus* (L.) Æ *Littorina obtusata* (L.) food chain. Journal of the Marine Biological Association of the United Kingdom, 55, 583-610.

Young, M. L. (1977). The roles of food and direct uptake from water in the accumulation of zinc and iron in the tissues of the dogwhelk, *Nucella lapillus*. Journal of Experimental Marine Biology and Ecology, 30, 315-325.

CHAPTER 5

FINE STRUCTURE OF THE CILIATED BANDS OF THE *DENTALIUM RECTIUS* MANTLE: EVIDENCE FOR GAS EXCHANGE AND IRON UPTAKE

ABSTRACT

The ultrastructure of the ciliated bands found in the scaphopod mantle cavity is described for the first time in *Dentalium rectius*. The bands consist of series of 20-30 ridges, which encircle the mid-region of the mantle cavity and are continuous through mantle and body wall epithelia. They are composed of ciliated and supporting cell types. The supporting cells are sharply demarcated from the surrounding mantle epithelium, and are characterised by a densely microvillous apical membrane which is highly domed; this produces a network of deep crevices between adjacent cells which extend to within 1 μm of the basal lamina and haemocoel. The supporting cells are also the site of iron uptake by pinocytosis. The iron-containing vesicles are incorporated into the lysosomal system or are secreted by an apocrine-like process into the extensive haemocoel beneath the bands, where they are phagocytosed by amoebocytes. The ciliated bands in *D. rectius* function in respiratory current production, and appear from their ultrastructure to be areas of the mantle epithelium specialized for gas exchange and active transport. As such, they may be considered the functional equivalents of ctenidia, which have been lost in this molluscan class.

INTRODUCTION

Among the characters that distinguish the Scaphopoda from other molluscan classes are several unique morphological features associated with the mantle cavity. During development, two mantle lobes originate dorso-laterally and fuse ventrally to form a narrow space which extends the length of the animal (Moor, 1983); the mantle cavity is therefore open at both ends. The Scaphopoda are the only molluscan class which are known to lack osphradia and ctenidia. Elaborations of scaphopod mantle tissues include the slit-like openings to the haemocoel (Lacaze-Duthiers (de), 1857) and the development of the posterior mantle into the sensory pavilion, which is also capable of shell secretion and dissolution (Chapters 6 and 7). Another such feature is a series of ciliated bands which runs transversly along both body and mantle walls just anterior to the anal opening (Distaso, 1905; Fol, 1889; Lacaze-Duthiers (de), 1857; Odhner, 1931; Plate, 1888; Plate, 1892; Yonge, 1937). While such bands are present in all scaphopods, there are generally fewer in the Gadilida than in the Dentaliida, and range from a single band in *Gadila metivieri* (Steiner, personal communication) to over thirty in *Dentalium rectius* .

The ciliated bands create water currents within the mantle cavity (Distaso, 1905; Lacaze-Duthiers (de), 1857; Taib, 1980; Yonge, 1937) which are thought to assist gas exchange. Plate (1892) considered the bands to be analogous to molluscan ctenidia, while Distaso (1905) suggested that they were homologous structures. In addition to their putative role in respiration, the high iron content of many tissues in *D. rectius* (Chapter 4) suggests that such a region of specialized epithelium may have a significant role in metal uptake, as has been shown for the ctenidia of the bivalve mollusc *Mytilus edulis* (George et al., 1975; 1976; Pentreath, 1973). Investigation of the ciliated bands of the scaphopod mantle cavity to date have been entirely histological. This study examines the ultrastructure of the ciliary bands and histochemical characteristics of their cellular inclusions in

Dentalium rectius with a view towards elucidating their role in the uptake of metals and gas exchange.

MATERIALS AND METHODS

Dentalium rectius was collected from dredged subtidal (60 m) sediments of Satellite Channel, British Columbia. Specimens for light microscopy were fixed in 10% seawater formalin, dehydrated in ethanol and embedded in paraffin. Histological sections were stained in eriochrome cyanin (Chapman, 1977). Tissues for electron microscopy were initially fixed in phosphate-buffered glutaraldehyde at room temperature, rinsed in phosphate buffer, and followed by a post-fixation treatment of phosphate-buffered osmium tetroxide at 4°C. Tissues were rinsed in distilled water and dehydrated in ethanol. For scanning electron microscopy (SEM), tissues were critical point dried from CO_2, gold coated and viewed using a JEOL JSM-35 scanning electron microscope. Tissues prepared for transmission electron microscopy (TEM) were infused with propylene oxide, embedded in epon resin and sectioned on a Reichert ultramicrotome. Sections with grey to pale gold interference colour were stained with uranyl acetate and lead citrate, and examined using a Philips EM-300 transmission electron microscope.

RESULTS

The ciliary bands in *Dentalium rectius* are ciliated transverse ridges located immediately anterior to the anal bulb, within the mantle cavity (Figures 1, 78). They vary in number (usually 20-35) and are found on both the body and mantle walls, each band running in a contiguous but discontinuous circuit around the mantle cavity (Figures 79,

80). When fixed, the cilia are usually directed anteriorly (Figure 79). The ridges are composed of both ciliated cells and supporting, non-ciliated cells (Figures 79-81).

Ciliated cells

Most ciliated cells bear hundreds of cilia reaching 25 μm in length, although some areas of the bands have fewer, shorter cilia (Figures 82, 83). The ciliated cells vary between 10-24 μm in height, with the higher cells usually located in the body wall epithelium (Figures 78, 84, 85). The apical membrane does not bear microvilli. Zonula adherens and septate junctions are found between the ciliated cells and supporting cells (Figure 86). The cilia have a basal rootlet which bulges just below the basal body to a maximum observed width of 162 nm, then tapers from approximately 105 nm to 58 nm towards its base (Figures 86, 87). The rootlets emerge from the basal body at a consistent angle and orientation (Figure 86); they extend into the mid region of the cell cytoplasm and reach as up to 13 μm in length in the largest observed cells. The rootlet appears finely striated in some instances, with a periodicity decreasing along the length of the rootlet from 30 to 10 nm (Figure 87).

The cytoplasm is characterised by the presence of golgi, mitochondria, a large quantity of glycogen and a variety of membrane delimited vesicles (Figures 86-89). These vesicles contain electron opaque, flocculent material in varying amounts (Figure 87) and range in diameter from 116 nm to 0.8 μm granules (Figures 87-89). Vacuoles (with a maximum observed diameter of 6.1 μm) are found in the basal cytoplasm and contain larger quantities of flocculent material with the same appearance (Figures 84, 88). The

Figure 78. Longitudinal section of *D. rectius* showing the ciliated ridges of the body wall (*upper arrowheads*) and mantle wall (*lower arrowheads*) within the mantle cavity (*M*) (*I*, intestine; *K*, kidney; *S*, stomach). Scale bar = 0.5mm.

Figure 79. Ciliated bands lining the mantle cavity. Scale bar = 0.1mm.

Figure 80. Ciliated bands of the body (*B*) and mantle (*M*) walls. Note the discontinuity of ciliated bands. *Arrowhead* indicates commensal trichodyne. Scale bar = 0.1mm.

Figure 81. Oblique transverse sections of ciliated bands, showing ciliated and supporting (*S*) cells. Note the posterior displacement of the ciliated cell nucleii (*arrowheads*) and network of channels between the supporting cells (*C*, cilia). Thick epon resin section, light photomicrograph. Scale bar = 20μm.

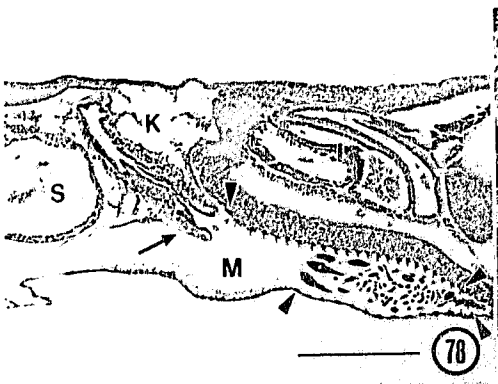
K
S
M
78

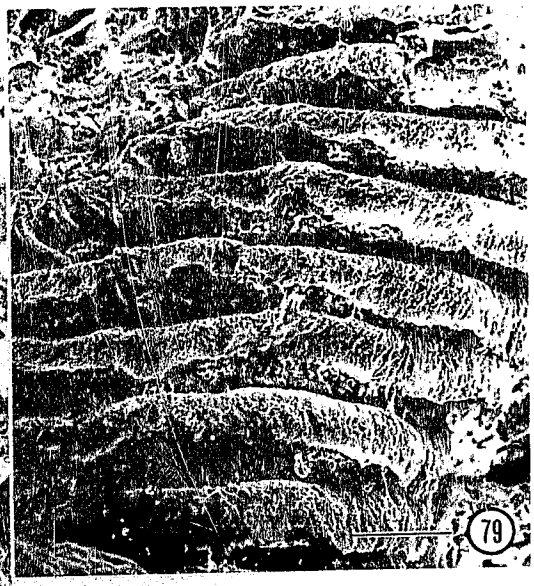
79


M
B
B
80

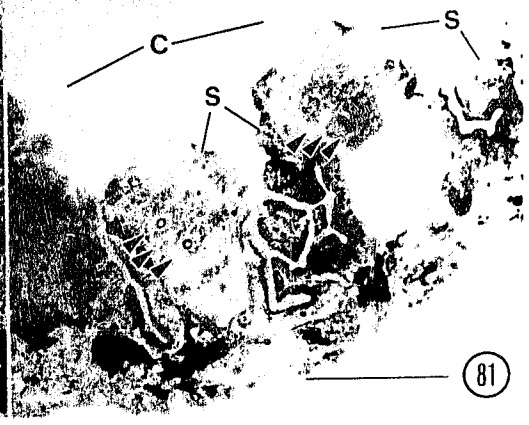
C
S
S
81

Figure 82. Ciliary tufts of ciliated bands of the mantle cavity. Scale bar = 40μm.

Figure 83. Low ridges and reduced ciliation in ciliated bands of the mantle cavity. Compare with Figure 82. Scale bar = 30μm.

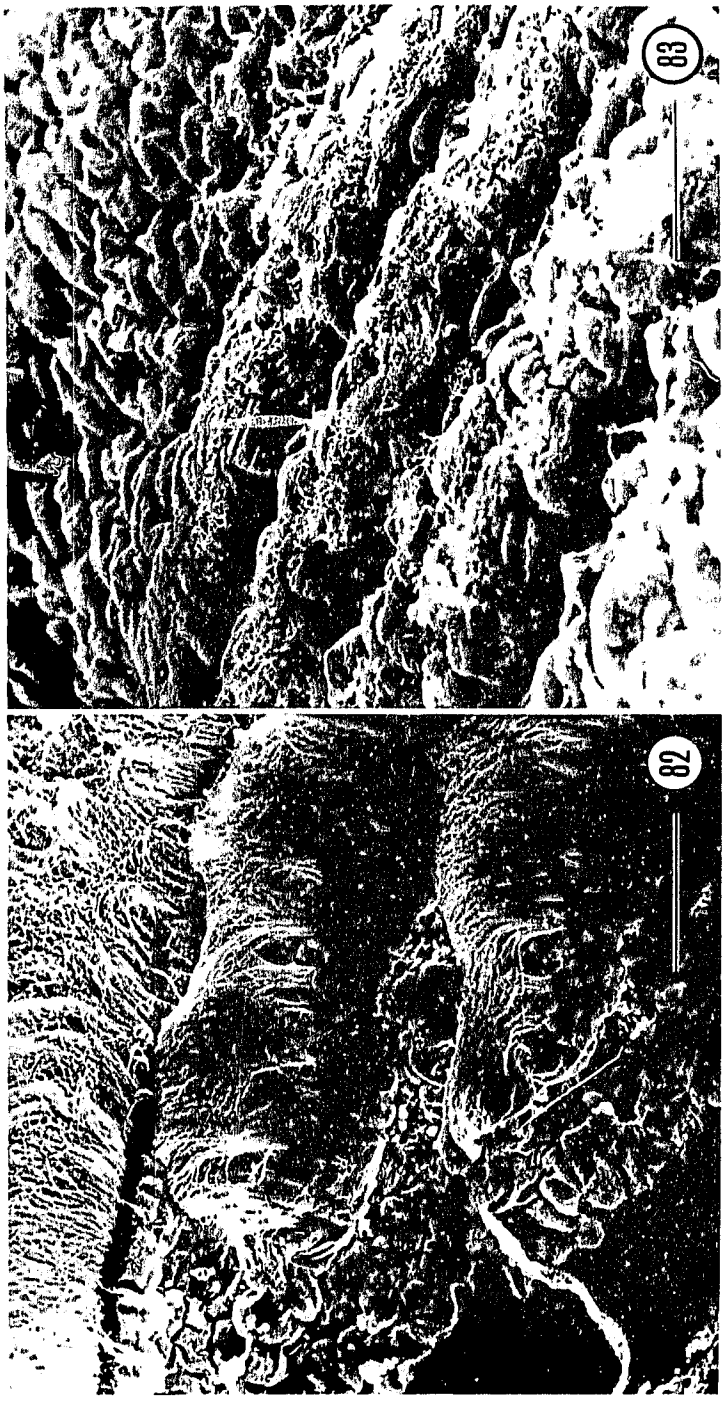
83
82

Figure 84. Longitudinal section through ciliated and supporting (*S*) cells of a ciliated band of the body wall (*large arrowhead*, granules of ciliated cell; *double arrowhead*, lamina densa; *thin arrow*, cell bodies of adjacent ciliated cells; *thick arrow*, vacuoles among high numbers of mitochondria; *M*, muscle layer). Scale bar = 3μm.

Figure 85. Longitudinal section through ciliated and supporting cells of a ciliated band of the mantle wall (*arrowheads*, outer mantle epithelium; *H*, haemocoel). Scale bar = 6μm.

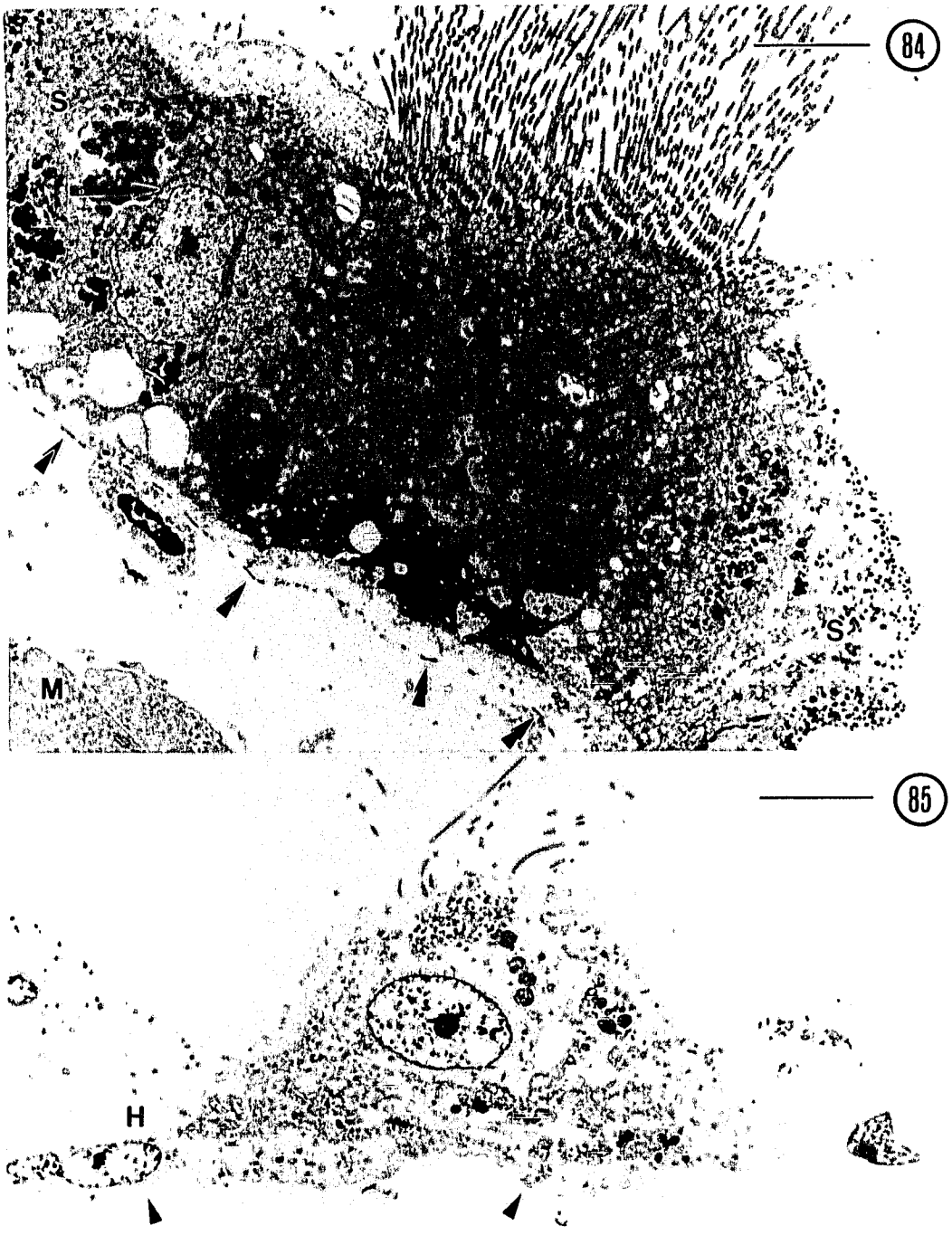
84
S
S
M
85
H

Figure 86. Ciliated and supporting cell apices. Note intracellular granules of the supporting cell, and basal rootlets of the ciliated cell. Scale bar = 2μm.

Figure 87. Apical cytoplasm of a ciliated cell, across plane of ciliary rootlets. Note glycogen, mitochondria, endoplasmic reticulum, basal apparatus of cilia (*B*) and striation of rootlets (*arrowheads*). Scale bar = 0.5μm.

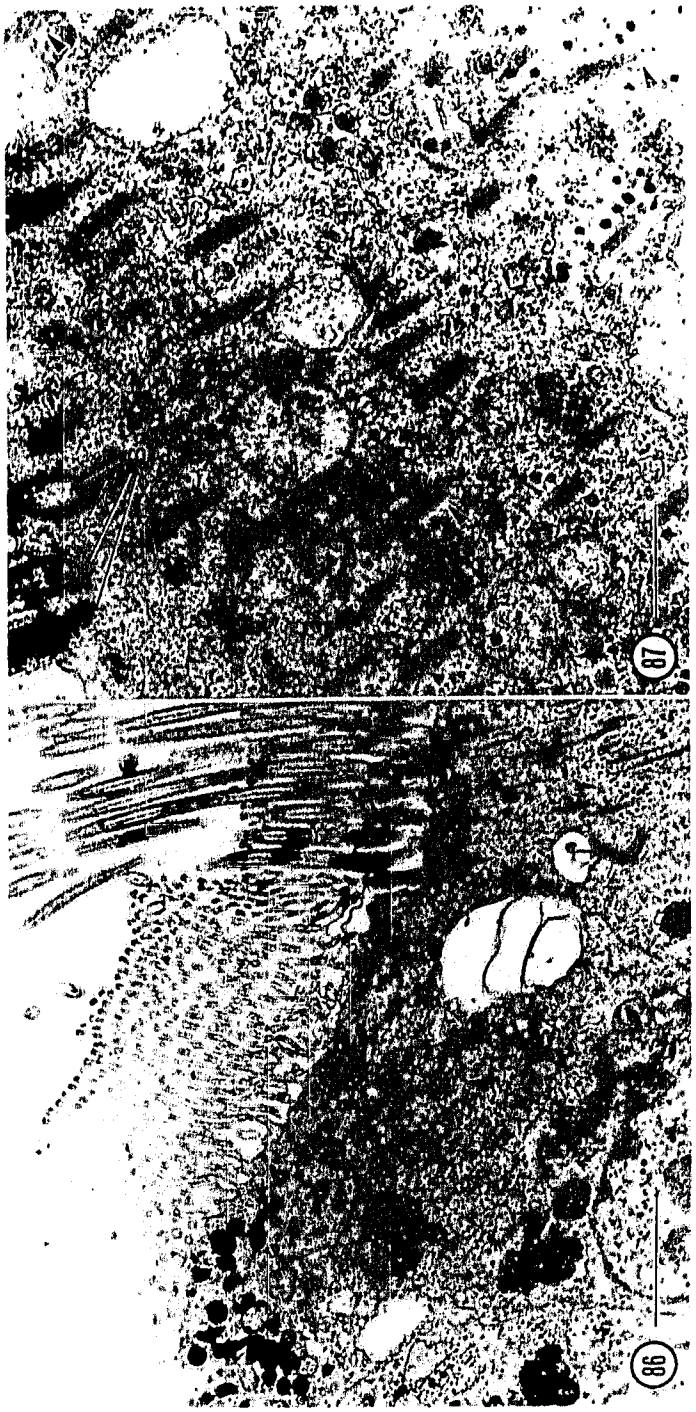
87
88

histochemistry of the granules and vacuolar contents are presented in Table 4. They are nearly identical in their composition, with protein and polysaccharide carbohydrates as the main organic constituents. Iron, probably present as phosphates, is a detectable inorganic component. There is a strong indication for the presence of lipofuscin which, with the ultrastructural evidence, suggests that these granules and vacuoles are tertiary lysosomes.

The nucleus of the ciliated cells is situated towards the base of the cell, and is consistently displaced towards the posterior cell membrane (Figures 81, 85). The cells are separated from the underlying haemocoel by a basal lamina, and by an additional electron opaque layer referred to here as the lamina densa (Figure 89, 90). The lamina densa is discontinuous, and appears to form a reticulum beneath the epithelium; it has a fibrous substructure (Figure 90). Nerve processes are located in basal intercellular spaces, above the basal lamina (Figure 89).

Supporting cells

The supporting cells of the ciliated ridges distinguish the region from the rest of the mantle, as their apices rise well above the general mantle epithelium (Figure 91). They form narrow clefts with neighbouring supporting cells (Figures 92, 93), producing an extensive system of channels which runs between and surrounds the cells (Figure 81). The crevices run to within 1 μm of the basal lamina in some instances (Figure 85, 93). The apical cell membrane forms a dense layer of microvilli which have a fibrillar coating, probably mucus (Figures 84, 85, 86, 91-96).

The cells range from 6-10 μm in height (Figure 94). The cytoplasm of the supporting cells contains glycogen, mitochondria, electron transparent vesicles and

Figure 88. Granules and vacuoles of the mid-region cytoplasm of the ciliated cells. Scale bar = 2μm.

Figure 89. Ciliated cell base. Note nerve axon profiles with synaptic vesicles (N) and lamina densa (arrowheads). Scale bar = 3μm.

Figure 90. Fibrous substructure of lamina densa. Scale bar = 0.5μm.

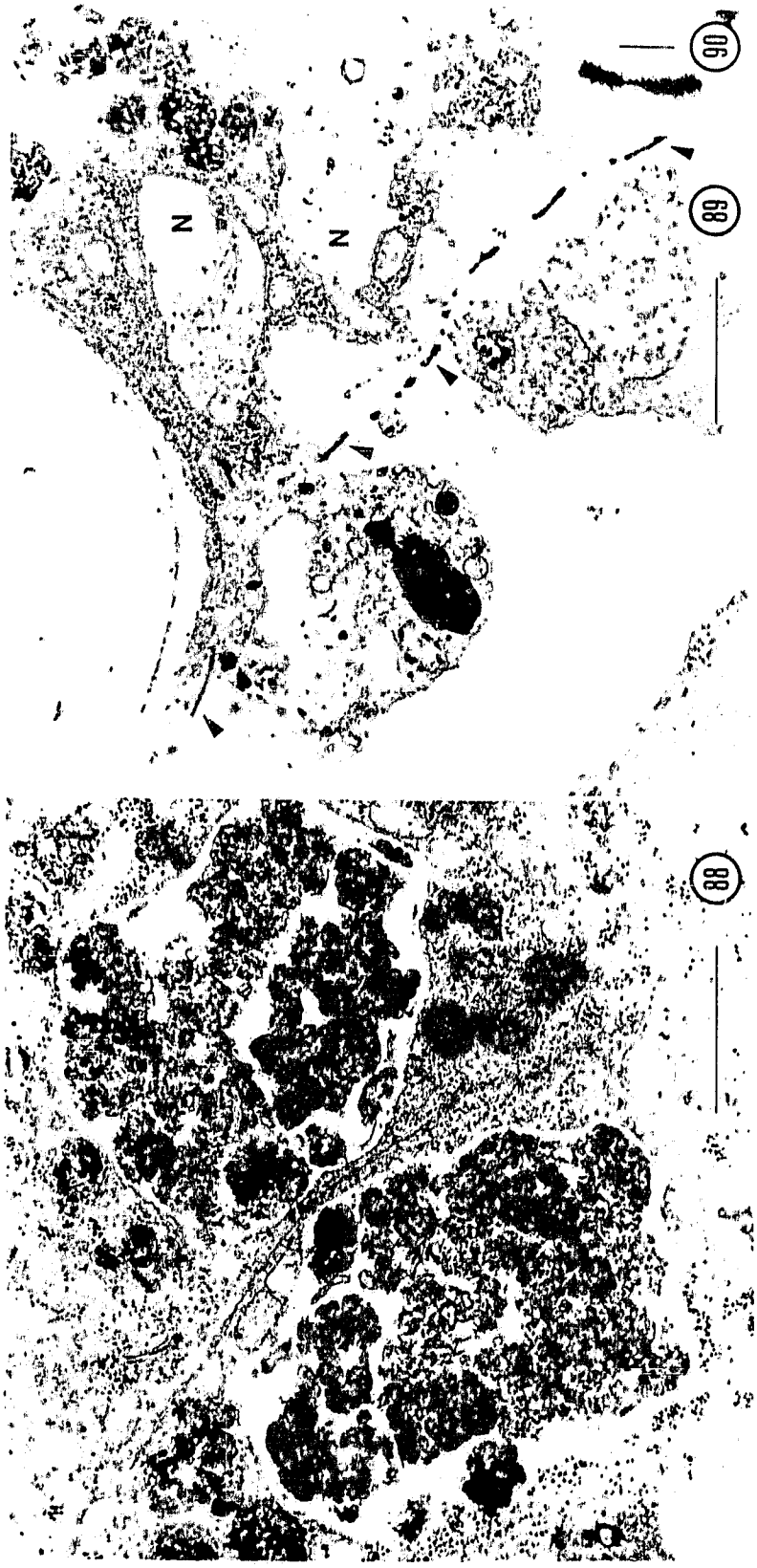
90
88
N
N
88

Table 4. Histochemical observations on the intracellular granules of the ciliated bands lining the mantle cavity.

Staining procedure	Reference	Constituent	C	S	M
Mercuric chloride-bromphenol blue	Pearse (1968)	proteins	++	+++	+++
Sudan black B	Humason (1979)	lipids	x	x	+*
Hexamine silver	Pearse (1972)	uric acid, urates	-	-	-
Periodic acid-Schiff†	Humason (1979)	carbohydrates	++	++	++
PAS with diastase†	Humason (1979)	carbohydrates, glycogen removed	++	++	+**
Best's carmine	Pearse (1968)	glycogen	++	++	++
Toluidine blue	Pearse (1968)	mucins	-	-	-
Alcian blue pH 2.5	Pearse (1968)	polysaccharides	+	++	++
Alcian blue pH 1.0	Pearse (1968)	sulphated polysaccharides	-	+	+
Autofluorescence	Pearse (1972)	} melanins	+	x	+
Schmorl	Pearse (1972)	} &	++	+++	+++
Nile blue	Pearse (1972)	} lipofuscin	+++	+++	+++
Sudan black B	Lillie (1965)	lipofuscin	++	++	++
Hueck	Pearse (1972)	lipofuscin	+++	+++	+++

Table 4. Histochemical observations on the intracellular granules of the ciliated bands lining the mantle cavity (cont'd).

Staining procedure	Reference	Constituent	C	S	M
Perl's	Pearse (1972)	Fe^{+++}	+	+	++
Hutchinson's	Humason (1979)	Fe^{+++}	-	+	++
Hutchinson's with H_2O_2	Humason (1979)	masked Fe^{+++}	+	+	++
Hutchinson's with HNO_3	Humason (1979)	masked Fe^{+++}	+	+	+++
Turnbull Blue	Pearse (1972)	Fe^{++}	-	-	-
Dithizone	Pearse (1972)	Zn^{++}	-	-	-
Rubeanic Acid	Pearse (1972)	Cu^{++}	-	-	-
von Kossa	Pearse (1972)	phosphate	++	x	++
Ebel's	Chayen et al. (1969)	polyphosphate	++	x	++
Ammonium molybdate	Pearse (1972)	phosphate	+	x	+

†control sections (Schiff reagent only) employed.

*large lipid droplet associated with cell, seperate from granules.

**indicates glycogen is present.

-, no detectable reaction; +, detectably positive; ++, moderately positive; +++, strongly positive; x, not tested.

C, ciliated cells of ciliated ridges; S, supporting cells of ciliated ridges; M, general epithelium lining mantle cavity.

Figure 91. Differentiated supporting mantle epithelium of the ciliated bands. Note smooth surface of indifferent mantle epithelium to the top and left. Scale bar = 0.1mm

Figure 92. Supporting cells of the ciliated bands. Note dense microvilli and deep, narrow crevices between cell apices which appear to be bridged by microvilli. Scale bar = 10μm.

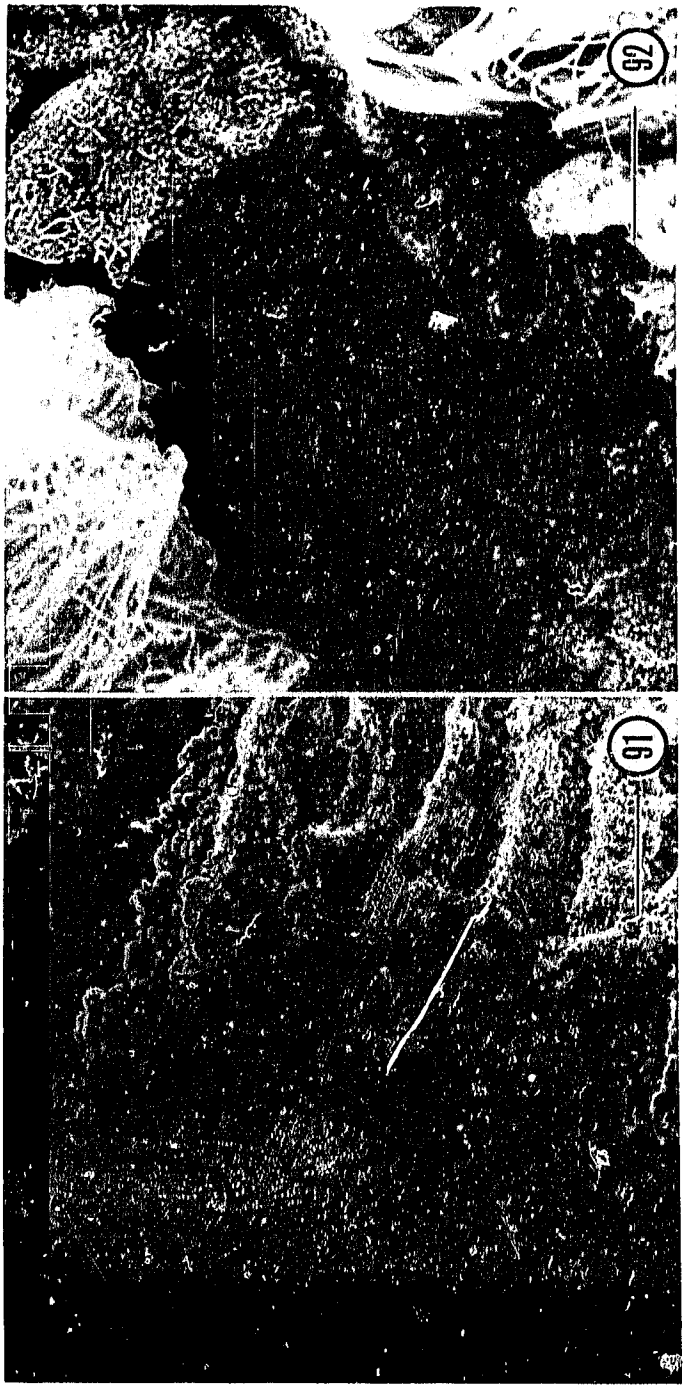
62
61

Figure 93. Supporting cells of the ciliated bands. Note deep crevices between cells (*arrowheads*, lamina densa). Scale bar = 4μm.

Figure 94. Supporting cell of the ciliated bands. Note microvillous apical membrane, dense intracellular granules of the apical cytoplasm, basal lamina (*arrowhead*) and lamina densa (*double arrowhead*) Scale bar = 3μm.

93

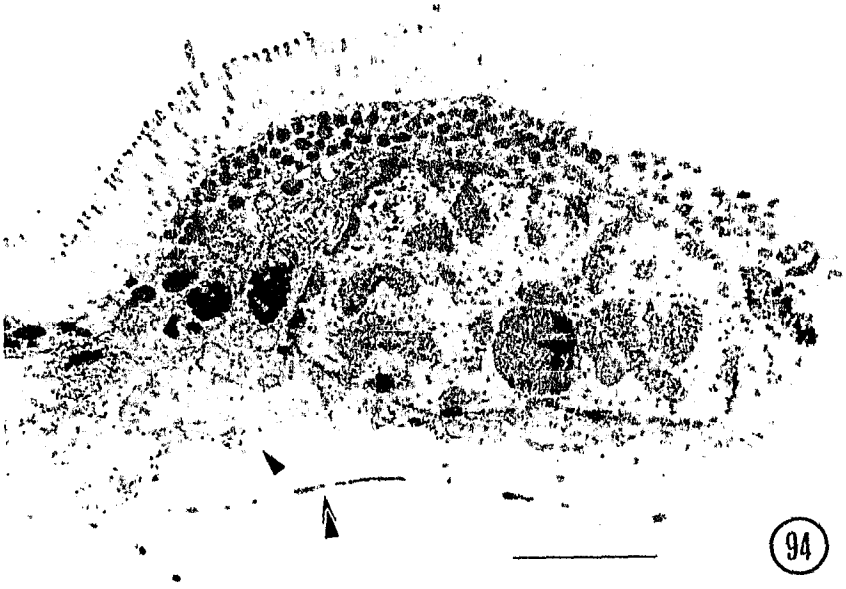

94

vacuoles containing heterogenous material similar to the tertiary lysosomes of the ciliated cells (Figure 94). The apical cytoplasm contains a high density of membrane delimited granules (maximum diameter 0.7 μm) which have an homogeneous, electron opaquematrix with scattered particles within it (Figures 94, 95). They are further distinguished from the tertiary lysosomes by the presence of glycogen and a moderate to strong reaction for ferric iron (Table 4). They appear to be endocytosed by the apical cell membrane (Figure 96). The nucleus is located basally, and the basal cell membrane has processes which extend through intercellular space to the basal lamina. In addition, the *lamina densa* noted beneath the ciliated cells also underlies the supporting cells (Figure 94).

Haemocoel and Amoebocytes

The haemocoel underlies the entire mantle cavity epithelium (Figure 97). In the region of the ciliated bands, this is more extensive beneath the body wall epithelium than the mantle epithelium. Additionally, there is a substantial muscle layer beneath the body wall ciliary bands, not found within the mantle wall (Figures 78, 84, 85).

Amoebocytes are found throughout the haemocoel (Figure 97; personal observation) and have a central nucleus and several pseudopodia (Figure 98). The cells possess mitochondria and vesicles which are largely electron transparent. Glycogen and granules similar to those of the supporting cells are also characteristic cytoplasmic inclusions. The amoebocytes were often in close association with the lamina densa at the base of the supporting cells (Figure 84). In some instances, cytoplasmic fragments of the

Figure 95. Apical cytoplasm of the supporting cells. Note endoplasmic reticulum, golgi apparatus and the particulate material scattered within the homogeneous matrix of the membrane-delimited granules. Scale bar = 1μm.

Figure 96. Endocytosis of granules by supporting cells of the ciliated bands. Scale bar = 20nm


95

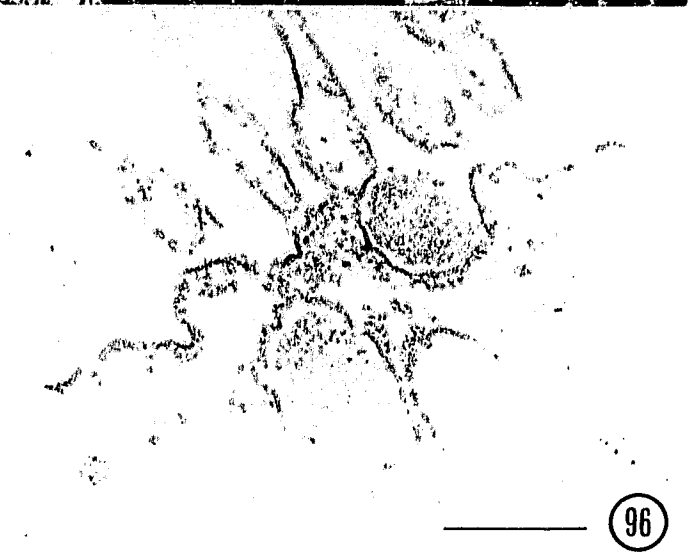
96

Figure 97. View of the body wall epithelium lining the mantle cavity. Note the extensive haemocoelic space containing numerous amoebocytes between the epithelium and underlying muscle layer. Scale bar = 10μm.


97

Figure 98. Amoebocyte within haemocoel beneath supporting cells of the ciliated bands. Note granule-containing cytoplasm within the amoebocyte (*N*, nerve axon profiles). Scale bar = 3μm.

Figure 99. Fragment of granule-containing cytoplasm passing through the lamina densa (*arrowheads*) beneath a supporting cell of the ciliated bands. Scale bar = 1μm.


98
N
99

support cells which contained granules were observed crossing the lamina densa (Figure 99); these seem to be subsequently phagocytosed by amoebocytes (Figure 98), which tested positively for iron using the histochemical tests listed in Table 4.

DISCUSSION

The ciliated bands of scaphopods have long been known to produce currents in the pallial cavity, drawing water from its posterior opening towards the anterior (Lacaze-Duthiers (de), 1857), and similar currents are produced in *Dentalium rectius* (personal observations). The initial intake of water into the scaphopod mantle cavity is produced by dilation of the foot (Yonge, 1937) and movement of the epipodial lobes (Taib, 1980). Water leaves the mantle cavity through the anterior mantle opening by the beating of the ciliary bands (Steiner, personal communication) and through the posterior opening by periodic expulsions due to withdrawal of the foot (Taib, 1980; personal observations), which also ejects feces (Yonge, 1937) and gametes (Dinamani, 1964) from the mantle cavity (personal observations). The currents produced by the ciliary bands produce a constant flow of water over structures which have been suggested as sites of gas exchange, such as the pulsating anal bulb, general mantle epithelium (Lacaze-Duthiers (de), 1857; Plate, 1892; Simroth, 1894; Yonge, 1937) and the ciliary bands themselves (Distaso, 1905).

The ciliated bands of *Dentalium rectius* are provided with an extensive haemocoel. Although only noting the ciliated bands on the body wall, the region was described in *Dentalium* by Lacaze-Duthiers (1857) as highly vascularized, just anterior to the bifurcation of the pallial blood vessels. He could not distinguish a consistent direction of blood flow, but observed that the bands received blood at various times from haemocoelic spaces

anterior and posterior to the ridges, and from the anal bulb. Blood moved from the ciliated bands to the mantle sinus upon contraction of the foot and abdominal sinus; dilation of these organs returned the blood to the bands lining the body wall (Lacaze-Duthiers (de), 1857). Distaso (1905) observed in other species of *Dentalium* that the bands received blood from the ventral vessel of the mantle which, after passing through the bands, was returned to the heart. Bidirectional blood flow has been observed through the perianal and abdominal blood sinuses of *D. rectius* (Chapter 1; Reynolds, 1990a); contraction of the extensive musculature of the body wall (Figure 1) and withdrawal of the foot and body within the shell would undoubtedly contribute to transport of the haemolymph supplying the ciliated bands.

Little is known of scaphopod respiratory proteins. Two reports of hemoglobin in the pharyngeal region and radular apparatus (Manwell, 1963; Smith, 1967) are thought to represent myoglobin in the radular musculature (Bonaventura & Bonaventura, 1983). Difficulty in obtaining sufficient quantities of haemolymph from *D. rectius*, one of the larger scaphopod species, has impeded investigation of blood proteins (Morse, personal communication).

Ultrastructural and histochemical data indicate uptake of iron-containing granules by pinocytosis into the apical cytoplasm of the supporting cells of the ciliary bands and the general mantle epithelium. In seawater, iron is largely present as particulate ferric hydroxide (Lewis & Goldberg, 1954; Sillén, 1961). The concentration of this particulate iron is highly correlated with total particulate matter in suspension, which in turn is greatly affected by physical and chemical changes in the environment. Consequently, recorded iron levels in seawater range widely, from 0-3420 µg/l (reviewed in Head, 1971). Iron is found in high quantities in certain tissues of the digestive system of *D. rectius* (Chapter 4), although uptake via gut epithelia from ingested material is likely the major source of this

iron as has been shown in the bivalve *Mytilus edulis* (Pentreath, 1973; Young, 1975) and gastropod *Nucella lapillus* (Young, 1977). George et al. (1975), however, showed that approximately 20% of total iron uptake in *Mytilus edulis* is via the ctenidia, occuring at a higher rate than across the rest of the mantle epithelium (George et al., 1976; Pentreath, 1973).

The processing of iron in the ciliated bands of *D. rectius* appears to follow one of three routes. Vesicles in the apical cytoplasm of the ciliated cells contain particulate matter without a mucous matrix and appear to be pinocytotic in origin. Their contents are incorporated into iron-containing granules and eventually into larger vacuoles which can be considered secondary lysosomes. In the support cells, mucus surrounding the microvilli and in which particulate iron is embedded is pinocytosed by the support cell apical membrane. This mucous may also be able to sequester soluble iron, and therefore be the initial binding site of both particulate and soluble iron, both of which contribute to the total iron content of the apical granules as has been described for the ctenidium of *Mytilus edulis* (Pentreath, 1973). This would account for the greater total iron content of the mucous-containing support cell granules compared to those of the ciliated cells. Some of these granules, which are similar to those found in the gill and mantle epithelium of *Crassostrea gigas* (Thomson et al., 1985), *Mytilus edulis* (George, et al., 1976) and *Littorina littorea* (Mason, Simkiss & Ryan, 1984), are likely processed in secondary lysosomes. The majority, however, appear to be released with surrounding cytoplasm into the haemocoel and engulfed by amoebocytes. The amoebocytes in the *D. rectius* haemocoel test positive for iron histochemically, and their distribution throughout the haemocoel suggests that they are involved in iron transport. Similar processing pathways have been proposed for *Mytilus* (George et al., 1975; 1976), *Mercenaria* (Fowler, 1975)and *Macrocallista* (Bevelander & Nakahara. 1966), although the mechanism by which the iron within the

amoebocytes is incorporated into other tissues remains uncertain (Simkiss & Mason, 1983). The demands of radula mineralisation in *Dentalium rectius* and the lack of iron excretion via the kidney (Chapters 3 and 4; Reynolds, 1990b) suggest that uptake via the mantle is a significant iron source in *Dentalium rectius* that augments uptake via the gut. Other radula-bearing molluscs have high iron concentrations in the haemolymph, with haemolymph ferritin identified as a high capacity iron-binding protein which could supply the mineralising region of the radula with iron (Burford, Macey & Webb, 1986). The presence of ferritin in the haemolymph of scaphopods, as with respiratory proteins, still remains to be investigated.

No distinct regional differentiation within the ciliary bands was observed. The morphological features of the support cells, such as the raised cell apices, attenuation of cell height between the apices and microvillous apical membrane suggest that these cells are specialized for diffusion between the haemolymph and external environment. Facilitating this, the ciliated cells provide a constant supply of fresh seawater over the supporting cells, and the haemolymph is continually circulated by the contractions of the adjacent perianal sinus, which may represent the reduced ventricle (Chapter 2; Reynolds, 1990a). The supporting cells possess ultrastructural features which suggest that they are also involved in active transport, as confirmed by the pinocytosis of iron-containing granules and subsequent transport by amoebocytes. The role of the ciliated bands in ammonia excretion, as has been demonstrated in the gills of other molluscs (Schipp et al., 1979) awaits further study. While gas exchange may occur to some extent over the entire mantle and body wall epithelium, including the anal bulb, the ciliary bands in the scaphopod mantle cavity appear to combine current producing, gas exchange and active transport specializations into one organ system as is found in the molluscan ctenidium. They therefore form a functional equivalent to ctenidia, given the loss of these organs from the scaphopod mantle cavity.

LITERATURE CITED

Bevelander, G. & Nakahara, H. (1966). Correlation of lysosomal activity and ingestion by the mantle epithelium. Biological Bulletin, 131, 76-82.

Bonaventura, C. & Bonaventura, J. (1983). Respiratory pigments: structure and function. In P. W. Hochachka (Ed.), Environmental Biochemistry and Physiology. (pp. 1-50). New York: Academic Press.

Burford, M. A., Macey, D. J. & Webb, J. (1986). Hemolymph ferritin and radula structure in the limpets *Patelloida alticostata* and *Patella peronii* (Mollusca: Gastropoda). Comparative Biochemistry and Physiology, 83A(2), 353-358.

Chapman, D. M. (1977). Eriochrome cyanin as a substitute for haematoxylin and eosin. Canadian Journal of Medical Technology, 39, 65-66.

Chayen, J., Bitensky, L. & Butcher, R. G. (1973). Practical Histochemistry. John Wiley and Sons, Ltd., London.

Dinamani, P. (1964). Burrowing behaviour of *Dentalium*. Biological Bulletin, 126, 28-32.

Distaso, A. (1905). Sull' Anatomia degli scafopodi. Zoologischer Anzeiger, 29, 271-278.

Fol, H. (1889). Sur l'anatomie microscopique du Dentale. Archives de Zoologie Experimentale et Génerale, Deuxième Série, 7, 91-148, pls. 5-8.

Fowler, B. A. (1975). Mercury and iron uptake by cytosomes in the mantle epithelial cells of quahog clams (*Mercenaria mercenaria*) exposed to mercury. Journal of the Fisheries Research Board of Canada, 32, 1767-1775.

George, S. G., Pirie, B. D. S. & Coombs, T. L. (1975). Transport of iron complexes in shellfish. In Hutchinson, T. C. (Ed.) International Conference on Heavy Metals in the Environment. Electrical Power Research Institute et al., Toronto.

George, S. G., Pirie, B. J. S. & Coombs, T. L. (1976). The kinetics of accumulation and excretion of ferric hydroxide in *Mytilus edulis* (L.) and its distribution in the tissues. Journal of Experimental Marine Biology and Ecology, 23, 71-84.

Head, P. C. (1971). Observations on the concentration of iron in sea water, with particular reference to southhampton water. Journal of the Marine Biological Association of the United Kingdom, 51, 891-903.

Hobden, D. J. (1967). Iron metabolism in *Mytilus edulis*. 1. Variation in total content and distribution. Journal of the Marine Biological Association of the United Kingdom, 47, 597-606.

Humason, G. L. (1979). Animal Tissue Techniques (fourth ed). Freeman, San Francisco.

Jutting, T. v. B. (1926). Scaphopoda. In G. Grimpe & E. Wagler (Ed.), Die Tierwelt der Nord- und Ostsee (pp. 67-80). Akad. Verlagsges., Leipzig.

Lacaze-Duthiers, H. de (1857). Histoire de l'organisation et du développement du Dentale. Annales des Sciences Naturelles, Quatrième Série, 7, 194-251, pls. 5-9.

Leeson, C. R. & Leeson, T. S. (1970). Staining methods for sections of epon-embedded tissues for light microscopy. Canadian Journal of Zoology, 48, 189-191.

Lewis, G. J. & Goldberg, E. D. (1954). Iron in marine waters. Journal of Marine Research, 13, 183-197.

Lillie, R. D. (1965). Histopathologic Technic and Practical Histochemistry (third ed). McGraw-Hill, New York.

Manwell, C. (1963). The chemistry and biology of hemoglobin in some marine clams- 1. Distribution of the pigment and properties of the oxygen equilibrium. Comparative Biochemistry and Physiology, 8, 209-218.

Mason, A. Z., Simkiss, K. & Ryan, K. P. (1984). The ultrastructural localization of metals in specimens of *Littorina littorea* collected from clean and polluted sites. Journal of the Marine Biological Association of the United Kingdom, 64, 699-720.

Moor, B. (1983). Organogenesis. In Verdonk, N. H., van den Biggelaar, J. A. M. & Tompa, A. S. (Eds.), The Mollusca, v. 3, Development (pp. 123-177). Academic Press, New York.

Morton, J. E. (1959). The habits and feeding organs of *Dentalium entalis*. Journal of the Marine Biological Association of the United Kingdom, 38, 225-238.

Odhner, N. H. (1931). Die Scaphopoden. In Bock, S. (Ed.), Further Zoological Results of the Swedish Antarctic Expedition 1901-1903 (pp. 1-8, pls. 1, 2). Norsedt, Stockholm.

Pearse, A. G. E. (1968). Histochemistry, Theoretical and Applied, 1 (third ed). Churchill, London.

Pearse, A. G. E. (1972). Histochemistry, Theoretical and Applied, 2, (third ed). Churchill Livingston, London.

Pentreath, R. J. (1973). The accumulation from water of ^{65}Zn, ^{54}Mn, ^{58}Co and ^{59}Fe by the mussel, *Mytilus edulis*. Journal of the Marine Biological Association of the United Kingdom, 53, 127-143.

Plate, L. H. (1888). Bemerkungen zur Organisation der Dentalien. Zoologischer Anzeiger, 14, 78-80.

Plate, L. H. (1892). Ueber den Bau und die Verwadtschaftsbeziehungen der Solenoconchen. Zoologische Jahrbucher Jena Abteilung für Anatomie, 5, 301-386, pls. 23-26.

Reynolds, P. D. (1990a). Functional morphology of the perianal sinus and pericardium of *Dentalium rectius* (Mollusca: Scaphopoda) with a reinterpretation of the scaphopod heart. American Malacological Bulletin, 7(2), 137-146.

Reynolds, P. D. (1990b). Fine structure of the kidney and characterization of secretory products in *Dentalium rectius* (Mollusca, Scaphopoda). Zoomorphology, 110(1), (in press).

Schipp, R., Mollenhauer, S. & von Boletzky, S. (1979). Electron microscopical and histochemical studies of differentiation and function of the cephalopod gill (*Sepia officinalis* L.). Zoomorphologie, 93, 193-207.

Sillén, L. G. (1961). The physical chemistry of seawater. In M. Sears (Ed.), Oceanography (pp. 549-581). American Association for the Advancement of Science, Washington, D. C.

Simkiss, K. & Mason, A. Z. (1983). Metal ions: metabolic and toxic effects. In P. W. Hochachka (Ed.) The Mollusca, v. 2, Environmental Biochemistry and Physiology (pp. 101-164). Academic Press, New York.

Simroth, H. (1894). I. Abteilung: Amphineura und Scaphopoda. Mollusca (pp. 356-467, tafel XV-XXII). Winter, Leipzig.

Smith, M. H. (1967). Occurrence of haemoglobin in some molluscs. Comparative Biochemistry and Physiology, 20, 361-364.

Taib, N. T. (1980). Some observations on the living animals of *Dentalium entalis* L. Journal of the College of Science, University of Riyadh, Saudi Arabia, 11, 129-144.

Thomson, J. D., Pirie, B. J. S. & George, S. G. (1985). Cellular metal distribution in the Pacific oyster, *Crassostrea gigas* (Thun.) determined by quantitative X-ray microprobe analysis. Journal of Experimental Marine Biology and Ecology, 85, 37-45.

Yonge, C. M. (1937). Circulation of water in the mantle cavity of *Dentalium entalis*. Proceedings of the Malacological Society of London, 22, 333-337.

Young, M. L. (1975). The transfer of ^{65}Zn and ^{59}Fe along a *Fucus serratus* (L.) Æ *Littorina obtusata* (L.) food chain. Journal of the Marine Biological Association of the United Kingdom, 55, 583-610.

Young, M. L. (1977). The roles of food and direct uptake from water in the accumulation of zinc and iron in the tissues of the dogwhelk, *Nucella lapillus*. Journal of Experimental Marine Biology and Ecology, 30, 315-325.

CHAPTER 6

DISTRIBUTION AND ULTRASTRUCTURE OF CILIATED SENSORY RECEPTORS IN THE POSTERIOR MANTLE EPITHELIUM OF *DENTALIUM RECTIUS* (MOLLUSCA, SCAPHOPODA)

ABSTRACT

The uniquely modified scaphopod mantle cavity opens posteriorly via the pavilion, a siphon-like extension of the posterior mantle through which the respiratory currents pass. The pavilion was examined for ciliated sensory cells in *Dentalium rectius* Carpenter 1864 using scanning and transmission electron microscopy. Three types of sensory receptor were distinguished on the basis of number, length and ultrastructure of the associated cilia. Receptors with 2-5 cilia of ~1.7 μm length lined the pavilion edge. A second type, possessing 1-2 cilia, ~8.2 μm in length, was found throughout the internal and on part of the external surface of the pavilion. The third receptor type consisted of a rigid bundle of 16-40 cilia with a length of ~14.4 μm, and was present close to the periphery and at the base of the pavilion near the entrance to the mantle cavity. The structure and distribution of these cells are similiar to peripheral chemo- and mechanoreceptors which sample respiratory currents and the surrounding environment in other molluscs, but they may assume a greater functional significance in scaphopods due to the absence of an osphradium in this class.

INTRODUCTION

Peripheral ciliated sensory cells have been described in detail from several classes of molluscs, and are considered to be primary receptors of chemical and physical information from the surrounding environment. This is reflected by their abundance in specialized regions of the external epithelium such as the pallial tentacles and mantle edge of gastropods (Crisp, 1971; Hackney et al., 1983; Wondrak, 1984; Hodgson et al., 1987) and bivalves (Moir, 1977; Owen & McCrae, 1979; Hodgson & Fielden, 1984). Ciliated receptors are particularly associated with the inhalent respiratory current and are found on the siphons of infaunal bivalves (Hodgson, et al., 1984; 1986) and within the mantle cavity on specialized sensory organs such as the bursicles of the Vetigastropoda (Haszprunar, 1987b). In addition, the molluscan osphradium possesses innervated ciliary tufts in high densities (Garton et al., 1984) and is thought to have a distance chemosensory role in reproduction or feeding (Altner & Prillinger, 1980; Haszprunar, 1987a).

In scaphopods, epithelial sensory structures which could test the water surrounding the animal or entering the mantle cavity are poorly known. Both inhalent and exhalent respiratory currents pass through the posterior or apical aperture of the shell (Yonge, 1937), which is directed towards or held above the surface of the sediment in these burrowing molluscs. The underlying mantle is developed into an tubular extension, termed the pavilion by Deshayes (1825); the entrance to the mantle cavity proper is partially occluded by a collar of tissue at the pavilion base (Boissevain, 1904; Lacaze-Duthiers (de), 1857). The sensitivity of the posterior mantle edge to chemical and physical stimuli has rarely been tested. Clark (1849) described a violent expulsion of water, probably due to withdrawal of the foot, when fine sand grains were introduced into the pavilion. Withdrawal or burrowing is also elicited by the touch of an eyelash brush and by a strong

salt solution (personal observations). Morphological description of epithelial sensory structures in the mantle include the unconfirmed description of an osphradium in several species of *Dentalium* by Distaso (1905), although Hazprunar (1987a), after examining three other species, concludes that scaphopods lack osphradia. A band of ciliated epithelium on the muscular collar at the base of the pavilion was described as sensory by Boissevain (1904). Due to the widespread presence of ciliated receptors in the mantle epithelia of other molluscan classes and the sensitivity of the scaphopod pavilion to chemical and physical stimuli, an ultrastructural examination for putative sensory structures in the pavilion of *Dentalium rectius* Carpenter 1864 was undertaken.

MATERIALS AND METHODS

Dentalium rectius was dredged from sediments at 60 m depth from Satellite Channel, near Victoria, British Columbia. Specimens were brought to the laboratory where they were dissected; the pavilion was fixed in 2.5% glutaraldehyde in 0.2M phosphate buffer (pH 7.4) and 0.14M NaCl for two hours at room temperature, rinsed in 0.2M phosphate buffer and 0.3M NaCl, and post-fixed in 1% osmium tetroxide in 0.1M phosphate buffer and 0.375M NaCl for one hour at 4°C. Tissues were rinsed in distilled water and dehydrated in ethanol. For scanning electron microscopy (SEM), some specimens were placed in 1% HCL for 5 minutes after fixation to remove mucus following Hodgson and Fielden (1984). After dehydration, tissues were critical point dried from CO_2, gold coated and viewed using a JEOL JSM-35 scanning electron microscope. SEM photomicrographs were used for analysis of cilia number and length, and for estimations of ciliated cell densities. Tissues for transmission electron microscopy (TEM) were tranferred to propylene oxide after dehydration, embedded in epon resin and sectioned on a Reichert

ultramicrotome. Ultrathin (grey to pale gold interference colour) sections were stained with uranyl acetate and lead citrate and examined using a Philips EM-300 transmission electron microscope.

RESULTS

Scanning electron microscopy

The pavilion of *Dentalium rectius* is similiar to that of other scaphopods, being a cylindrical extension of the posterior mantle with a medial slit along the ventral side (Figures 1, 100). Internally, a large dorsal tissue mass creates an oblique passageway to the mantle cavity. A ventral crescent of tissue, part of a discontinuous collar of tissue at the base of the pavilion, projects into the entrance leaving only a slit-like opening (Figures 101, 102). On the internal surface of the pavilion, tufts of cilia are scattered throughout the epithelium; a plot of cilia number per tuft against length distinguishes three distinct types of ciliated cells (Figure 103). Type 1 (Figures 104, 105) have 2-5 cilia with a mean length of 1.8 µm (± 0.6 S.D.; n=27), while Type 2 (Figure 105) have 1-2 cilia each 8.2 µm mean length (± 1.9 S.D.; n=20). Type 3 cells have approximately 20-30 cilia of 14.4 µm mean length (± 2.89 S.D.; n=26); they were further distinguished by the rigidity and tightly packed arrangement of the cilia, in many instances helically wound (Figure 106). Cilia number in Type 3 cells could not be easily counted using SEM and are likely underestimated. Cilia length, by contrast, was most easily measured in cell Type 3, in which the cilia were relatively straight and near perpendicular to the epithelial surface. The cilia of all cell types appear to emerge from a pit or depression in the mantle epithelium.

Figure 100. Ventral view of posterior mantle or pavilion. Note medial slit. Scale = 0.5mm.

Figure 101. Internal view of left side of pavilion (ventral to left) (*G*, gonad; *M*, mantle cavity;*arrowheads*, collar of tissue at base of pavilion; *arrow*, entrance to mantle cavity). Scale = 0.5mm.

Figure 102. Posterior view of entrance to the mantle cavity, pavilion rolled back (*D*, dorsal mass of tissue; *P*, pavilion; *V*, ventral crescent of collar at pavilion base; *arrowheads*, slit-like entrance to the mantle cavity). Scale = 0.3mm.

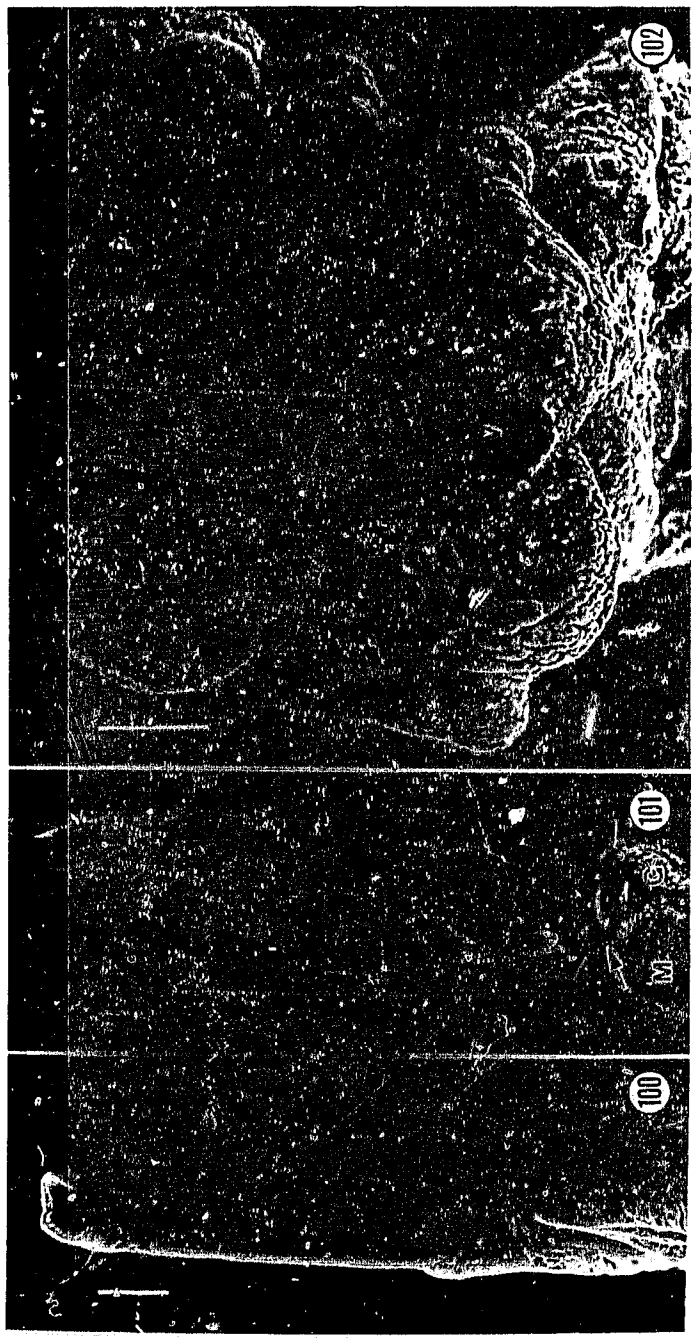
100
101
102

Figure 103. Plot of cilia length against number for putative ciliated receptor cells in pavilion.

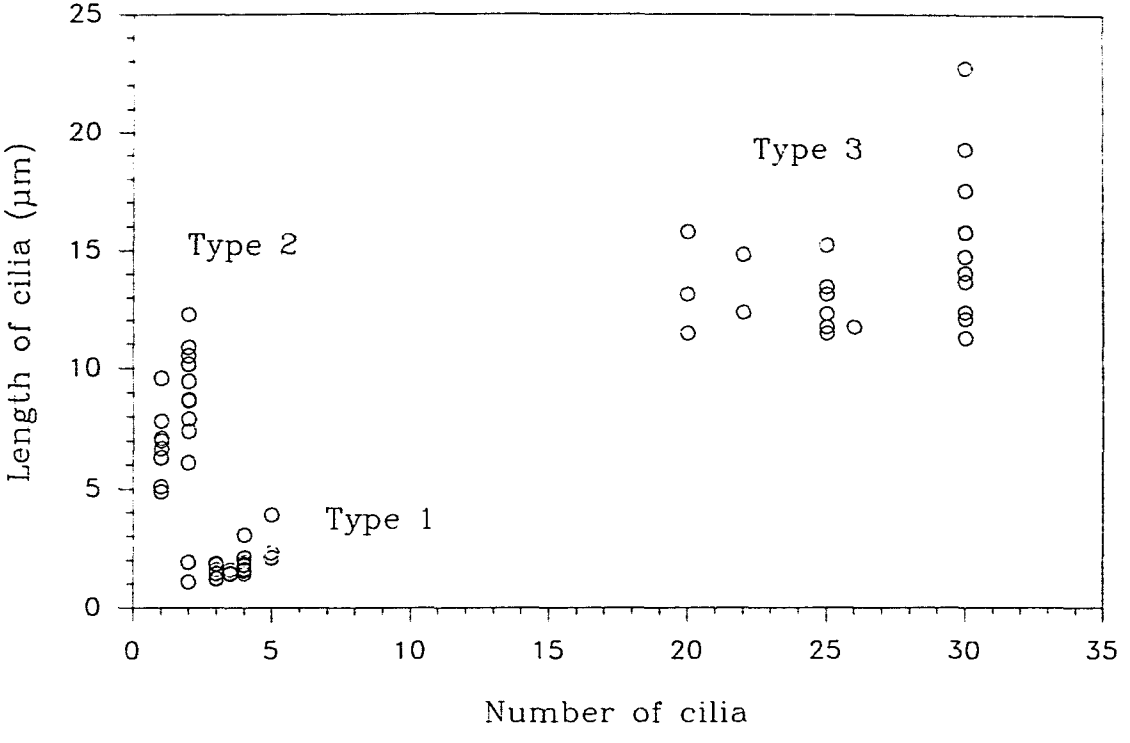
Length of cilia (µm)
25
20
15
10
5
0
Type 2
Type 1
Type 3
0
5
10
15
20
25
30
35
Number of cilia

103

Figure 104. Ciliated cell Type 1. Scale = 5 μm.

Figure 105. Ciliated cell Type 2. Scale = 5 μm.

Figure 106. Ciliated cell Type 3. Note upright rigidity and tightly packed arrangement of the cilia, and slight twist in the left ciliary bundle. Scale = 10 μm.

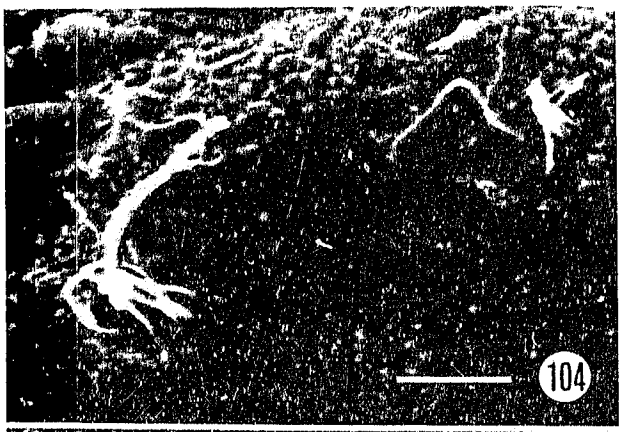
104

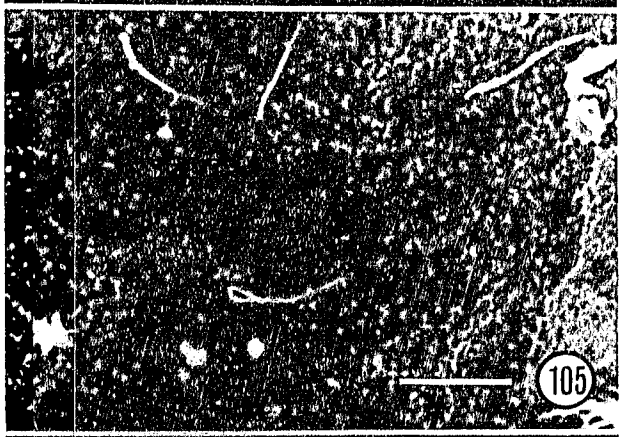
105

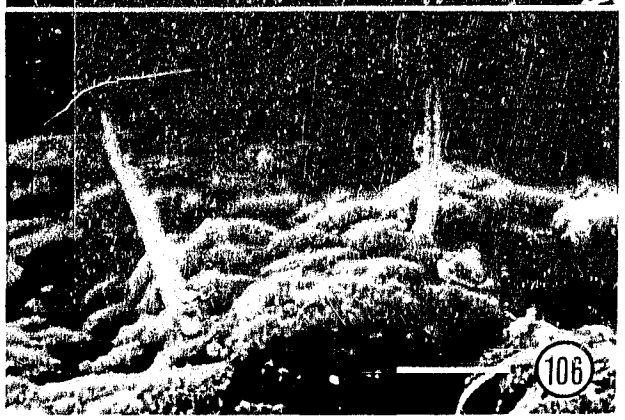
106

There was a heterogeneous distribution of the ciliated cell types over the pavilion epithelium. Type 1 cells are limited to the mantle edge (Figures 107, 108). Spaced at approx. 4 μm intervals, they form nearly a complete ring around the apex of the pavilion, just inside the posterior aperture of the shell, and extend partially along both sides of the medial slit which runs the length of the pavilion. Type 2 ciliated cells are also found in this area but are less common (7-8 μm apart) (Figure 108) and, with Type 3 cells, are found scattered throughout the internal surface of the pavilion at a combined density of approx 3.3 x 10^3 mm^{-2} (Figure 109). Type 3 cells are found in greater abundance in a band near the apex of the pavilion (7-8 μm apart), separated from the edge by a region of heavily ciliated epithelium (Figures 108, 110). With the near exclusion of the other ciliated cells, Type 3 is found in the highest density (approx. 3 x 10^3 mm^{-2}) in the ventral crescent and dorsal tissue mass of the pavilion base, at the entrance to the mantle cavity (Figure 111). On the external surface of the pavilion, only Type 2 ciliated cells were found; they were limited to the posterior-mid region, where they were relatively abundant (3.2 x 10^3 mm^{-2}).

Vesicles, probably mucous droplets, were distributed throughout the internal surface of the pavilion (Figure 109). Within a groove posterior to the ventral portion of the collar is a band of cilia, which appear to beat in limited synchrony (Figure 112).

Transmission electron microscopy

The supporting epithelium of the internal surface of the pavilion consists of columnar cells, 13-17 μm in height (Figures 113, 114). These cells have a densely microvillous apical membrane, and the cytoplasm is rich in mitochondria, Golgi bodies, rough endoplasmic reticulum, free ribosomes and electron opaque granules. Electron tranparent secretory vesicles are present throughout the cytoplasm and among the

Figure 107. Distribution of Type 1 cells (*arrowheads*) at pavilion edge, along the medial slit near the posterior rim. Scale = 20 μm.

Figure 108. Ciliated cell types along the posterior rim of the pavilion. Type 2 cells are found along the rim (*arrowheads*), separated by a ciliary band (*C*) from a band of Type 3 cells (*arrows*) on the interior (*double arrowheads*, Type 1 cells). Scale = 20 μm.

Figure 109. Ciliated cell Types 2 (*arrowheads*) and 3 (*arrows*) of the internal pavilion epithelium (*double arrowheads*, mucous globules). Scale = 20 μm.

Figure 110. View of posterior rim, showing distribution of ciliated cell Types 1 and 3, and the ciliated band near the pavilion apex. Scale = 80 μm.

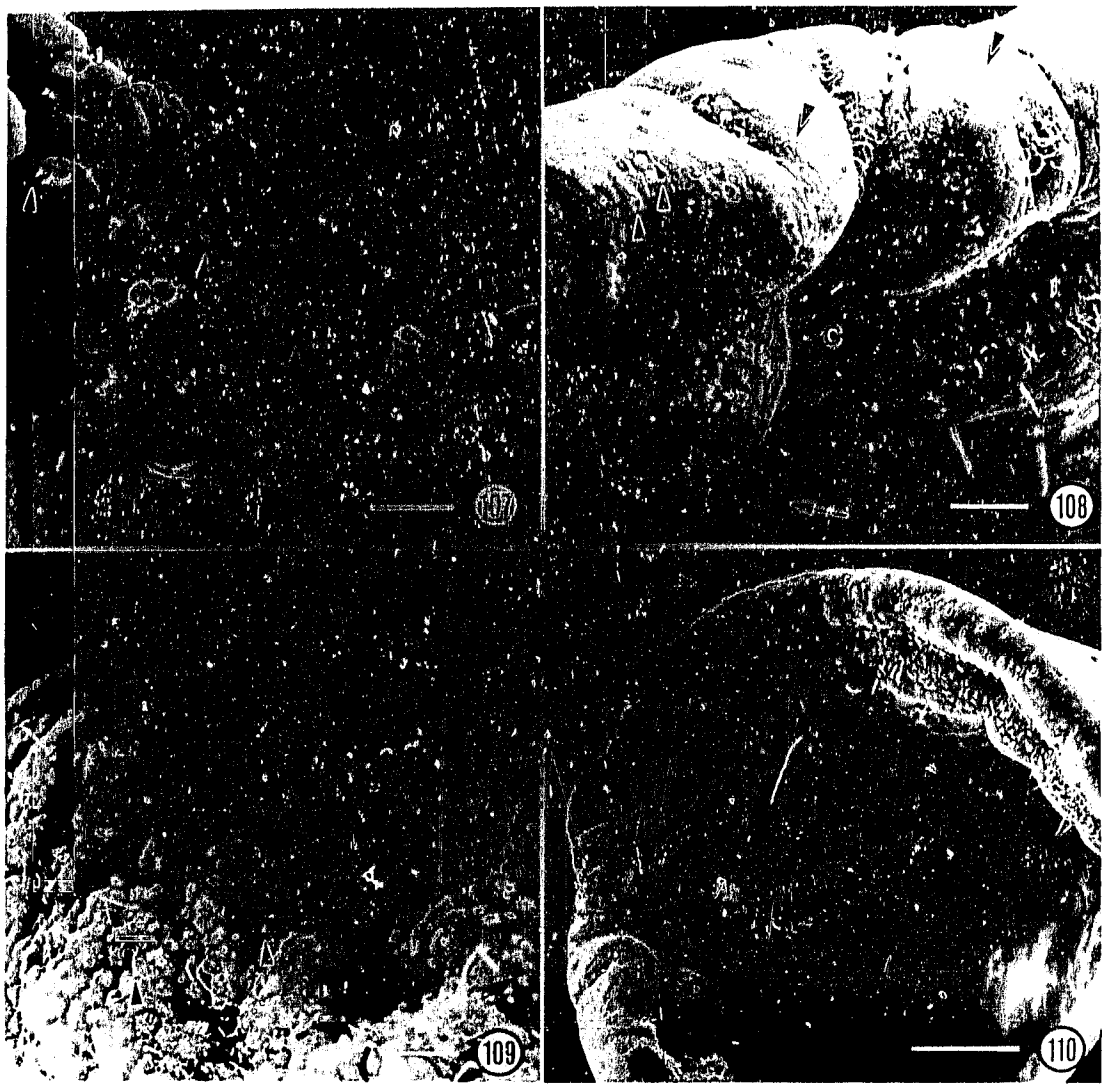
107
108
109
110

Figure 111. Distribution of ciliated cell Type 3 in ventral crescent of collar and dorsal tissue mass at the pavilion base (*D*, dorsal tissue mass; *E*, entrance to mantle cavity; *V*, ventral crescent of pavilion collar; *arrowheads*, Type 2 cells; *arrows*, Type 3 cells). Scale = 50 μm.

Figure 112. Band of cilia in groove posterior to the ventral crescent of the collar. (*E*, entrance to mantle cavity; *V*, ventral crescent of pavilion collar) Scale = 50 μm.


M
(112)
E
V
(111)

Figure 113. Pavilion rim epithelium (*BL*, basal lamina; *N*, nerve profiles; *T2*, Type 2 ciliated cell; *C*, ciliated band; *S*, supporting epithelium). Scale = 5 μm.

Figure 114. . Elongate neural process (*arrowheads*) of ciliated cell Type 1and adjoining subepithelial nerves (*N*) (*BL*, basal lamina; *arrow*, neurotubules). Scale = 5 μm.


114
113
N
BL
BL
N
C
S
T2
S
C

microvilli, corresponding to the membrane limited vesicles noted under SEM. There is a prominent nucleus basally, and hemidesmosomes are interspersed along the basal membrane. A basal lamina separates the epithelium from a layer of collagen fibrils. Muscles cells and nerves were found beneath the epithelium (Figures 113, 114).

The three ciliated cell types were distinguished under TEM by position, cilia number and length. The cilia of cell Types 2 and 3 have a striated rootlet attached to the basal body, with a maximum width of 87 μm and a banding periodicity ranging from 45-65 nm; near the basal body, alternating light and dark banding with a periodicity of 22 μm could be discerned (Figure 115). Cilia of Type 1 cells did not possess rootlets (Figure 116). All cilia possessed a typical arrangement of nine doubled outer microtubules and two single central elements (Figure 117). Transverse sections of Type 3 cells show a collar of cytoplasm around the cilia, the width and depth of which varies considerably (Figures 118-120); over 40 cilia are often present, which can be tightly packed. Basal feet are not strictly aligned but appear to have a consistent orientation with respect to adjacent cilia (Figure 119), which may be linked to the rigid arrangement of the ciliary bundle. Basal rootlets extend into cytoplasm rich in mitochondria (Figures 120, 121).

The ciliated cells shared cytoplasmic characteristics which differentiated them from the surrounding epithelium. The pitted appearance of the apices is due to the shortness or absence of microvilli from the cell apex (Figures 114-116). The ciliated cells consist of an elongate process running between the surrounding columnar epithelial cells; in instances where serial sections permitted, the processes could be followed through the basal lamina to the cell bodies, which adjoin nerve tissue within the pavilion (Figure 114). The cell cytoplasm is typically less electron opaque than that of the surrounding columnar epithelium (Figures 114, 118, 120). Intracellular organelles are relatively sparse; those that characterize the ciliated cells are elongated mitochondria near the cell apex (Figures 113-

Figure 115. Basal apparatus of ciliated cell Type 2. Note banding periodicity of basal rootlets. Scale = 0.4 μm.

Figure 116. Basal apparatus of ciliated cell Type 1. Note absence of basal rootlets (*arrowheads*, neurotubules). Scale = 1 μm.

Figure 117. Transverse sections of cilia from cell Type 3. Note typical 9+2 microtubule arrangement. Scale = 0.2 μm.


115
116
117

Figure 118. Tightly packed arrangement of cilia in ciliated cell Type 3 (transverse section) (*arrowhead*, zonula adherens; S, supporting epithelium). Scale = 1 μm.

Figure 119. Orientation of basal feet (*arrowheads*) in ciliated cell Type 3 (transverse section). Scale = 1 μm.

Figure 120. Basal appartatus (*arrowheads*) of cilia in ciliated cell Type 3 (transverse section). Scale = 1 μm.

Figure 121. Mitochondria (*arrowheads*) among basal rootlets of ciliated cell Type 3 (transverse section). Scale = 1 μm.

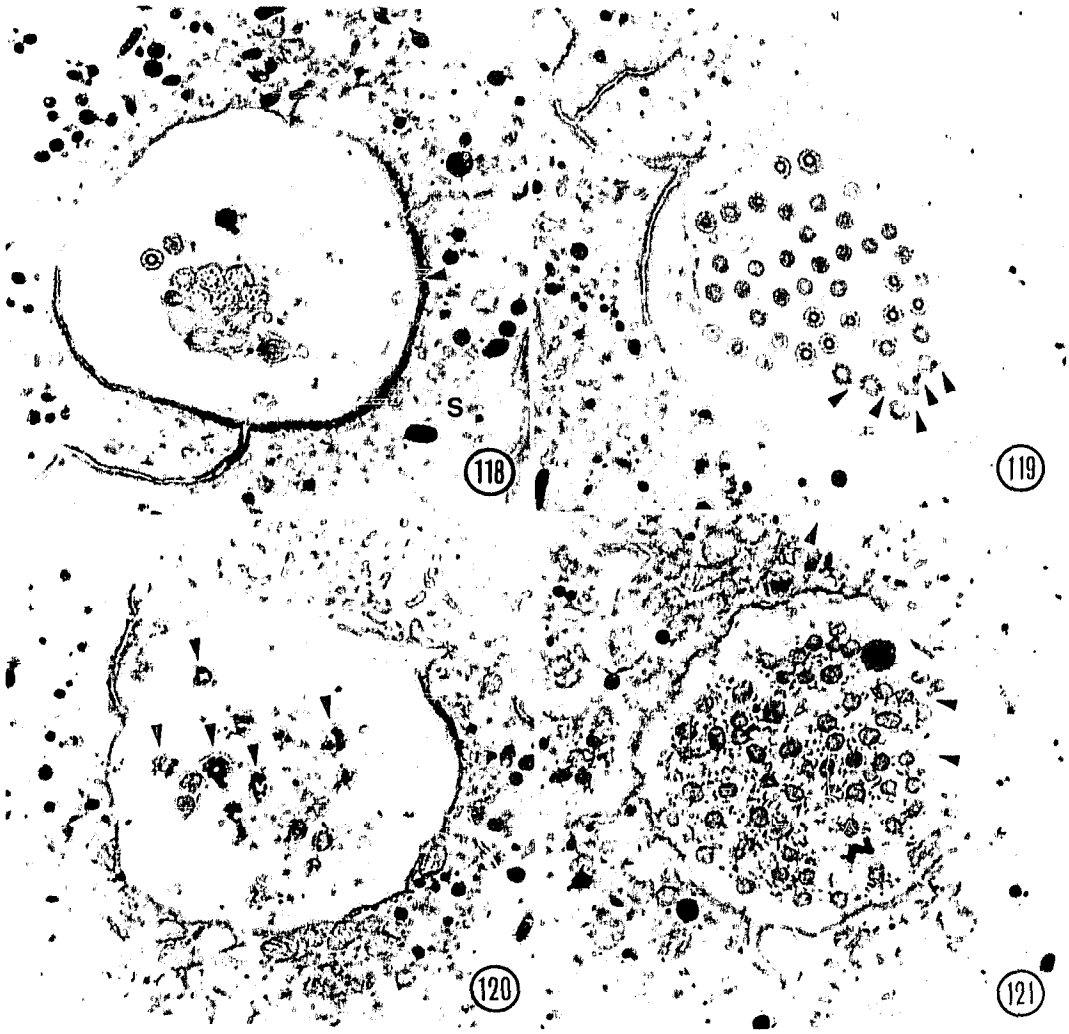
S
118
119
120
121

115, 121), neurotubules which generally run along the long axis of the process (Figures 114, 116), and numerous small vesicles (Figures 115,116, 118-121). Intermediate junctions (zonula adherens) are found between the processes and the columnar epithelial cells (Figures 114-116, 118-120).

The ciliary band near the apex of the pavilion was composed of cilia with a 9 + 2 microtubular structure and basal rootlet. Unlike cell Types 1-3, the cilia are borne by indifferent columnar epithelium (approx. 22 μm in height), with no evidence of associated neural elements (Figure 114).

DISCUSSION

The three types of ciliated cells described from the pavilion of *Dentalium rectius* possess ultrastructural characteristics resembling those of dendritic processes, which adjoin neural elements within the mantle tissue subepithelially. Innervation of the pavilion is served by two visceral nerves which arise from the visceral ganglia (Lacaze-Duthiers, 1856; Fischer-Piette & Franc, 1969). These ciliated cells can be considered primary receptors and are similiar to ciliated sensory cells found in the mantle epithelium of other molluscs. Sites of receptor occurrence include the pallial tentacles of limpets (Hackney, et al., 1983; Hodgson, et al., 1987) and bivalves (Moir, 1977; Owen, et al., 1979), and the siphons of bivalves (Hodgson, et al., 1984; 1986) and gastropods (Crisp, 1971). In all of these studies, ciliary receptors have been differentiated into specific types on the basis of cilia number and length, and this has often been supported by cilia ultrastructure and tuft distribution. The densities of putative receptor cells in the pavilion of *D. rectius* are similiar to those reported from the siphons and external epithelium of a variety of bivalves and gastropods (Crisp, 1971; Davis, 1982; Hodgson, et al., 1984; Hodgson, et al., 1986).

There is, however, considerable variation in these receptor characters between species, and no correlation between Types 1, 2 and 3 in the present study and those of previous studies should be inferred.

Apart from cilia number and length, the differences between the receptor types in *D. rectius* are found in the ultrastructure of the basal apparatus. The cilia of Types 2 and 3 have basal rootlets in common with most ciliated receptors described in molluscs, and may be correlated with directional mechanoreception (Moir, 1977; Hodgson and Fielden, 1984). The unique ciliary arrangement of receptor Type 3 is particularly suggestive of a mechanosensory function. The large numbers of tightly bound cilia are probably non-motile, and the rigidity, numbers and orientation of the cilia perpendicular to the epithelial surface suggest a receptor which would maximize and withstand vigorous mechanical stimulation; the extensive collar of cytoplasm which surrounds the ciliary bundle may also play a role in reception of mechanical stimuli. Zylstra (1972), investigating gastropod epithelial receptors, suggests a mechanoreceptive function for free nerve endings possessing cilia with well developed basal apparatus. Similiar receptor types are rare in other mollusca; a peg-like receptor at the anterior part of Hancock's organ in the cephalaspids *Bullaria striata* and *Haminea navicula* superficially ressemble receptor type 3 described here, but there is little information on its fine structure (Edlinger, 1980). Haszprunar (1986) described mechanoreceptive anterolateral cirri in the solenogastre *Aesthoherpia glandulosa* which also consisted of bundles of rigid cilia, but having a modified microtubular arrangement. The absence of striated rootlets in receptor Type 1 could indicate, by default, a chemosensory role for Type 1 receptors in *D. rectius*. Ciliated receptors which lack basal rootlets are also found in the pavilion of the gadilid scaphopod *Entalina quinquangularis* (Steiner, personal communication), the infaunal bivalve *Donax* (Hodgson, et al., 1984), and a variety of pulmonates (Wondrak, 1984).

While *D. rectius* responds to both mechanical and chemical stimulation to the pavilion epithelium, there is no evidence of the putatively mechanosensitive "collar receptors" (stereocilia) described in other molluscs (Crisp, 1981; Haszprunar, 1985; Moir, 1977) or of "paddle cilia" (discocilia) which are associated with chemoreception (Davis, 1982; Haszprunar, 1987a; 1989). Paddle cilia, however, are dynamic structures that may not always be evident, and many suspected chemosensory structures do not posses them (Matera & Davis, 1982). While behavioural assay has shed some light on the function of these two cilia types, molluscan sensory receptors show a wide variety of cilia ultrastructure for which it is difficult to assign specific sensory modalities in the absence of electrophysiological data (for review of sensory cilia ultrastructure and function, see Barber, 1974; Altner & Prillinger, 1980).

The supporting epithelial cells are largely secretory, producing mucus-filled vesicles and embedding the microvilli of the epithelial cells. The nature of the electron opaque granules seen throughout the epithelium is not known, although they are similiar to intracellular iron-containing granules from the epithelial cells of the mantle cavity of *D. rectius*, which is a significant site of iron uptake and storage (Chapter 4).

The ciliated band near the apex of the pavilion is not innervated and may be motile. The band of cilia just above the collar of tissue at the base of the pavilion was assigned a sensory function by Boissevain (1904), but from SEM appears to be capable of metachronal movement. It is likely that neither of these ciliary bands are sensory, but their beating could facilitate receptor function by maintaining water flow over areas of high receptor density.

The pavilion in *D. rectius* lacks extensive musculature and is not extended out of the shell like the siphons of infaunal bivalves, but instead largely conforms to the cylindrical

shape of the shell. However, the pavilion edge can be protruded slightly and partially reflected over the shell rim (personal observations), which is likely the position it adopts while secreting the secondary shell (Chapter 7). This behaviour, given the arrangement of receptor Types 2 and 3 near the pavilion edge, increases the effectiveness of this sensory band in sampling the external environment. The widespread distribution f receptor Type 2 and the abundance of Type 3 on the collar of tissue at the pavilion base, which is capable of closing the slit-like passage, are well situated to test the inhalent respiratory current before it enters the mantle cavity. The pavilion sensory receptors probably play an important role in the maintenance of respiratory current quality, prevention of mantle cavity fouling and predator avoidance. Food detection is more likely to be carried out by the subradular organ (Fischer-Piette, et al., 1969), and putative sensory structures in the captacula (Shimek, 1988) and anterior mantle edge (Steiner, personal communication), all of which yet require ultrastructural confirmation.

The pavilion is one of several unique modifications of the scaphopod mantle, such as the loss of ctenidia and osphradia. In addition to shell secretion, the scaphopod pavilion is also responsible for increasing posterior aperture size, by dissolution of shell at the aperture rim or decollation of the shell apex as in *D. rectius* (Chapter 7). The development of its sensory structures generally parallels that observed in the mantle edge of other molluscan classes, and may functionally compensate for the absence of an osphradium in this molluscan class.

LITERATURE CITED

Altner, H. & Prillinger, L. (1980). Ultrastructure of invetebrate chemo-, thermo-, and hygroreceptors and its functional significance. International Review of Cytology, 67, 69-139.

Barber, V. C. (1974). Cilia in sense organs. In M. A. Sleigh (Ed.), Cilia and Flagella (pp. 403-433). Academic Press, New York.

Boissevain, M. (1904). Beiträge zur Anatomie und Histologie von Dentalium. Jenaische Zeitschrift für Naturwissenschaft, 38, 553-572, pls. 17-19.

Clark, W. (1849). On the animal of *Dentalium tarentinum*. The Annals and Magazine of Natural History, Series 2., 4, 321-378.

Crisp, M. (1971). Structure and abundance of receptors of the unspecialized external epithelium of *Nassarius reticulatus* (Gastropoda, Prosobranchia). Journal of the Marine Biological Association of the United Kingdom., 51, 865-890.

Crisp, M. (1981). Epithelial sensory structures of trochids. Journal of the Marine Biological Association of the United Kingdom, 61, 95-106.

Davis, W. J. (1982). Chemoreception in gastropod molluscs: electron microscopy of putative receptor cells. Journal of Neurobiology, 13(1), 79-84.

Deshayes, M. (1825). Anatomie et monographie du genre Dentale. Memoires de la Société d'histoire naturelle de Paris, 2, 321-378, pls. 1-4.

Distaso, A. (1905). Sull' Anatomia degli scafopodi. Zoologischer Anzeiger, 29, 271-278.

Edlinger, K. (1980). Beiträge zur Anatomie, Histologie, Ultrastruktur und Physiologie der chemischen Sinnesorgane einiger Cephalaspidea (Mollusca, Opisthobranchia). Zoologischer Anzeiger, 205(1/2), 90-112.

Fischer-Piette, E. & Franc, A. (1968). Classe des scaphopodes, Scaphopoda (Bronn 1862). In Grassé, P.-P. (Ed.) Traité de zoologie, anatomie, systematique, biologie, 5(3), Mollusques, Gasteropodes et Scaphopodes (pp. 987-1017). Masson et Cie, Paris.

Garton, D. W., Roller, R. A. & Caprio, J. (1984). Fine structure and vital staining of osphradium of the southern oyster drill, *Thais haemastoma canaliculata* (Gray) (Prosobranchia: Muricidae). Biological Bulletin, 167, 310-321.

Hackney, C. M., McCrohan, C. R. & Hawkins, S. J. (1983). Putative sense organs on the pallial tentacles of the limpet, *Patella vulgata* (L.). Cell and Tissue Research, 231, 663-674.

Haszprunar, G. (1985). On the anatomy and fine-structure of a peculiar sense organ in *Nucula* (Bivalvia, Protobranchia). The Veliger, 28(1), 52-62.

Haszprunar, G. (1987a). The fine morphology of the osphradial sense organs of the Mollusca. III. Placophora and Bivalvia. Philosophical Transactions of the Royal Society of London. B, 315, 37-61.

Haszprunar, G. (1987b). The fine structure of the ctenidial sense organs (bursicles) of Vetigastropoda (Zeugobranchia, Trochoidea) and their functional and phylogenetic significance. Journal of Molluscan Studies, 53, 46-51.

Haszprunar, G. (1989). The fine morphology of the osphradial sense organs of the mollusca. I. Gastropoda, Prosobranchia. Philosophical Transactions of the Royal Society of London. B. Biological Sciences., 307, 457-496.

Hodgson, A. N. & Fielden, L. J. (1984). The structure and distribution of peripheral ciliated receptors in the bivalve molluscs *Donax serra* and *D. sordidus*. Journal of Molluscan Studies, 50, 104-112.

Hodgson, A. N. & Fielden, L. J. (1986). The ultrastructure of the ciliated cells from the siphon of *Solen capensis* (Mollusca, Bivalvia). Journal of Molluscan Studies, 52, 161-168.

Hodgson, A. N., Hawkins, S. J., Cross, R. H. M. & Dower, K. (1987). Comparison of the structure of the pallial tentacles of seven species of south african patellid limpet. Journal of Molluscan Studies, 53, 229-240.

Lacaze-Duthiers (de), H. (1857). Histoire de l'organisation et du développement du Dentale. Annales des Sciences Naturelles, Quatrième Série, 7, 194-251, pls. 5-9.

Lacaze-Duthiers, H. (1856). Histoire de l'organisation et du développement du Dentale. Annales des Sciences Naturelles, Quatrième Séries, Paris, 6, 319-385, pls. 11-13.

Matera, E. M. & Davis, W. J. (1982). Paddle cilia (discocilia) in chemoreceptive structures of the gastropod mollusk *Pleurobranchaea californica.* Cell and Tissue Research, 222, 25-40.

Moir, A. J. G. (1977). Ultrastructural studies on the ciliated receptors of the long tentacles of the giant scallop, *Placopecten magellanicus* (Gmelin). Cell and Tissue Research, 184, 367-380.

Owen, G. & McCrae, J. M. (1979). Sensory cell/gland cell complexes associated with the pallial tentacles of the bivalve *Lima hians* (Gmelin), with a note on specialized cilia on the pallial curtains. Philosophical Transactions of the Royal Society of London. B, 287, 6-62.

Shimek, R. L. (1988). The functional morphology of scaphopod captacula. The Veliger, 30(3), 213-221.

Wondrak, G. (1984). Ultrastructure of the sensory epithelia of oral tube, fungiform sensory bodies, and terminal knobs of tentacles of *Ovatella myosotis* Draparnaud (Archaeopulmonata, Gastropoda). Journal of Morphology, 181, 333-347.

Yonge, C. M. (1937). Circulation of water in the mantle cavity of *Dentalium entalis.* Proceedings of the Malacological Society of London, 22, 333-337.

Zylstra, U. (1972). Distribution and ultrastructure of epidermal sensory cells in the freshwater snails *Lymnaea stagnalis* and *Biomphalaria pfeifferi.* Netherlands Journal of Zoology, 22(3), 283-298.

CHAPTER 7

MANTLE-MEDIATED SHELL DECOLLATION INCREASES POSTERIOR APERTURE SIZE IN *DENTALIUM RECTIUS* (SCAPHOPODA: DENTALIIDA)

ABSTRACT

The scaphopod mantle cavity communicates with the external environment via the posterior aperture located at the apex of a tusk-shaped shell. Implicit in shell ontogeny is a potential difficulty in maintaining a sufficiently large posterior mantle opening to the exterior. As shell growth occurs anteriorly, the progressive enlargement of the anterior aperture is accompanied by a diminishing of the posterior aperture relative to body size. An increase in posterior aperture size correlated with growth of the organism is therefore necessary to facilitate the passage of respiratory currents, gametes and waste materials from the mantle cavity. Shell morphometrics, ultrastructure and direct observation of live specimens of *Dentalium rectius* confirm that such an increase does take place, and is due primarily to decollation of the shell through dissolution by the posterior mantle. While an increase in posterior aperture size by shell dissolution and truncation had been previously predicted, shell decollation has not been previously recorded from the Class. The removal of an apical portion of shell, as opposed to dissolution of the aperture rim, is necessitated in *D. rectius* and some other Dentaliida by the secondary shell secretion of the posterior mantle margin.

INTRODUCTION

The shell of *Dentalium rectius* Carpenter 1864 is typical of the Dentaliida, being a slightly curved translucent cone reaching 7 cm in length. As with all members of the Class Scaphopoda it is open at both ends, anteriorly for protrusion of the burrowing foot and feeding captacula (Figure 1), and posteriorly for the passage of both inhalent and exhalent respiratory currents to the mantle cavity (Yonge, 1937). A thin, secondary tube of shell often extends from the apex of the primary shell (Figure 122), a shell character which is found only among several dentaliid scaphopod genera (Stasek & McWilliams, 1973; Palmer, 1974). Shell secretion to accommodate soft tissue growth proceeds anteriorly, by a widening of the anterior aperture accompanied by an asymmetrical increase in shell length, producing the characteristic tusk-like shape (Shimek, 1989).

The consequences of this shell growth pattern to certain physiological requirements have been noted by Lacaze-Duthiers (1856), Pilsbry & Sharp (1897) and Fischer-Piette & Franc (1969). With increasing size of the animal, a constant posterior aperture size would become progressively smaller in relation to body size, and eventually be quantitatively inadequate for the passage of respiratory currents, the release of gametes, and the elimination of feces. While the apical larval shell is lost at an early stage (Lacaze-Duthiers, 1856), a continual increase in posterior aperture size with growth of the animal has been predicted to occur to ensure the maintenance of adequate exchange with the external environment (Lacaze-Duthiers, 1856; Pilsbry & Sharp, 1897; Fischer-Piette, et al., 1969).

Fischer-Piette & Franc (1969) and Stasek & McWilliams (1973) suggest that, in addition to secondary shell secretion, the posterior mantle margin of scaphopods may increase posterior aperture size by dissolution or reabsorptive truncation of the shell apex. A laboratory observation of shell decollation (the loss of the posterior or apical portion of

the shell) in *Dentalium rectius* prompted an investigation of the posterior shell growth pattern and an examination of discarded and intact shell apices for evidence of the shell loss mechanism.

MATERIALS AND METHODS

Live *Dentalium rectius* for observation were dredged from Barkely Sound near Bamfield, British Columbia, in June, 1985, while specimens for shell morphometrics were collected form Satellite Channel near Victoria, British Columbia, from October, 1987, to February 1988.

Specimens were maintained at the Bamfield Marine Station, British Columbia, over a four day period in 1 litre plastic beakers, filled with sediment from the biotope sieved to ≤ 1 mm and placed in running sea water ($10 \pm 0.5^{o}C$). Containers with double 1mm mesh sides were used to maintain aeration of sediment. Shell decollation was observed in one of the specimens; the discarded shell apex was later fractured and examined by scanning electron microscopy (SEM).

Shell measurements (Figure 122) were made at x10 magnification using a Zeiss dissecting microscope and ocular micrometer. The primary shells of many specimens were broken during the sampling process (23%) and were excluded from subsequent analyses of shell characters. Shells which appeared to have had breakages with subsequent shell repair were not excluded. Character relationships were described by linear regression using least mean squares (Zar, 1985). Of the measurements taken, anterior aperture height best represented growth (soft tissue dry weight) as described by the allometric relationship

Figure 122. Schematic diagram showing measurements taken on all shells (*a*, total length; *b*, primary shell length; *c*, anterior aperture height; *d*, primary shell apex height; *e*, secondary shell base height; *f*, secondary shell apex height; *g*, secondary shell length).

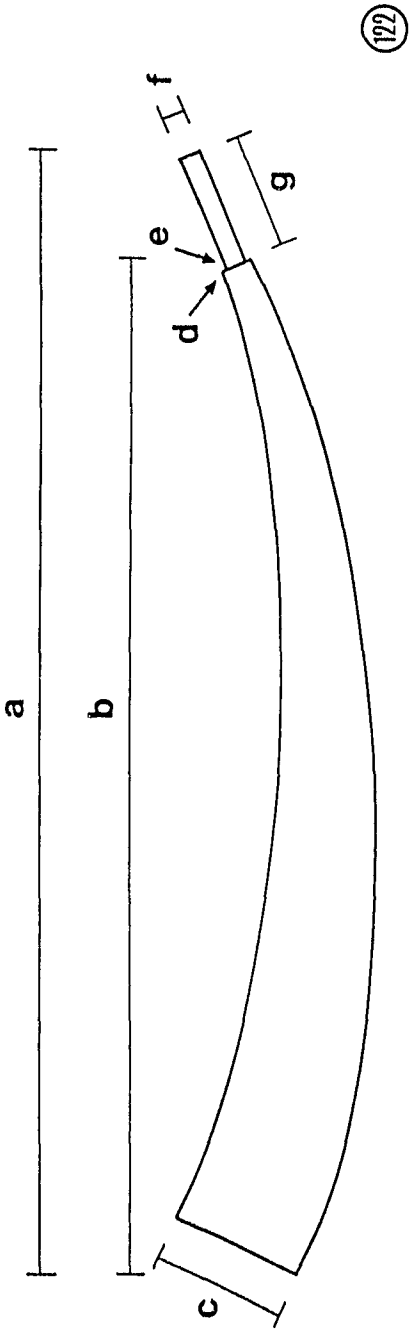
122
a
b
c
d
e
f
g

$\log(Y) = 0.238 \log(X) + 0.197$, $r^2 = 0.94$, $P<0.0001$, $n=43$ (Figure 123). The presence and position of a shallow ventral notch at the apex of the primary shell (Figure 124) were noted in 131 specimens (Table 5). The rate of decrease in the size of the posterior aperture per unit length, or taper, of the primary and secondary shells were calculated using the equations:

$$\text{Primary shell taper} = \frac{\text{primary shell base (anterior aperture) - primary shell apex}}{\text{primary shell length}}$$

$$\text{Secondary shell taper} = \frac{\text{secondary shell base - secondary shell apex (posterior aperture)}}{\text{secondary shell length}}$$

The means of primary and secondary shell taper were compared using the Student t-test (Zar, 1985).

Shells examined by SEM were rinsed with double distilled water, dried at room temperature, mounted on aluminium stubs and, in some cases, fractured using a fine stainless steel probe. Specimens were gold coated prior to viewing in a JEOL JSM-35 scanning electron microscope.

RESULTS

Apical shell morphology

Observations on the morphology of the shell apex are presented in Table 5. The primary shell apex of most shells (86.26%) have a notch (Figures 124, 125), which is usually found on the convex (ventral) side (94.69%). Otherwise, specimens have a shattered or broken primary shell apex (10.69%) (Figures 126, 127) or an intact apex with no notch (3.05%). The primary shell is secreted by the anterior mantle margin which is reflected by the presence of circular growth lines (Figures 126, 127), although these are often not apparent at the apex of the primary shell due to erosion (Figures 124, 125).

A secondary shell was present in 89.31% of the specimens (Table 5). The secondary shell is secreted by the posterior mantle margin, which produces V-shaped growth increments and a central suture line ventrally (Figures 124, 125). The apex of the secondary shell was usually broken, although a notch was noted at the apex on intact shells. The secondary shell growth was discontinuous in 13 cases (7.6% of all specimens with a secondary shell); nine of these had a notched primary shell with a subsequent break in the secondary shell repaired (one with two breakages), three had a notched primary shell with a notched disruption in the secondary shell, and one had a breakage repaired in the primary shell apex with a notched disruption in the secondary shell.

Figure 123. Plot of log (anterior aperture height) against log (soft tissue dry weight).

$\log(Y) = 0.238 \log(X) + 0.197$, $r^2 = 0.94$, $P<0.0001$, $n=43$.

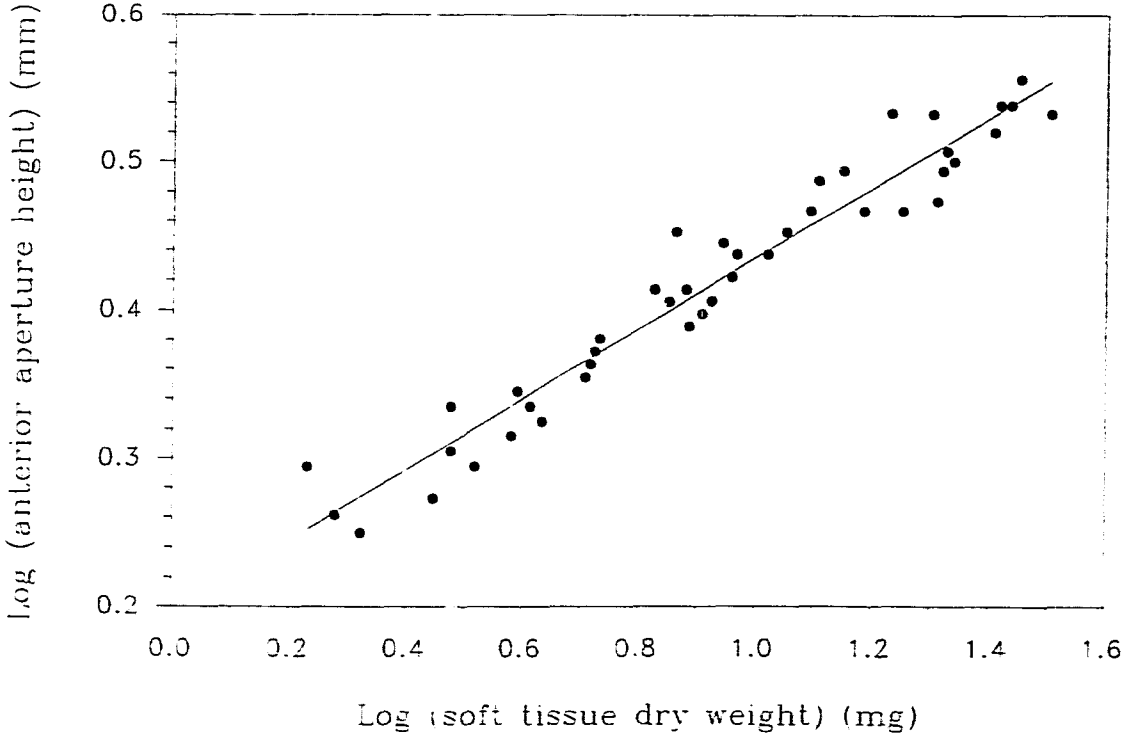
Log (anterior aperture height) (mm)
0.6
0.5
0.4
0.3
0.2
0.0
0.2
0.4
0.6
0.8
1.0
1.2
1.4
1.6
Log (soft tissue dry weight) (mg)

123

Figures 124-127. Junction of primary (lower) and secondary (upper) shells.

Figure 124. Ventral view of notched primary-secondary shell junction. Note the V-shaped notch at the primary shell apex, the V-shaped growth lines and median suture line (*arrowhead*)of the secondary shell, and the eroded primary shell. Scale = 0.3mm.

Figure 125. Ventral view of notched primary-secondary shell junction. Note the circular growth lines of the primary shell (*arrowheads* and lower left corner), V-shaped notch at the primary shell apex, and the V-shaped growth lines, median suture line, and simple prismatic structure (*arrow*) of the secondary shell. Scale = 0.2mm.

Figure 126. Lateral view of primary-secondary shell junction which lacks a notch (ventral to the right). Note the circular growth lines and shattered apex of the primary shell. Scale = 0.2mm

Figure 127. Dorsal view of primary-secondary shell junction which lacks a notch (ventral to the right). Note the shattered apex of the primary shell. Scale = 0.2mm

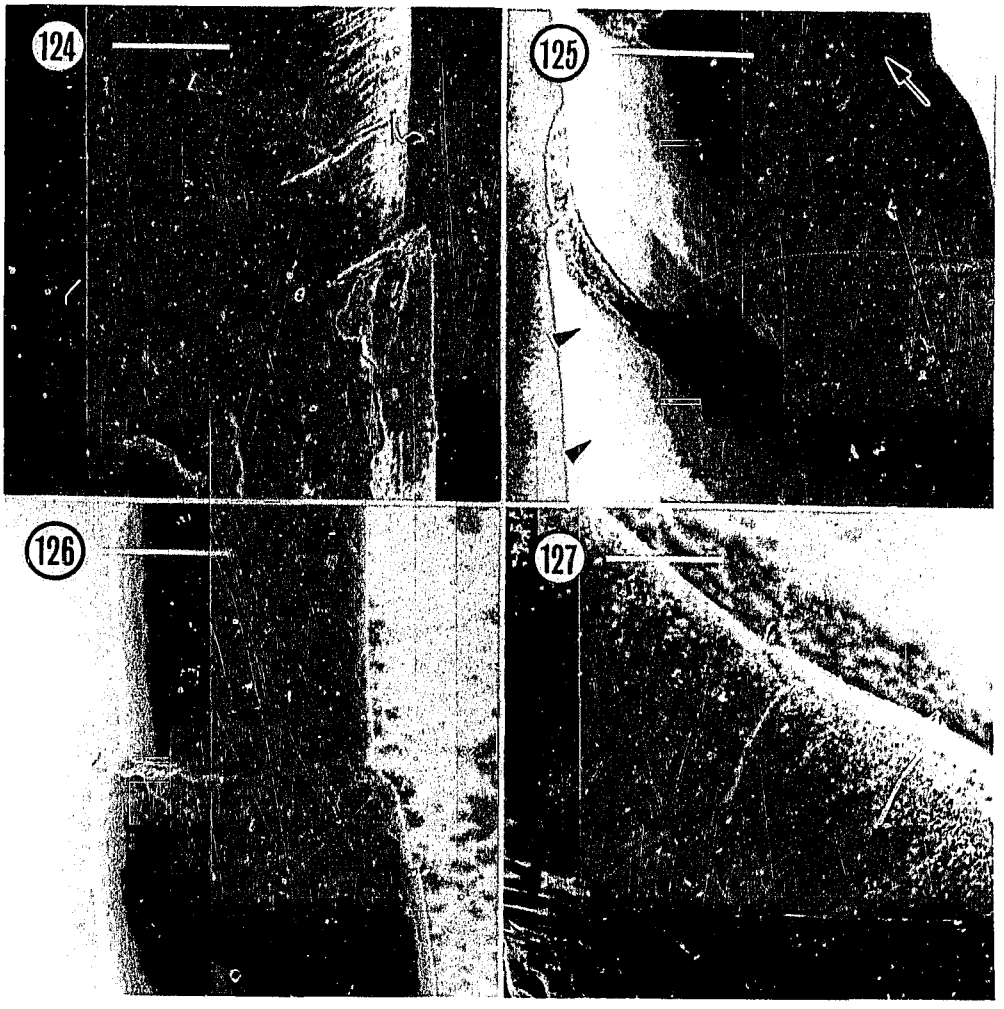
124
125
126
127

Table 5. Summary of primary shell morphological characteristics.

All specimens	With secondary shell	Without secondary shell	Totals
notched	102	11	113 (86.26%)
not notched	1	3	4 (3.05%)
repaired breakage	14	—	14 (10.69%)
Totals	117 (89.31%)	14 (10.69%)	131 (100.00%)

Notched shells	With secondary shell	Without secondary shell	Totals
ventral notch	98	9	107 (94.69%)
dorsal notch	3	1	4 (3.54%)
both	1	1	2 (1.77%)
Totals	102 (90.27%)	11 (9.73%)	113 (100.00%)

Observation of shell decollation and evidence of shell dissolution

During observation of live *Dentalium rectius*, the apical shell of 80% of the specimens (n = 100) protruded above the sediment surface at some time, when examined hourly over a 24 hour observation period. Shell decollation was observed in a specimen approximately 3 cm in length, with the shell protruding 7-9 mm from the sediment. The shell apex had detached, fallen over and was found resting at an angle between the sediment surface and the new aperture rim. The scaphopod had not changed position appreciably over the previous hour. When the container was disturbed several minutes later the scaphopod burrowed deeper into the sediment, leaving the detached portion of shell on the sediment surface. The animal appeared healthy (vigorous burrowing movements by foot) when examined two days later.

The discarded shell apex was examined under SEM and measured 5.15 mm in length and 0.67 mm in diameter at the point of separation, tapering to 0.38 mm posteriorly (Figure 128). The posterior aperture of the scaphopod therefore increased by 0.29 mm, or x1.8 the original diameter. The edge of the discarded shell, where detachment from the primary shell occurred, clearly showed evidence of dissolution (Figure 129) in contrast to a fractured edge of the same discarded shell (Figure 130). The anterior edge of the discarded shell shows the two layers of aragonitic calcium carbonate of the primary shell, an outer crossed lamellar structure (Figure 131) and an inner simple prismatic layer (Figure 132) which is continuous with the secondary shell (Figure 125). Comparison with the corresponding shell layers at the edge where detachment from the scaphopod occurred (Figures 133, 134) shows that much of the mineralised shell was lost, with some crystal orientation discernable between separate secretory layers.

The internal surface of the discarded shell revealed partial shell dissolution at a

Figure 128. Dorsal view of discarded shell apex, with lower dorsal portion removed (fracture line indicated by *large arrows*). Note the V-shaped line of decollation from the primary shell (*small arrows*). Scale = 0.5mm.

Figure 129. Etched shell layers where decollation from the primary shell occurred. Note the deeply eroded appearance of the two distinct shell layers. Scale = 30μm.

Figure 130. Fractured edge of same shell. Note the clearly defined shell microstructure, in the same orientation as in Figure 129 (cross section). Scale = 30μm.


129
130
128

Figure 131. Outer crossed lamellar layer of the decollated shell, fractured region. Scale = 5μm.

Figure 132. Inner simple prismatic layer of the decollated shell, fractured region. Scale = 5μm.

Figure 133. Outer crossed lamellar layer of the decollated shell at site of decollation, showing evidence of dissolution. Same orientation as in Figure 131. Scale = 5μm.

Figure 134. Inner simple prismatic layer of the decollated shell at site of decollation, showing evidence of dissolution. Same orientation as in Figure 132. Scale = 5μm.

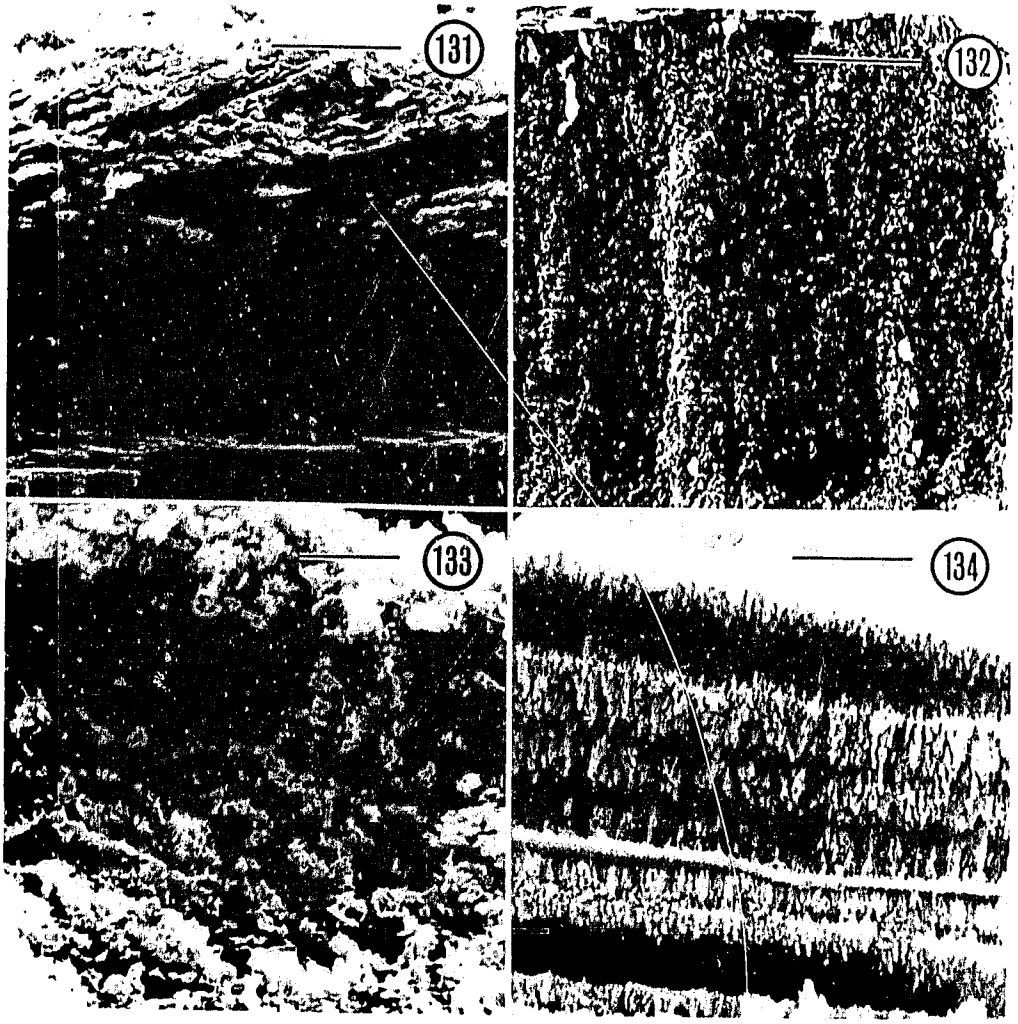
131
132
133
134

number of locations posterior to the edge of detachment (Figures 135, 136), and stereoscopic SEM observations confirmed these markings to be depressions into the shell. Close examination revealed a rough surface which differed substantially from the normally smooth, slightly undulating topography of the internal shell surface (Figure 136). The V-shaped, ventral orientation of these scars was consistent with the edge where separation of the shell eventually occurred (Figure 135), and with the notches normally found at the primary shell apex. SEM examination of the internal shell surface of several specimens revealed no other markings posterior to the point of retractor muscle insertion.

Analysis of shell measurements

Analysis of shell characters show that decollation (indicated by a notch on the primary shell apex) produces increased posterior aperture sizes (represented at time of decollation by notched primary shell apex height) with growth (Figure 137). While subsequent secondary shell growth originates from the internal surface of the primary shell apex (Figures 124-127), it does not taper as much as the primary shell (Table 6) and so maintains the increased aperture size (Figure 138).

DISCUSSION

Maintaining communication between the external environment and the mantle cavity of scaphopods predicts an ontogenetic increase in posterior aperture size. Such an increase occurs in *Dentalium rectius* , and so accomodates greater respiratory currents circulating

Figure 135. Discarded shell, view of internal ventral surface. Note three sets of V-shaped scars (*arrowheads*). *Arrows*, fracture edge; *double arrowhead*, detachment edge. Scale = 0.1mm.

Figure 136. Scar on internal ventral surface of detached shell, produced by shell dissolution. Scale = 20μm.

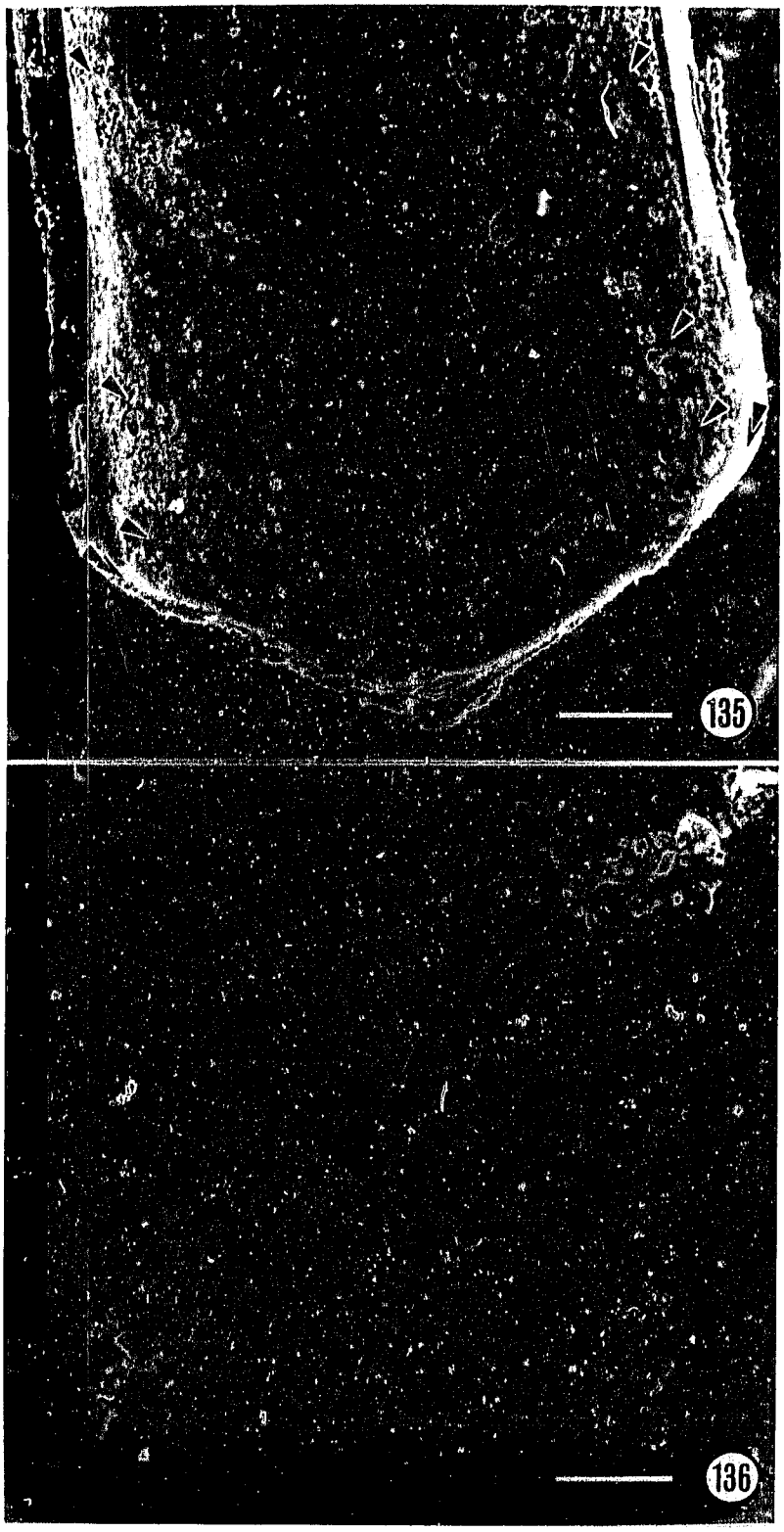
135
136

Figure 137. Plot of anterior aperture height against primary apex height for notched shells (shells which have been decollated), with or without a secondary shell. $Y = 0.22X + 0.05$, $r^2 = 0.63$.

Figure 138. Plot of anterior aperture height against secondary apex height, notched shells. $Y = 0.16X + 0.11$, $r^2 = 0.51$.

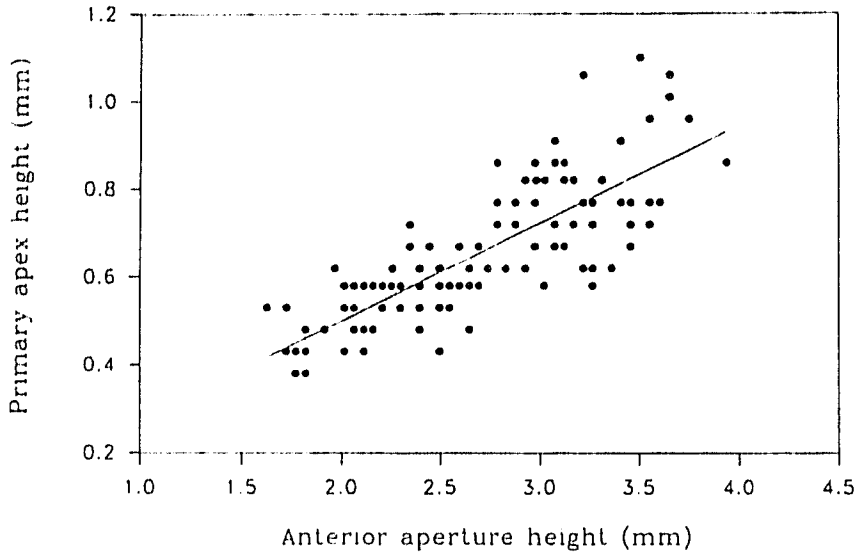
Primary apex height (mm)
1.2
1.0
0.8
0.6
0.4
0.2
1.0
1.5
2.0
2.5
3.0
3.5
4.0
4.5
Anterior aperture height (mm)

137

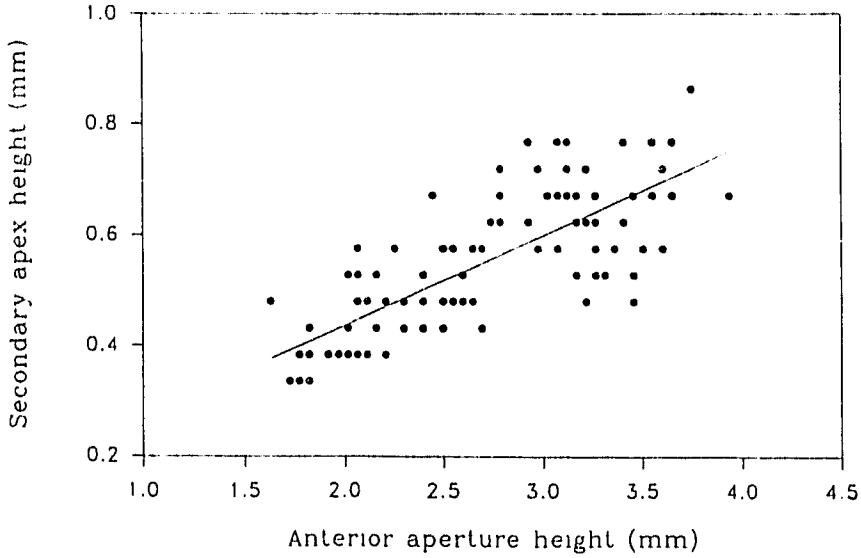
Secondary apex height (mm)
1.0
0.8
0.6
0.4
0.2
1.0
1.5
2.0
2.5
3.0
3.5
4.0
4.5
Anterior aperture height (mm)

138

Table 6. Comparison of primary and secondary shell taper, for shells which have been decollated (have a notch on the primary shell apex). The negative minimum value indicates a secondary shell which increased in width with length. n = 102.

Taper rate (mm)	Primary shell	Secondary shell
mean ± SE*	0.053 ± 0.001	0.01 ± 0.006
minimum	0.037	-0.056
maximum	0.086	0.500

* t - test: $0.001 < P(|t| \geq 7.289) < 0.0001$

within a larger mantle cavity, and facilitates the passage of increasing fecal material and gametes with growth of the animal. The removal of shell material to achieve this could occur in a number of ways, such as weathering or abrasion by sediments while burrowing, or the gradual dissolution of the aperture rim by the mantle. However, the secretion of a secondary shell by the posterior mantle in *D. rectius* precludes continual dissolution or erosion of the primary shell rim as a mechanism for increasing posterior aperture diameter. Instead, the entire secondary shell and a posterior portion of the primary shell must be removed. While haphazard and potentially fatal to the scaphopod, periodic accidental breakage of the primary shell apex, with subsequent repair by secondary shell growth, apparently serves to increase posterior aperture size in a small percentage (10.69%, Table 5) of the sampled population. Shell decollation, by dissolution of the shell anterior to the primary shell aperture resulting in the detachment of an apical portion of the shell, would be a more effective mechanism for increasing aperture size with growth of the animal. While observed only under laboratory conditions, *Dentalium rectius* can decollate the posterior portion of its shell in this way. Repeated periodically, this would account for the observed increase in posterior aperture size in this species (Figure 139). The V-shaped internal scars and detachment edge of the discarded shell, producing a notch in the new primary shell apex similiar to that found in most specimens, resemble surfaces subjected to shell dissolution (Deith, 1985; Signor, 1985). The consistent orientation, shape and size of the scars suggests that removal of shell material resulted from secretions of a limited band of the underlying mantle, in contrast with the large area of outer pavilion epithelium thought to be involved in secondary shell secretion (Stasek & McWilliams, 1973). It is not possible, however, to specify the precise mechanism of shell removal involved beyond invoking some type of dissolution or chemical erosion of calcium carbonate; shell reabsorption would require active uptake by the mantle of shell materials (Signor, 1985).

Figure 13. Schematic diagram of shell growth and and model for posterior aperture enlargement through decollation of the primary shell. The shell is viewed from the ventral side, showing notches in primary and secondary shells. Most recent (*arrowhead*) and possible future (*double arrowheads*) sites of shell decollation are indicated (*large arrows*, direction of primary shell growth; *small arrows*, direction of secondary shell growth).

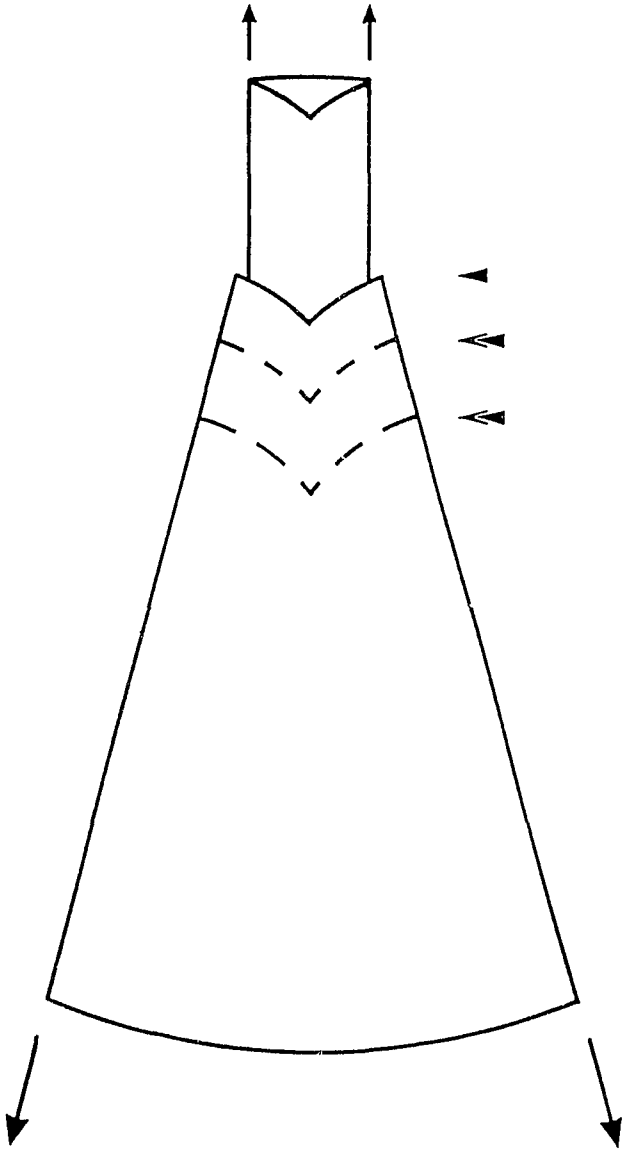

(139)

Shell decollation has been noted in several terrestrial gastropod families such as the Truncatellidae (Morrison, 1963), Potamidae, Pleuroceridae (Vermeij, 1974) and Subulinidae (Hochpöchler & Kothbauer 1975; Kat, 1981). Although also occurring in the marine Caecidae, the phenomenon is usually associated with tall-spired terrestrial species found on hard substrates in which the shell is wholly supported by the foot (Kat, 1981; Vermeij, 1974). The loss of one or more whorls is accomplished by dissolution of the internal shell surface, although separation of the apex could be achieved through erosion of the weakened shell. The new apex is closed off or plugged by subsequent shell secretion (Morrison, 1963; Kat, 1981). Removal of the shell apex is thought to increase the stability of the terrestrial snail by shifting the center of gravity to lie over the aperture; in contrast, gastropods which live in soft sediments have the shell supported in part by the substrate (Vermeij, 1974). In the terrestrial pulmonate gastropod *Rumina decollata* , the change in shell shape through loss of apical whorls has been related to increased mobility, reduction in shell weight, and reduced water loss, with a resultant increase in body and gonad size increasing fitness (Kat, 1981). The selective advantage of shell decollation in the Scaphopoda differs from that in gastropods. With no mechanism for enlarging the posterior aperture, there would be a severe restriction on growth in the Dentaliida; with this restriction removed, the larger body and gonad sizes which could be attained would increase fitness, as argued for *R. decollata* (Kat, 1981).

In scaphopods of the genus *Cadulus* and other members of the Gadilida which do not secrete a secondary shell, posterior aperture increase could occur simply by a steady rate of dissolution at the aperture rim. In some species, there are several notches in the posterior aperture producing a lobate apex (Abbott, 1974), although the number of notches can be highly variable (Shimek, 1989). Removal of apical shell material in scaphopods can be considered one of several growth related shell shape changes that molluscs achieve

through shell dissolution or reabsorption, such as the creation of slits or holes in some limpets (Fretter & Graham, 1962), removal of apertural spines (Carriker, 1972), internal remodelling of uppermost whorls in prosobranchs (Vermeij, 1974), and surficial dissolution of the pentultimate whorl in prosobranchs and *Nautilus* (Signor, 1982; 1985).

As Fischer-Piette & Franc (1969) point out, the process by which scaphopods enlarge the shell anteriorly while progressively shortening it at the posterior end results in the gradual loss of the complete juvenile shell, and the progressive loss of the older portions of the adult shell. This necessitates an anterior shift in the point of retractor muscle insertion as growth proceeds. While no SEM evidence for this was found in the shells examined, it is likely that any scars resulting from such a shift would be quickly hidden by shell secretion of the underlying mantle.

It is also of importance to note that the original description of *Dentalium rectius* (Carpenter, 1864 in Palmer, 1964; 1865) and the description of the subgenus *Rhabdus* by Pilsbry & Sharp (1897), which cites *D. rectius* Carpenter 1864 as the type species, do not mention the presence of an apical notch. Apical shell morphology is an important shell character in scaphopod taxonomy (e.g., Emerson, 1962; Palmer, 1974) although the reliability of this and other shell characters has been questioned (Shimek, 1989). Since in all other respects the study population fits the description of *D. rectius*, it is very likely that the shallow ventral notch in the primary shell apex of this species was missed by the earlier workers.

These results indicate that the interrupted shell growth between the primary and secondary shell of *D. rectius* is not caused primarily by shell repair due to accidental breakages or predation by the ratfish *Hydrolagus* as suggested for other populations of this species (Shimek, 1989), but by mantle-mediated shell decollation. Decollation results in

loss of the secondary shell and the oldest portion of the primary shell, the production of a notch in the shell apex prior to secondary shell regrowth, and an increase in posterior aperture size. Decollation is likely repeated periodically during growth and is an important physiological mechanism for maintenance of a sufficient opening to the mantle cavity, which would otherwise be progressively restricted by the ontogenetic shell growth pattern in scaphopods. Decollation of the shell is necessary to achieve this change in shell shape, as direct dissolution of the aperture rim would be ineffective given the continuity of secondary shell secretion. The presence of a secondary shell in *D. rectius* and some other dentaliid species may be significant to the maintenance of the burrow or in providing protection for the sensory structures of the posterior mantle tissue or pavilion (Chapter 6).

LITERATURE CITED

Abbott, R. T. (1974). American Seashells (second ed.). Van Nostrand Reinhold, New York.

Carpenter, P. P. (1865). Diagnoses Specierum et Varietum novarum Molluscorum, prope Sinum Pugetianum a Kennerlio Doctore, nuper decesso, collectorum. Proceedings of the Academy of Natural Sciences of Philadelphia, 1865, 54-64.

Carriker, M. R. (1972). Observations on the removal of spines by muricid gastropods during shell growth. The Veliger, 15(2), 69-74.

Deith, M. R. (1985). The composition of intertidally deposited growth lines in the shell of the edible cockle, *Cerastoderma edule*. Journal of the Marine Biological Association of the United Kingdom, 65(573-581), 573-581.

Emerson, W. K. (1962). A classification of the scaphopod mollusks. Journal of Paleontology, 36(3), 461-482.

Fischer-Piette, E. & Franc, A. (1968). Classe des scaphopodes, Scaphopoda (Bronn 1862). In Grassé, P.-P. (Ed.) Traité de zoologie, anatomie, systematique,

biologie, 5(3), Mollusques, Gasteropodes et Scaphopodes (pp. 987-1017). Masson et Cie, Paris.

Fretter, V. & Graham, A. (1962). British Prosobranch Molluscs . Ray Society, London.

Hochpöchler, F. & Kothbauer, H. (1975). Der mechanismus der Dekollation bei *Rumina decollata* (L.) (Gastropoda: Stylomatophora). Archiv Molluskenk, 106 (1-3), 119-121.

Kat, P. W. (1981). Shell shape changes in the Gastropoda: shell decollation in *Rumina decollata* (Pulmonata: Subulinidae). The Veliger, 24(2), 115-119.

Lacaze-Duthiers, H. (1856). Histoire de l'organisation et du développement du Dentale. Annales des Sciences Naturelles, Quatrième Séries, Paris, 6, 319-385, pls. 11-13.

Morrison, J. P. E. (1963). *Cecina* from the state of Washington. Nautilus, 76, 150-151.

Palmer, C. P. (1974). A supraspecific classification of the scaphopod Mollusca. The Veliger, 17(2), 115-123.

Palmer, K. van W. (1958). Type specimens of marine mollusca described by P. P. Carpenter from the west coast (San Diego to British Columbia). Geological Society of America, Memoir 76.

Pilsbry, H. A. & Sharp, B. (1897). Class Scaphopoda. Manual of Conchology, Series 1, 17, i-xxxii, 1-144.

Shimek, R. L. (1989). Shell morphometrics and systematics: a revision of the slender, shallow water *Cadulus* of the northeastern Pacific (Scaphopoda: Gadilida). The Veliger, 32(3), 233-246.

Signor, P. W. (1982). Growth-related surficial resorption of the penultimate whorl in *Terebra dimidiata* (Linnaeus, 1758) and other marine prosobranch gastropods. The Veliger, 25(1), 79-82.

Signor, P. W. (1985). Surficial shell resorption in *Nautilus macrophalus* Sowerby, 1849. The Veliger, 28(2), 195-199.

Stasek, C. R. & McWilliams, W. R. (1973). The comparative morphology and evolution of the molluscan mantle edge. The Veliger, 16(1), 1-19.

Vermeij, G. J. (1974). Molluscs in mangrove swamps: physiognomy, diversity, and regional differences. Systematic Zoology, 22, 609-624.

Yonge, C. M. (1937). Circulation of water in the mantle cavity of *Dentalium entalis*. Proceedings of the Malacological Society of London, 22, 333-337.

CHAPTER 8

GENERAL DISCUSSION

SIGNIFICANCE OF SCAPHOPODA IN MOLLUSCAN STUDIES

Haemocoel and coelom

Circulation and excretion in molluscs, as in most higher invertebrates and vertebrates, are intimately associated. The excretory pathway of ultrafiltration across the heart wall, with subsequent modification by reabsorption and secretion as the urine passes from pericardial to kidney lumina to the exterior, has been well established; both ultrastructural description and physiological experimentation has provided this evidence from four classes, the Bivalvia (Hevert, 1984; Meyhöfer et al., 1985), Gastropoda (Little, 1965; Andrews, 1981), Cephalopoda (Martin & Aldrich, 1970; Schipp & Hevert, 1981) and Polyplacophora (Økland, 1981). These studies have focussed on both the fluid dynamics of circulation (for review, see Jones, 1983) and the production and modification of urine (for review, see Martin, 1983; Andrews, 1988). The heart of molluscs therefore has a dual role, in excretion and in the movement of blood; oxygenated hemolymph is brought from the gills or ctenidia to the paired auricles, passes into the ventricle and is then pumped to the rest of the body. The blood pressures created by the musculature of the heart simultaneously drive ultrafiltration, and therefore initiate the excretory process.

In contrast, circulation and excretion in the scaphopods present difficulties in interpretation. The morphology of the heart and pericardium in *Dentalium rectius* is highly modified; the heart appears to be very reduced with a complete loss of auricles, the ventricle is represented by a muscular perianal blood sinus, the pericardial rudiment is contractile and

does not fully enclose the perianal sinus, podocytes are limited in distribution and poorly developed, and the communication between pericardium and the kidneys is incomplete. Furthermore, the merocrine secretory process of the *D. rectius* kidneys described here is rare among examined Mollusca.

This investigation of the scaphopod heart/kidney complex reveals several features unique in molluscan circulation and excretion. The extensive reduction of the scaphopod heart is probably due to the specializations of the mantle cavity, and particularly the loss of ctenidia. The ciliated bands in the mid region of the mantle cavity, with supporting cells seemingly specialized for diffusion between mantle cavity and haemocoel, are generally considered to represent a specialized respiratory surface. Although there is an extensive underlying haemocoelic space, the ciliated bands do not have the distinct efferent and afferent blood vessels associated with molluscan ctenidia. The auricles, which in other molluscs receive blood from the ctenidia, may have been lost due to this reduction of circulatory requirements in the Scaphopoda. The presence of a contractile blood sinus around the rectum, homologous to the molluscan ventricle, and a considerable "pericardial" coelomic cavity may be essential to excretory function despite the reduced circulatory role. Ultrafiltration, as evidenced by the presence of podocytes in the pericardium, requires elevated blood pressures which are likely provided by the perianal sinus musculature.

The molluscan kidneys are mesodermal in origin, considered modified coelomoducts (Andrews, 1988) that were originally responsible for the passage of gametes, or separate pericardioducts (Salvini-Plawen, 1985) which were subsequently modified for excretion. In either case, the connection between the kidneys and pericardium has persisted, with ultrafiltration into the pericardial coelom of many molluscs localised in the auricular epicardium (Andrews, 1988). While loss of the auricles in the Scaphopoda is associated with diminished circulatory requirements, the excretory functions of the

remaining heart and pericardial structures are maintained. What remains to be identified is the efficiency of ultrafiltration, the excretory process most closely associated with circulation, that is being driven by the blood pressures created by the reduced scaphopod heart.

Metal uptake, accumulation and excretion

The accumulation of metals by marine fauna has been of great interest in the past twenty years, stemming particularly from the prospective use of indicator species, particularly molluscs, to signal pollutant levels of toxic metals in the environment (Simkiss & Mason, 1983). Greater understanding of the factors governing metal metabolism has demonstrated that complex systems are involved in uptake, accumulation and excretion, altering early concepts of organisms acting simply as heavy metal "sinks". In response to the need for a broader and more detailed understanding of metal processing by molluscs, greater attention has been given to the physiological role of metals in organisms not under environmental stress (Mason et al., 1984). There is considerable data on the identification and sites of metal accumulation in marine mollusca; these repeatedly identify the kidney and digestive gland as major sites of metal storage (Simkiss & Mason, 1983).

Apart from calcium, only zinc and iron were accumulated in the kidneys and tissues of the digestive tract in *D. rectius*. The storage of iron in the oesophagus and stomach epithelia and its excretion by radular mineralisation differs from iron metabolism studies in the bivalve *Mytilus* and gastropod *Littorina* (George, 1974; Young, 1977). It is uncertain what factors influence the departure of *D. rectius* from the pathways of iron processing shown in other molluscs; more information is required to better define the mechanisms of

metal uptake and transport, and the influence of the form and quantity of environmental sources of iron.

Mantle form and function

The molluscan mantle is a distinguishing feature of the phylum. In addition to secretion of the shell, the mantle encloses the mantle cavity, which can be considered a buffer between the organism and the external environment; materials released to the exterior, such as feces, urine and gametes, and those brought to the organism, such as respiratory currents, must pass through it. The protection afforded by the mantle cavity is utilised by the elaboration of the organs housed within it, such as the gills or ctenidia, and the sensory osphradia.

In the Scaphopoda, ctenidia and osphradia are absent. This is perhaps due to the reduced space available within the mantle cavity, a consequence of the narrow elongate body form. However, two regions of the mantle are specialised for gas exchange and sensory reception. The ciliated bands, found on the body and mantle wall and encircling the mid-region of the mantle cavity, consist of ciliated and supporting epithelium which functions in the creation of respiratory currents and facilitates diffusion. As stated above, the loss of ctenidia has had consequences for circulation and the structure of the heart/kidney complex, which shows a comcomitant reduction. While not approaching the structural complexity of most molluscan ctenidia, the ciliated bands are a functional equivalent within the constraints of a reduced mante cavity.

Another unique feature of the scaphopod mantle is the modification of the posterior region, known as the pavilion. Most macrofaunal molluscs which burrow into sediments

(gastropods and bivalves) have the mantle margin elaborated into one or two siphons, which serve to bring in clean respiratory water currents from above the surface of the sediment. The quality of the respiratory stream is tested by sensory receptors present on the tip of the siphon, and by the osphradia which are located in the path of the inhalent current. The scaphopod pavilion does not possess the musculature of the bivalve or gastropod siphon, and cannot be extended far out of the shell. It is, however, the opening to the mantle cavity through which the respiratory current enters, and ciliated sensory receptors are concentrated in areas of the pavilion which would serve to test the inhalent water stream. Once again, this is a modification of the mantle that is unique to the Scaphopoda that fills functional roles left vacant by the absence of more typical molluscan organs.

The dissolution of shell by the pavilion is not unusual among mollusca. Secondary removal of shell material by the mantle margin occurs in all classes which possess a shell, but are applied under widely differing circumstances. Essentially, these can be summarised under three headings; removal of physical impediments to further growth, the reduction of weight, and conservation of shell material. However, the decollation of the posterior or apical end in scaphopods appears to be a solution to a design flaw in the ontogenetic growth pattern of the shell. The restriction of the respiratory current to the posterior end is seemingly incongruous with the relative diminishing of the posterior aperture that occurs with increase in total body size; a larger posterior aperture is needed for passage of greater respiratory currents and the expulsion of feces and gametes. An analogous requirement for modification of shell shape is thought to occur in key-hole limpets (Fretter & Graham, 1962). As in those gastropods, it is likely that in most scaphopods there is a gradual dissolution of shell from the posterior aperture rim. However, the secretion of a secondary shell in *D. rectius*, found in some other members of the Dentaliida, necessitates decollation.

Thus, the ability of the molluscan mantle margin to remove as well as secrete shell is demonstrated in the Scaphopoda, but is applied to a unique modification of the shell in response to physiological requirements of the organism.

CONCLUDING REMARKS

The Scaphopoda have long been neglected as a significant comparative element in many areas of molluscan biology. Early studies of scaphopod anatomy provided a morphological base from which little progress has been made, an unusual case during the historical development of invertebrate functional morphology. In recent years, identification of accessible, high density populations of scaphopods in nearshore waters of the Northeast Pacific plus a greater awareness of the value of comparative studies has renewed interest in the biology of this group. This is evidenced by recent publications on scaphopod feeding behaviour, captacular and gut morphology, diet and ecology.

The results reported in this dissertation provide the first detailed morphological analysis of several scaphopod organ systems, and indicate convincingly that in many areas of morphology and physiology the scaphopods do not follow bivalve or gastropod models. As such, these studies offer insights into the role of morphological constraint in functional adaptation within the phylum, and complement studies on more studied groups of molluscs of similar habitat and lifestyle such as the protobranch bivalves. Nevertheless, several areas of scaphopod biology, such as reproduction, continue to be relatively untouched. Those areas in which I have provided more extensive information still lack data from the other taxon of the class, the Gadilida. The analysis of structure and function in the studies presented here provide models which can now be tested among other scaphopod taxa and by appropriate physiological techniques.

A critical analysis of molluscan functional morphology and phylogeny requires a comparable range and detail of data from the minor groups to augment that from the more diverse gastropod, bivalve and cephalopod classes. Apart from the Scaphopoda, much morphological and physiological work remains to be done in the Aplacophora, Monoplacophora and Polyplacophora. Until these are addressed, our understanding of the biology of this phylum will be overly influenced by the more conspicuous, well studied and widely radiated classes of the Mollusca.

LITERATURE CITED

Andrews, E. B. (1981). Osmoregulation and excretion in prosobranch gastropods, part 2: structure in relation to function. Journal of Molluscan Studies, 47, 248-289.

Andrews, E. B. (1988). Excretory systems of Molluscs. In Trueman, E. R. & Clarke, M. R. (Eds.), The Mollusca, v. 11, Form and Function (pp. 381-448). Academic Press, New York.

Bilyard, G. R. (1974). The feeding habits and ecology of *Dentalium entale stimpsoni* Henderson. The Veliger, 17(2), 126-138.

Dinamani, P. (1964). Burrowing behaviour of *Dentalium*. Biological Bulletin, 126, 28-32.

Fretter, V. & Graham, A. (1962). British Prosobranch Molluscs. Ray Society, London.

Gainey, L. F. Jr. (1972). The use of the foot and the captacula in the feeding of *Dentalium* (Mollusca: Scaphopoda). The Veliger, 15(1), 29-34.

George, S. G., Pirie, B. J. S. & Coombs, T. L. (1976). The kinetics of accumulation and excretion of ferric hydroxide in *Mytilus edulis* (L.) and its distribution in the tissues. Journal of Experimental Marine Biology and Ecology, 23, 71-84.

Hevert, F. (1984). Urine formation in the Lamellibranchs: evidence for ultrafiltration and quantitative description. Journal of Experimental Biology, 111, 1-12.

Jones, H. D. (1983). The circulatory system of gastropods and bivalves. In Salueddin A. S. M. & Wilbur K. M. (Eds.) The Mollusca, v. 5, Physiology, part 2 (pp. 189-238). Academic Press, New York.

Little, C. (1965). The formation of urine by the prosobranch gastropod mollusc *Viviparus viviparus* Linn. Journal of Experimental Biology, 43, 39-54.

Martin, A. W. (1983). Excretion. In Saleuddin, A. S. M. & Wilbur, K. M. (Eds.) The Mollusca, v. 5, Physiology, part 2 (pp. 353-405). Academic Press, New York.

Martin, A. W. & Aldrich, F. A. (1970). Comparison of hearts and branchial heart appendages in some cephalopods. Canadian Journal of Zoology, 48, 751-756.

Mason, A. Z., Simkiss, K. & Ryan, K. P. (1984). The ultrastructural localization of metals in specimens of Littorina littorea collected from clean and polluted sites. Journal of the Marine Biological Association of the United Kingdom, 64, 699-720.

McFadien-Carter, M. S. (1973). Zoogeography and ecology of seven species of Panamic-Pacific Scaphopoda. The Veliger, 15(4), 340-347.

Meyhöfer, E., Morse, M. P. & Robinson,W. E. (1985). Podocytes in bivalve molluscs: morphological evidence for ultrafiltration. Journal of Comparative Physiology B, 156, 151-161.

Nott, J. A. & Nicolaidou, A. (1989). The cytology of heavy metal accumulations in the digestive glands of three marine gastropods. Proceedings of the Royal Society of London, B 237, 347-362.

Økland, S. (1981). Ultrastructure of the pericardium in chitons (Mollusca: Polyplacophora), in relation to filtration and contraction mechanisms. Zoomorphology, 97, 193-203.

Poon, P. A. (1987). The diet and feeding behaviour of *Cadulus tolmiei* Dall, 1897 (Scaphopoda, Siphonodentalioida). The Nautilus, 101(2), 88-92.

Potts, W. T. W. 1967. Excretion in the Molluscs. Biological Reviews, 42, 1-41.

Salvini-Plawen, L. v. (1985). Early evolution and the primitive groups. In Trueman, E. R. & Clarke, M. R. (Eds.) The Mollusca, v. 10, Evolution (pp. 59-150). Academic Press, New York.

Schipp, R. & Hevert, F. (1981). Ultrafiltration in the branchial heart appendage of dibranchiate cephalopods: a comparative ultrastuctural and physiological study. Journal of Experimental Biology, 92, 23-35.

Shimek, R. L. (1988). The functional morphology of scaphopod captacula. The Veliger, 30(3), 213-221.

Shimek, R. L. (1989). Shell morphometrics and systematics: a revision of the slender, shallow water *Cadulus* of the northeastern Pacific (Scaphopoda: Gadilida). The Veliger, 32(3), 233-246.

Shimek, R. L. (1990). Diet and habitat utilization in a Northeastern pacific ocean scaphopod assemblage. American Malacological Bulletin, 7(2), 147-169.

Simkiss, K. & Mason, A. Z. (1983). Metal ions: metabolic and toxic effects. In Hochachka, P. W. (Ed.) The Mollusca, v. 2, Environmental Biochemistry and Physiology (pp. 101-164). Academic Press, New York.

Taib, N. T. (1980). Some observations on the living animals of *Dentalium entalis* L. Journal of the College of Science, University of Riyadh, Saudi Arabia, 11, 129-144.

Taib, N. T. (1981). Sites of absorption and food storage in the gut of *Dentalium entalis* L.. Journal of the College of Science, University of Riyadh, Saudi Arabia, 12(1), 147-154.

Trueman, E. R. (1968). The burrowing process of *Dentalium* (Scaphopoda). Journal of Zoology, London, 154, 19-27.

Young, M. L. (1977). The roles of food and direct uptake from water in the accumulation of zinc and iron in the tissues of the dogwhelk, *Nucella lapillus*. Journal of Experimental Marine Biology and Ecology, 30, 315-325.